

March 2015

Agricultural Waste Remediation and H₂ Production by Hyperthermophilic Heterotrophs: Bioinformatics, Taxonomy, and Physiology

Sarah A. Hensley
University of Massachusetts - Amherst

Follow this and additional works at: https://scholarworks.umass.edu/dissertations_2



Part of the [Biotechnology Commons](#)

Recommended Citation

Hensley, Sarah A., "Agricultural Waste Remediation and H₂ Production by Hyperthermophilic Heterotrophs: Bioinformatics, Taxonomy, and Physiology" (2015). *Doctoral Dissertations*. 303.
https://scholarworks.umass.edu/dissertations_2/303

This Open Access Dissertation is brought to you for free and open access by the Dissertations and Theses at ScholarWorks@UMass Amherst. It has been accepted for inclusion in Doctoral Dissertations by an authorized administrator of ScholarWorks@UMass Amherst. For more information, please contact scholarworks@library.umass.edu.

**AGRICULTURAL WASTE REMEDIATION AND H₂ PRODUCTION BY
HYPERTHERMOPHILIC HETEROTROPHS: BIOINFORMATICS, TAXONOMY, AND
PHYSIOLOGY**

A Dissertation Presented

by

SARAH A. HENSLEY

Submitted to the Graduate School of the
University of Massachusetts Amherst in partial fulfillment
of the requirements for the degree of

DOCTOR OF PHILOSOPHY

February 2015

Microbiology Department

© Copyright by Sarah A. Hensley 2015

All Rights Reserved

**AGRICULTURAL WASTE REMEDIATION AND H₂ PRODUCTION BY
HYPERTHERMOPHILIC HETEROTROPHS: BIOINFORMATICS, TAXONOMY, AND
PHYSIOLOGY**

A Dissertation Presented

by

SARAH A. HENSLEY

Approved as to style and content by:

James F. Holden, Chair

Klaus Nüsslein, Member

Kristen DeAngelis, Member

Caitlyn Butler, Member

John Lopes, Department Head
Microbiology Department

DEDICATION

In memory of Katarina Ölsson Gudmundsson, this dissertation is dedicated to everyone who lights up another's day just by their love of life and joyful presence.

ACKNOWLEDGMENTS

I would like to thank absolutely everyone who helped me in any way during this journey. Especially my professor, Dr. James Holden for his eternal optimism and motivation, as well as his belief in me as an individual. To my parents, Gary and Robyn Hensley, and my sister, Samantha Hensley, for their constant motivation, pride and support. Without their guiding light, I would have been lost many times over. To Jason Horowitz, who is more than I could ever have wished for in a partner and whose love has bolstered me greatly when I needed it most. To all my friends and co-workers, thank you for all of your support you've given me and all of the laughs we've shared. I couldn't have kept my chin up when times were tough, nor fully realized how wonderful my research was without you.

Also, I would like to thank the all-too-frequently unsung heroes. To my professors throughout the years, who fed my thirst for knowledge while supplying the tools to keep it alive and who taught me that education is not just about a letter grade. Of these professors, I would especially like to thank Deana Reynolds (who renewed my drive to learn when I needed it most), Elaine Freeland (who taught me to think outside the box and to trust my impulses), Stephen Gibbs (who taught me the value of academic determination and perseverance) and Dr. Romi Burks (who created in me a drive and showed me the path towards achieving a PhD).

Without any of these individuals and support networks, I would not be where I am today. I thank you all from the bottom of my heart.

This work could not have been completed without the efforts of Jesús Alvelo, Alex Basu, James F. Holden, Eun-Jung Leon, Jong-Hyun Jung, You-Tae Kim, Michael

Lavine, Ju-Hoon Lee, Emily Moreira, Katarina Ölsso, Cheon-Seok Park, and Dong-Ho Seo.

ABSTRACT

AGRICULTURAL WASTE REMEDIATION AND H₂ PRODUCTION BY HYPERTHERMOPHILIC HETEROTROPHS: BIOINFORMATICS, TAXONOMY, AND PHYSIOLOGY

FEBRUARY 2015

SARAH A. HENSLEY, B.S., SOUTHWESTERN UNIVERSITY

M.S., UNIVERSITY OF MASSACHUSETTS AMHERST

Ph.D., UNIVERSITY OF MASSACHUSETTS AMHERST

Directed by: Dr. James F. Holden

In the United States, nearly 35 million tons of food waste are delivered to landfills and wastewater treatment plants for disposal each year. This places a burden on landfills and the environment through the introduction of foreign chemicals. Utilizing hyperthermophilic heterotrophs for waste treatment in a consolidated bioprocess could potentially remediate these organics, increase reaction rates, kill pathogens, produce a bioenergy product (H₂), and lower costs relative to mesophilic waste treatment options. However, it is unknown how various agricultural waste streams will affect hyperthermophilic growth and metabolite production. We investigated *Thermococcales* species for this purpose. Specifically, we chose *Pyrococcus furiosus* and *Thermococcus paralvinellae* because of their use as a model organism and their potential H₂ production, respectively. In this set of studies, we determined 1) the genomic sequence of *T. paralvinellae*, 2) how representative these two microorganisms are of *Thermococcales* species, and 3) the physiology of both organisms when grown in different defined and waste-mediated environmental conditions. We found that *T. paralvinellae* is genomically most

similar to *T. barophilus* and that *P. furiosus* and *T. paralvinellae* are good representatives of different potential metabolisms of the *Thermococcales*. Both *P. furiosus* and *T. paralvinellae* are amenable to the catabolism of carbohydrates and peptides with H₂ production over a range of pH and acetate concentrations with little impact on growth and H₂ production rates. The mechanisms that *P. furiosus* and *T. paralvinellae* are using for redox balance may not be the same, as seen by the differential expression of a number of enzymatic activities. *T. paralvinellae* consistently produced more H₂ on both raw milk and spent grain wastes. Mesophilic bacteria were eliminated from the wastes in the process of hyperthermophilic growth, indicating that it is feasible to use hyperthermophilic heterotrophs in a single process step to reduce the organic load of food and agricultural wastes, generate H₂ as an energy byproduct, and remove pathogens.

TABLE OF CONTENTS

	Page
ACKNOWLEDGMENTS	v
ABSTRACT	vii
LIST OF TABLES.....	xii
LIST OF FIGURES.....	xiii
CHAPTER	
1. INTRODUCTION	1
1.1 Central Objectives and Goals.....	1
1.2 Existing Waste Treatment Technology.....	2
1.2.1 Methods of Food Waste Disposal.....	4
1.2.2 Feasibility of Different Food Waste Types for Biofuel Production.....	7
1.3 Biohydrogen: Potential and Production Capabilities	9
1.3.1 Biohydrogen Production Processes.....	10
1.4 Glycolysis, Respiration, and Fermentation	13
1.4.1 The Embden-Meyerhof-Parnas Pathway	14
1.4.2 Fermentative Mechanisms	16
1.5 Acetogens and Fermentation Balance.....	17
1.5.1 Acetic Acid Production	17
1.5.2 Acetogenic Metabolite Switching.....	19
1.5.3 Hydrogenases: Vital for Hydrogen Metabolism.....	21
1.5.4 Potential for Hydrogen Production.....	22
1.6 Biohydrogen and Biofuel Production by Thermophiles and Hyperthermophiles.....	24
1.6.1 Benefits and Limitations of Thermophilic Biohydrogen Production.....	24
1.6.2 Hyperthermophiles.....	26
1.6.3 Hyperthermophile Hydrogen Production Models.....	27

1.7 Introduction to the Thermococcales	28
1.8 Metabolism in the Thermococcales	31
1.8.1 Modifications to the Embden-Meyerhof-Parnas Pathway.....	31
1.8.2 Hydrogen Production by <i>P. furiosus</i>	33
1.8.3 Alternative Hydrogenases in the Thermococcales.....	34
1.8.4 Metabolite Switching by <i>P. furiosus</i> in the Absence of Sulfur	36
1.9 Possibilities of Waste Remediation by Thermococcales.....	37
1.9.1 Brewery Waste Remediation.....	38
1.9.2 Dairy Waste Remediation	38
1.9.3.1 Mastitis and Antibiotic Treatment of Dairy Cows	39
1.9.3.2 Antibiotic Activity on Cell Wall Synthesis.....	40
1.9.3.3 Disposal of Waste Milk.....	42
1.9.3.4 Lactose and Protein Transporters in Thermococcales.....	46
1.10 Summary of Thesis	47
2. COMPLETE GENOME SEQUENCE OF THE HYPERTHERMOPHILIC ARCHAEON <i>THERMOCOCCUS PARALVINELLAE</i>	49
2.1 Summary.....	49
2.2 Genomic Analysis of <i>Thermococcus paralvinellae</i>	49
2.3 Nucleotide Sequence Accession Number.....	52
3. <i>THERMOCOCCUS PARALVINELLAE</i> SP. NOV. AND <i>THERMOCOCCUS CLEFTENSIS</i> CL1 SP. NOV., NEW SPECIES OF HYPERTHERMOPHILIC HETEROTROPHS FROM DEEP SEA HYDROTHERMAL VENTS.....	53
3.1 Summary.....	53
3.2 Growth Parameters of Strains ES1 ^T and CL1 ^T	54
3.3 Overall Genomic Relatedness Index Analyses.....	57
3.4 Description of <i>Thermococcus paralvinellae</i> sp. nov.....	70
3.5 Description of <i>Thermococcus cleftensis</i> sp. nov.....	73
4. HYDROGEN PRODUCTION BY <i>PYROCOCCUS FURIOSUS</i> AND <i>THERMOCOCCUS PARALVINELLAE</i> ES1 GROWN ON SPENT BREWERY GRAIN AND RAW BOVINE MILK.....	74
4.1 Summary.....	74
4.2 Introduction	75

4.3 Materials and Methods	78
4.3.1 Organisms used	78
4.3.2 Growth conditions.....	78
4.3.3 Metabolite measurements	81
4.3.4 Protein fractionation.....	82
4.3.5 Enzyme assays	83
4.3.6 Waste remediation.....	85
4.3.7 Statistical analysis	87
4.4 Results.....	87
4.4.1 Growth and metabolite production in defined media	87
4.4.2 Growth and H ₂ production in waste media.....	88
4.4.3 Remediation of raw milk waste.....	93
4.4.4 Growth in a 20-liter bioreactor.....	98
4.4.5 Enzyme activities.....	98
4.5 Discussion	112
5. CONCLUSIONS	117
5.1 Direction and Future Work.....	117
BIBLIOGRAPHY	121

LIST OF TABLES

Table	Page
Table 2.1 <i>Thermococcus paralvinellae</i> Genome Statistics.....	51
Table 3.1: Comparison of <i>in silico</i> ANIb and GGDC Analysis of Genomic DNA of <i>Thermococcus</i> sp. strains ES1 ^T and CL1 ^T	60
Table 3.2: SpeCI Analysis of <i>Thermococcus</i> sp. Strains ES1 ^T and CL1 ^T	62
Table 3.3: ORFs Found in <i>Thermococcus</i> sp. strains ES1 ^T Without Homologs in <i>Thermococcus barophilus</i>	63
Table 3.4: Comparison of ORFs Present in Select Thermococcales Species.....	68
Table 3.5: ORFs Found in <i>Thermococcus</i> sp. Strains CL1 ^T Without Homologs in <i>Thermococcus</i> sp. Strain 4557.....	71
Table 4.1: Kinetic Parameters for <i>P. furiosus</i> and <i>T. paralvinellae</i> on Various Defined Media (\pm 90% Confidence Interval).....	91
Table 4.2: Product Formation by <i>P. furiosus</i> and <i>T. paralvinellae</i> After 18 Hr of Growth on Defined Media.....	92
Table 4.3: Eradication of Culturable Microbes in 10% Raw Milk Media After 100hr of Incubation.....	100
Table 4.4: <i>P. furiosus</i> and <i>T. paralvinellae</i> Specific Enzyme Activities.....	103

LIST OF FIGURES

Figure	Page
Figure 1.1: Embden-Meyerhof-Parnas Pathway	15
Figure 1.2: Acetate Production Via the Wood-Ljungdahl Pathway.....	18
Figure 1.3: Metabolite Switching Between Acidogenic and Solventogenic Phases in <i>C. acetobutylicum</i>	20
Figure 1.4: Modified Embden–Meyerhof Pathway Present in <i>P. furiosus</i>	32
Figure 1.5: Bacterial Cell Wall Structure.....	43
Figure 1.6: Archaeal Cell Wall Structure.....	44
Figure 1.7: Distribution of Cell Wall Physiologies Among Archaea	45
Figure 3.1: Growth of Strains ES1 ^T and CL1 ^T in the Presence and Absence of Elemental Sulfur.....	56
Figure 3.2: 16S Phylogenetic Tree of Thermococcales Species with Strains ES1 ^T and CL1 ^T	58
Figure 4.1: Proposed Redox and ATP synthesis enzyme reactions in <i>P. furiosus</i> and <i>T. paralvinellae</i>	77
Figure 4.2: Hydrogen Production by <i>P. furiosus</i> and <i>T. paralvinellae</i> on Defined Wastes.....	89
Figure 4.3: Hydrogen Production by <i>P. furiosus</i> and <i>T. paralvinellae</i> on Agricultural Wastes.....	90
Figure 4.4: Clarification of Agricultural Waste Media with 100hr of Incubation.....	94
Figure 4.5: Microscopy of <i>P. furiosus</i> and <i>T. paralvinellae</i> Cells in the Presence of Spent Grain.....	95
Figure 4.6: Protein Degradation Concomitant with Hydrogen Production by <i>P. furiosus</i> and <i>T. paralvinellae</i> on 0.1% (vol/vol) Raw Milk Media.....	96
Figure 4.7: Reducing Sugar Assay for <i>P. furiosus</i> and <i>T. paralvinellae</i> on 0.1% (vol/vol) Raw Milk Media.....	97

Figure 4.8: COD Measurements of <i>P. furiosus</i> and <i>T. paralvinellae</i> Grown on 0.1% (vol/vol) Raw Milk Media.....	99
Figure 4.9: Growth Rates of <i>P. furiosus</i> and <i>T. paralvinellae</i> Grown in Bottles and 20-liter Bioreactors.....	101
Figure 4.10: Growth of <i>P. furiosus</i> and <i>T. paralvinellae</i> in the 20-liter Bioreactor on Defined and Agricultural Media.....	102
Figure 4.11: Distribution of <i>P. furiosus</i> and <i>T. paralvinellae</i> Enzymatic Specific Activities.....	105

CHAPTER 1

INTRODUCTION

1.1 Central Objectives and Goals

This dissertation uses microbiology, biochemistry, bioinformatics, and environmental engineering to understand the effect of varying environmental conditions on the H₂ production capabilities and enzymatic expression patterns of two Thermococcales species: *Pyrococcus furiosus* and *Thermococcus paralvinellae*. The central objective is to determine if these species are genetically distinct from each other and other Thermococcales species, if they react similarly to environmental conditions, which result in an increase in H₂ production and if these species can grow on varying concentrations of agricultural feedstock. The agricultural feedstocks tested were spent brewery grain and raw cow's milk from cows treated with antibiotic and from untreated cows.

The goals of this dissertation are: 1) to compare the predicted proteomes of *P. furiosus* and *T. paralvinellae* ES1 with those of other Thermococcales species using fully sequenced and annotated genomes with emphasis on enzymes related to metabolite production and energy conservation; 2) to model shifts in metabolites in defined media by determining how growth rates, H₂ production rates, other product formation, and the activities of 13 key metabolite-related enzymes vary with changes in carbon source, pH, and the presence of acetate; and 3) to test the model with dairy and brewery wastes and to correct the model where it differs with predicted results.

This dissertation consists of five chapters. This introductory chapter will review the literature on waste treatment technology, biohydrogen production, methods of microbial respiration (e.g., fermentation, glycolysis, and acetogenesis), the potential of thermophiles and hyperthermophiles, the physiology and characteristics of Thermococcales species (including an in-depth look into the fermentative-like metabolic pathways of *P. furiosus*), and possible agricultural wastes that could be treated by Thermococcales species. Chapter 2 will delve into sequencing the genome of *Thermococcus paralvinellae* and the unique features it possesses. Chapter 3 will examine the commonalities between all of the currently published complete Thermococcales genomes and will include a concise genome analysis of *Thermococcus cleftensis* – another Thermococcales species in the Holden lab that produces H₂. Through this work, it was determined that *T. paralvinellae* and *T. cleftensis* are novel taxonomic species and were formally named. Chapter 4 will focus on the growth kinetics, metabolite production, and enzymatic activities of 13 enzymes in *P. furiosus* and *T. paralvinellae* under five defined and three waste growth conditions. Chapter 5 provides the implications and significance of this dissertation, as well as some possible avenues for future work.

1.2 Existing Waste Treatment Technology

Every year, the U.S. loses an estimated \$3 billion in freshwater systems to eutrophication, (i.e., an increase in nutrient load into an ecosystem) due to habitat destruction and loss of species (Dodds *et al.*, 2009; Smith *et al.*, 1999). There are two main sources of eutrophication: diffuse and point (Cloern, 2001; Koelmans *et al.*,

2001). Diffuse sources are from water-run off associated with land use change, such as deforestation or agricultural practices (Novotny, 1999; Tilman *et al.*, 2002). Point sources are from domestic and industrial waste streams, such as sewage treatment plants and landfills (Dodds *et al.*, 2009; Koelmans *et al.*, 2001). Both of these sources make up different portions of municipal solid waste (MSW), commonly known as garbage (Dodds *et al.*, 2009).

Per capita, MSW generation is the highest in the U.S. at 800 kg per person per year (Sakai *et al.*, 2011; Van Haaren *et al.*, 2010). MSW is composed of agricultural, sanitary, and solid residues, based on the origin of the waste. Traditionally, agricultural and food waste was an overlooked component of MSW, but this trend is changing as it becomes more evident that this waste has the potential to be used as animal feedstock, a source of compost, and carbon neutral fuel.

Recent estimates show that as much as 50% of food produced is lost or wasted worldwide, which amounts to 1.3 billion tons of food per year (Parfitt *et al.*, 2010). In the U.S. over the last decade, food waste has risen to account for the largest percentage (21%) of MSW (EPA, 2011; Staley and Barlaz, 2009). As of 2010, over 97% of food waste in the U.S. was estimated to be part of MSW and buried in landfills (Levis *et al.*, 2010). This is compared to the 9% of food waste entering landfills in the U.K. for the same year (Bartlett, 2010). This discrepancy is in part due to the fact that, in the U.S., there is currently just over 200 composting facilities that accept food waste (Olivares *et al.*, 2008), as compared to the over 7,600 curbside recycling programs (Simmons *et al.*, 2006). In the U.S., programs and facilities to manage yard waste are well established (in 2008, 60% of yard waste

was composted), but the management of food waste in composting facilities is only just beginning (in 2008, 3% of food waste was composted) (Levis *et al.*, 2010).

In general, food and MSW can be disposed of in a variety of ways (Lin *et al.*, 2013). However, MSW management strategies are often implemented at the state and local level, making it difficult to have a uniform set of policies across the U.S.

1.2.1 Methods of Food Waste Disposal

In the U.S., current management strategies for food waste are, in order of decreasing practice, to dispose of them via landfills, animal feed, composting, and incineration (Lin *et al.*, 2013). To limit landfill growth, as well as to make use of an organic-rich carbon source, diverting food waste to composting and biological treatment is generally considered to be the most promising for the future (Hermann *et al.*, 2011). Biological treatment generally requires the separation of organic material from the rest of MSW via a waste management facility. The organic compounds that would need to be separated are called source-separated organics (SSO) and include materials such as food and yard waste, paper, diapers, and pet wastes (Levis *et al.*, 2010). For the most part, SSO can be degraded biologically through aerobic composting or anaerobic digestion.

The major aerobic composting methods are windrows, aerated static piles, the Gore Cover system, tunnel composting, and in-vessel composting (Diaz *et al.*, 2007; Haug, 1993). Windrow methods are those for which long parallel rows are constructed that contain a mixture of semi-solid non-hazardous sludge and nutritional amendment (Hay and Kuchenrither, 1990). The rows are then turned

frequently with the aid of machinery. Forced or natural ventilation may be used. Aerated static piles, where the waste is not manipulated during composting other than to provide air for circulation, require less energy but more time than windrows (Brodie *et al.*, 2000). The Gore Cover system is the same as an aerated static pile but includes a breathable expanded polytetrafluoroethylene fabric covering the composting pile that keeps odors from exiting but allows CO₂ to flow freely (Schmidt *et al.*, 2009). Tunnel composting systems are aerated containers that have air forced through the floor and internal air circulation (Partanen *et al.*, 2010). In-vessel composting is a static treatment in which the waste is placed in a rigid container (Mohee and Mudhoo, 2005). All of these methods use aerobic bacteria and fungi to degrade waste (Partanen *et al.*, 2010).

Although aerobic composting is relatively cheap and produces natural compost to be used as fertilizer or soil conditioner, there are a number of downsides. Chiefly reported are odor and air quality problems, as well as the release of nutrients into the environment and negative effects on water quality (Pell, 1997). Perhaps more importantly, there is little to no concomitant generation of fuel that could further offset the cost of composting and growth conditions are prime for the development of pathogenic contamination of the waste (Pell, 1997).

In contrast, anaerobic reactors can produce biogas (primarily H₂ or CH₄) as well as liquid biofuel (primarily ethanol or butanol), making them more cost-effective (Angenent *et al.*, 2004; Braber, 1995). Anaerobic digestors in one form or another have been used for the better part of a century because of their high organic removal rates, low energy-input requirements, energy production (in the form of

CH₄, H₂, or alcohols), and low sludge production (Angenet *et al.*, 2004). As discussed more in-depth below, anaerobic digestors can also operate at higher temperatures than aerobic digestors, decreasing the possibility of pathogen contamination in the environment.

The most common anaerobic reactors currently in place to treat food waste at an industrial level can be classified into different systems based on their feed's solids content, the number of stages, the operating temperature, and the method of introducing feed into the reactor (Rilling, 2005). Regardless of operational procedure, the industrial anaerobic fermentation process is generally divided into three steps: hydrolysis, acidification, and CH₄ formation. During hydrolysis, bioavailable polymers like carbohydrates, proteins, and fats are decomposed to smaller dimers and monomers (Rilling, 2005). This can be through the action of enzymes added abiotically or through the function of fungi or polymer-degrading fermenters (Rilling, 2005). During acidification, the substrates obtained from hydrolysis (chiefly, amino acids, glucose, and fatty acids) are broken down completely to H₂, CO₂, and acetate to be fed to methanogens in the CH₄ formation stage (Rilling, 2005).

Anaerobic digestion is beginning to be used in the U.S. to stabilize wastewater biosolids (e.g., the aqueous fraction of treated sewage sludge), but there are only a few pilot scale operations using food waste (Sakai *et al.*, 2011). Food waste treatment is more common in the E.U., where there are laws in place under the Waste Framework Directive that require member states to reduce the amount of organic waste entering landfills by 65% relative to 1995 levels by 2016 (European

Commission, 2009). Every year, the E.U. generates approximately 89 million tons of food waste (Monier *et al.*, 2010), but 41% of these wastes are recycled (Sakai *et al.*, 2011). Thus, the E.U. performs the second-most amount of food waste recycling in the world, next to South Korea, where almost half of all recycled material is organic waste (Sakai *et al.*, 2011).

Food waste is produced at every stage of processing, from farms and food processing facilities as pre-consumer waste to domestic waste (Lin *et al.*, 2013). Although the amount of waste for each sector is fairly evenly spread, waste produced by the agricultural and manufacturing sectors is generated in a more concentrated manner and would therefore be easier to collect, process, and treat to keep it from entering landfills and help offset the costs of the processing center. Therefore, recent developments in technology focus on food processing facilities.

1.2.2 Feasibility of Different Food Waste Types for Biofuel Production

The main factors that are used to determine whether a substrate can be utilized in waste treatment technology are availability, cost, carbohydrate content, and biodegradability (Kapdan and Kargi, 2006). Simple sugars such as glucose, sucrose, and lactose are preferred substrates for biofuel – especially biohydrogen – production because carbohydrates are the main substrates for fermenters (Kapdan and Kargi, 2006). Cellulose and hemicellulose are the most abundant polysaccharides in nature, with xylose and glucose being the predominant metabolites that are fermented (Kapdan and Kargi, 2006). However, pure compounds are relatively expensive while waste streams from food processing

plants offer a rich and inexpensive carbon source.

Some carbohydrate-rich, non-toxic effluents that have been examined for biohydrogen production are from the dairy industry, olive mill, baker's yeast, sugar refineries, tofu production, brewery wastewaters, mixed food waste, potato, apple, rice winery, molasses, domestic wastewater, and sweet potato (see Kapdan and Kargi, 2006 for a review). Hydrogen yields and production rates from these feedstocks have been determined, with H₂ yields as high as 2.7 H₂/glucose from sweet potato starch residue by *Clostridium butyricum* and *Enterobacter aerogenes* (Yoki *et al.*, 2002). Other wastes are protein-rich, such as slaughterhouse waste, but many regions have restrictions on meat entering food waste SSO biological treatment facilities (Levis *et al.*, 2010).

Depending on the waste source and the microbes producing biofuels from them, many of these wastes require pretreatment. The longest and most expensive part of the pretreatment of plant-based agricultural wastes is to grind, delignify and hydrolyze the (hemi)cellulose content of the waste (Kapdan and Kargi, 2006). Other forms of carbohydrate-rich food waste may also require pretreatment to remove undesirable components (e.g., antibiotics, hormones, pathogenic microorganisms) or to optimize the growth parameters for fermentative microorganisms, as discussed below (Kapdan and Kargi, 2006; Rilling, 2005).

Incomplete pretreatment, as well as differing chemical compositions of a given waste type (due to different nutrients / sources), frequently leads to variations in the composition of food waste. The greatest effected of these are the concentrations of carbohydrates and protein types available. Moreover, for

anaerobic bacteria, mixing waste types does not necessarily improve the H₂ production rate (Kim *et al.*, 2004). This variability frequently leads to metabolic shifts in the microorganisms in the acidification step of anaerobic digestion and differences in compound production and yield. This issue seems to arise in the acidification step in particular because the microorganisms are processing the large organic molecules of the waste into smaller organic molecules and hydrogen through fermentative shifts. Thus, it is imperative to understand the causes of these metabolic shifts and to try to optimize the biofuel production rate.

1.3 Biohydrogen: Potential and Production Capabilities

Biogases (and biofuel, if the gas is combustible) are generated when organic matter is anaerobically degraded by microbes (Rilling, 2005). In nature, biogas production is seen in marshlands, marine sediments, flooded rice fields, the rumen of various animals, and landfill sites (Rilling, 2005). Depending on the microorganism used, the biofuel produced from food waste could come in many forms, including CH₄, ethanol, butanol, and H₂. Alcohols, while easy additives to gasoline, are currently produced in extremely small quantities and offer lower potential combustive potential than CH₄ or H₂. Methane offers good combustive potential and is readily available through the methanogens present in many types of wastes. However, methanogens are extremely sensitive to O₂ and contamination by sulfur reducers, both of which lower CH₄ productivity at an industrial scale. Hydrogen, however, is not a greenhouse gas and its combustion generates no pollutants. Moreover, H₂ offers the highest potential energy yield.

1.3.1 Biohydrogen Production Processes

There are three main processes to produce biological H₂: 1) biophotolysis of water by algae, 2) dark-fermentative H₂ production during the acidogenic phase of anaerobic digestion of organic matter, and 3) two stage dark/photo-fermentation (Kapdan and Kargi, 2006). Algal H₂ production is often touted as an economical and sustainable method both because of its low water utilization per mole of H₂ produced and because of the CO₂ sequestration it allows (Prince and Kheshgi, 2005; Sakurai and Masukawa, 2007). However, this process does not use any waste stream and has low overall H₂ production potential compared to the other two methods (Hallenbeck and Ghosh, 2009; Prince and Kheshgi, 2005). This low potential is due to the fact that the algal H₂ production process simultaneously produces O₂, which destabilizes the algal hydrogenase (Ghiradi *et al.*, 2007; Tamagnini *et al.*, 2007). Thus, dark fermentative methods are considered to be more advantageous due to their simultaneous waste treatment and H₂ production.

There are a wide range of fermenting microorganisms that produce H₂ at around 1-1.2 mol H₂/mol glucose when cultures are grown anaerobically (see Kapdan and Kargi, 2006 for a review). Many of these are *Clostridia* species, because of their wide substrate utilization and compatibility with industrial methods (Kapdan and Kargi, 2006). The maximum possible H₂ yield obtained from traditional mesophilic fermenters on glucose under optimal conditions is around 2 H₂/glucose (Fang and Liu, 2002; Kumar and Das, 2000; Morimoto *et al.*, 2004; Ueno *et al.*, 2001). To date, *Enterobacter cloacae* IIT-BT08 produces the highest amount of H₂/glucose (2.2 H₂/glucose) by a mesophilic culture in batch dark fermentation

(Kumar and Das, 2000). Many researchers have shown that, even under optimal conditions, mesophiles could only ever produce 4 H₂/hexose (Verhaart *et al.*, 2010). This theoretical limit for mesophilic cultures, which is far below the possible 12 H₂/glucose, is due to a number of factors, chief among these being growth parameters. Perhaps the most relevant to this research is that H₂ yield is strongly determined by the thermodynamics of the metabolic reactions leading to its formation (Verhaart *et al.*, 2010). Under standard conditions (1 M reactants, 25°C, pH 7, 1 atm), the complete oxidation of glucose has a Gibb's energy of +3.2 kJ/mol. Therefore, ATP must be produced by the microorganism in order for it to be capable of glucose fermentation. To this end, most microorganisms utilize the Embden-Meyerhof pathway to yield 2 ATP/glucose. Having to produce additional energy by generating acetate is a major factor for lowering the potential H₂ yield from glucose (and other hexoses). Additionally, for the 4 H₂/glucose to be achieved by mesophiles, the H₂ partial pressure in the system must be kept low (less than 0.022 kPa) or H₂ formation is severely inhibited (Schink and Stams, 2006). This means that cultures must be degassed and mixed vigorously, which increases production costs. Moreover, the dark fermentative method requires strict monitoring of microbial growth conditions.

For most fermenters, medium pH affects biogas content, the type of organic acids produced, and both the specific H₂ production yield and rate. There are many studies looking into the optimal pH range for maximum H₂ yield and the specific H₂ production rate (see Kapdan and Kargi, 2006 for a review). Most of these studies indicate, despite the initial or optimal pH, in a closed environment (e.g. batch

system) the final pH in anaerobic bacterial H₂ production is around pH 4.0-4.8. This decrease in pH during fermentation is due to production of organic acids, which deplete the buffering capacity of the medium and result in a low final pH (Khanal *et al.*, 2004). As the pH decreases, H₂ production becomes inhibited because it affects the activity of the iron-containing hydrogenase enzyme (Dabrock *et al.*, 1992) (discussed in more detail below).

Other important considerations for dark fermentative H₂ production are composition of the waste substrate, media composition, temperature, and the type of microbial culture utilized (Hallenbeck, 2009; Kapdan and Kargi, 2006). Despite H₂ being the goal, most of these fermenters predominantly produce acetic, butyric, and propionic acids when grown on carbohydrate wastes (Kapdan and Kargi, 2006; Verhaart *et al.*, 2010). Other by-products, such as ethanol, lactic acid, and CH₄ can also be produced, all depending on the consortia and species present (Angenent *et al.*, 2004). The combination of nutrients required for fermenters (high iron concentrations for the hydrogenase enzymes, bioavailable nitrogen supplementation, reducing agents, an anaerobic atmosphere, and other additional nutritional supplements (e.g., yeast extract)) combine to increase the cost of dark fermentation and make H₂ gas production currently uneconomical in the short term (Kapdan and Kargi, 2006). A two-stage process could help to eliminate some of the downsides of each process individually.

The ideal microorganisms to participate in these processes are those that can breakdown a variety of large organic molecules, such as a long chain sugars or peptides, while generating some form of potential energy (e.g., H₂ or smaller

molecules ideal for later processes) (Alper and Stephanopoulos, 2009; Angenent *et al.*, 2004). These microorganisms should also be aerotolerant, genetically tractable, and not easily contaminated. There are a number of microorganisms that fit most of this description and are currently being studied for biofuel production, such as the *Enterobacter* and *Clostridia* spp. briefly discussed above (Antoni, 2007). Almost all of these microorganisms can catabolize glucose and many are fermenters (Antoni *et al.*, 2007; Hallenbeck, 2009).

1.4 Glycolysis, Respiration, and Fermentation

There are three major catabolic pathways that provide chemical precursors to other pathways for cellular metabolism: the Pentose-Phosphate Pathway, the Entner-Doudoroff pathway, and the Embden-Meyerhof-Parnas (glycolysis) pathway (White *et al.*, 2011). These pathways are markedly different and yet are similar in function. Namely, all three pathways convert glucose to glyceraldehyde-3-phosphate, and the second stage of each of the three pathways (wherein the glyceraldehyde-3-phosphate is oxidized to pyruvate) is identical. From an energetic point of view, the reactions that convert glyceraldehyde-3-phosphate to pyruvate are extremely important because they generate ATP from inorganic phosphate and ADP. The fate of the pyruvate that is formed during the catabolism of the carbohydrate depends on whether the cells are respiring or fermenting. We will focus on glycolysis since it is most similar to the species investigated in anaerobic food waste digestion and in this study, and it is more widespread than the Entner-Doudoroff Pathway and the Pentose-Phosphate Pathway.

1.4.1 The Embden-Meyerhof-Parnas Pathway

Glycolysis occurs in two stages (Figure 1.1). The first stage splits the glucose molecule (C_6) into two glyceraldehyde-3-phosphate (C_3) molecules. This occurs in four steps and consumes two ATPs per glucose. The pathway begins with the phosphorylation of glucose by hexokinase to form glucose-6-phosphate. Glucose-6-phosphate is isomerized by an isomerase to fructose-6-phosphate. Fructose-6-phosphate is phosphorylated at the expense of ATP by fructose-6-phosphate kinase to fructose-1,6-bisphosphate. The fructose-1,6-bisphosphate is cleaved into glyceraldehyde-3-phosphate and dihydroxyacetone phosphate by fructose-1,6-bisphosphate adolase. The dihydroxyacetone phosphate is then isomerized to the second glyceraldehyde-3-phosphate (White *et al.*, 2011).

The second stage catalyzes the oxidation of glyceraldehyde-3-phosphate to pyruvate. It occurs in five steps and generates two ATPs per glyceraldehyde-3-phosphate. Therefore, there is a net gain of two ATP from each glucose molecule catabolized. Each glyceraldehyde-3-phosphate is oxidized to 1,3-bisphosphoglycerate with two electrons passed to NAD^+ to form $NADH + H^+$. The 1,3-bisphosphoglycerate is the phosphoryl donor for a substrate-level phosphorylation step catalyzed by 3-phosphoglycerate kinase to form 3-phosphoglycerate. 3-phosphoglycerate is converted into 2-phosphoglycerate by phosphoglycerate mutase, which is then dehydrated by enolase to form phosphoenolpyruvate. Phosphoenolpyruvate is the phosphoryl donor for the second substrate-level phosphorylation step by pyruvate kinase to form ATP and pyruvate (White *et al.*, 2011).

Figure 1.1: Embden-Meyerhof-Parnas Pathway

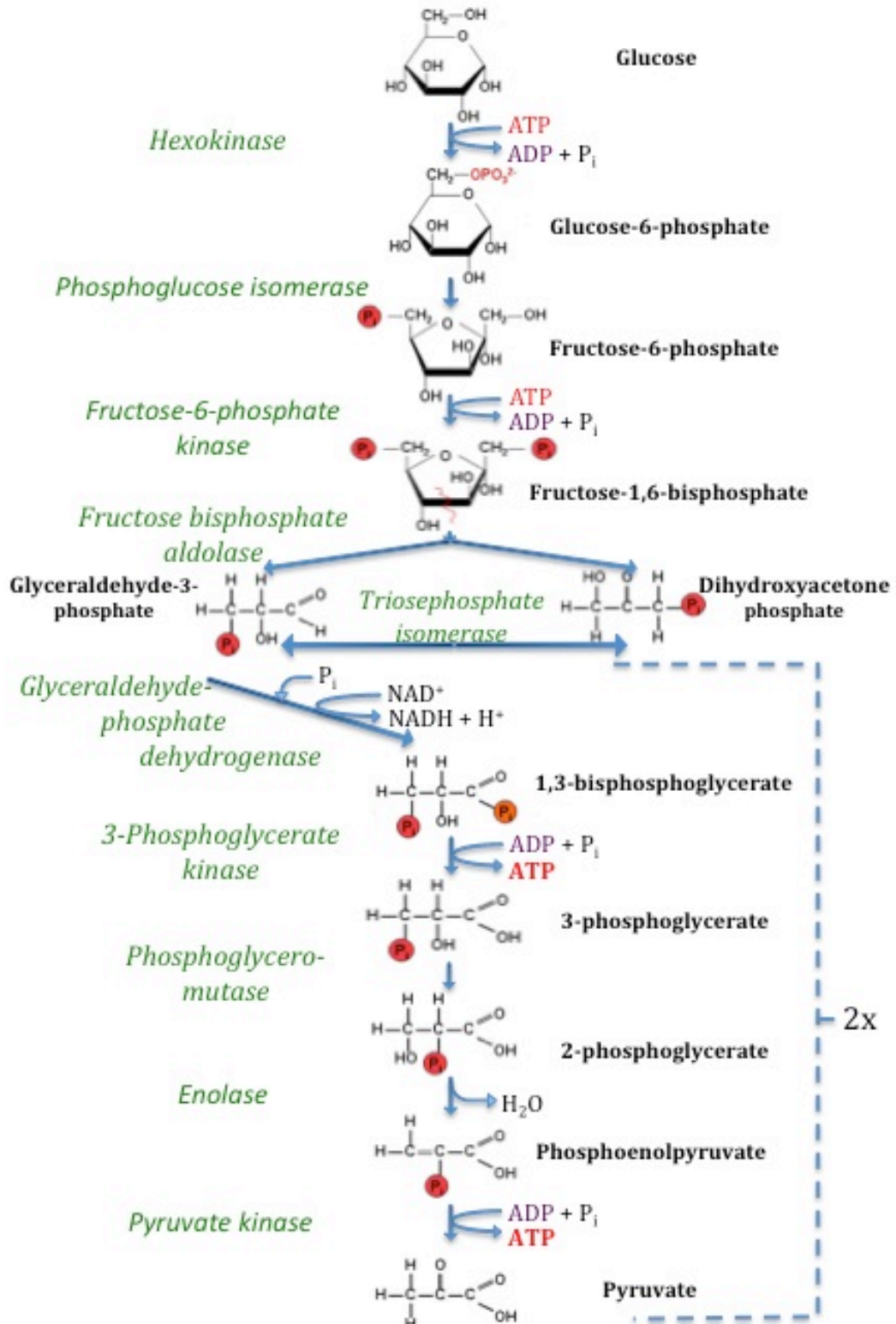


Figure 1.1. Adapted from White *et al.* (2011). Enzymes are italicized and in green.

In addition to generating pyruvate, which is vital for various cellular processes, glycolysis is important for the generation of reduction potential in the form of reduced electron carriers (e.g., NADH). In respiring organisms, this reduction potential is used to form an electrochemical gradient across the cytoplasmic membrane that is then used to drive ATP synthesis by oxidative phosphorylation (see below). In fermenting organisms, this reduction potential is used to reduce an intracellular metabolic intermediate for the purpose of regenerating NAD⁺ for further catabolism.

1.4.2 Fermentative Mechanisms

In fermenting cells, reduced electron carriers are reoxidized in the cytoplasm by an endogenous electron acceptor, but ATP is not made in the reaction. Instead, ATP is formed separately through substrate-level phosphorylation. There are several fermentative pathways that are named for their end products (e.g., ethanol, lactic acid, propionic acid, butyric acid, mixed acid). Some fermenters possess what some researchers call a 'fermentative ion pump mechanism' (Skulachev, 1989). It is similar to oxidative phosphorylation in that membrane-bound enzymes establish an ion gradient to produce ATP. It differs from oxidative phosphorylation in that it does not involve a membrane electron transport chain. Instead, membrane-bound redox reactions (e.g., hydrogenase, RNF complex) are linked to ion translocation across the membrane to establish an ion gradient across the membrane. ATP synthesis is then linked to a membrane-bound ion-translocating ATP synthetase. This allows

microorganisms to grow in an environment that otherwise would not support growth.

1.5 Acetogens and Fermentation Balance

1.5.1 Acetic Acid Production

The most thoroughly studied fermentation pathway, especially for mesophiles, is acetate production by acetogens via the Wood-Ljungdahl Pathway (Drake *et al.*, 2008). Acetate production is favorable because it leads to ATP production by substrate-level phosphorylation by phosphotransacetylase and acetate kinase. Acetogens are phylogenetically diverse anaerobes that display at least one of the following characteristics: chemolithoautotrophic growth using H₂ and CO₂, conversion of sugar to acetate, and use of aromatic compounds (Drake, 1994; Drake *et al.*, 2008). Technically, while any organism that produces acetic acid is an acetogen, the term only applies to those organisms that use the Wood-Ljungdahl pathway (Drake, 1994; Drake *et al.*, 2008).

The Wood-Ljungdahl pathway, also known as the acetyl-CoA pathway, functions in three main capacities for acetogens: as a terminal electron accepting process, as a means of energy conservation, and as a mechanism for the autotrophic assimilation of carbon (Drake, 1994). In this pathway, two molecules of CO₂ are reduced to acetate, one forms the methyl group of acetate; the other, the carboxyl group (Figure 1.2). While the pathway does not yield any net energy from substrate-level phosphorylation (one ATP is produced when acetyl-phosphate is converted to acetate, but another ATP is used to link formate with tetrahydrofolate), energy

Figure 1.2: Acetate Production Via the Wood-Ljungdahl Pathway

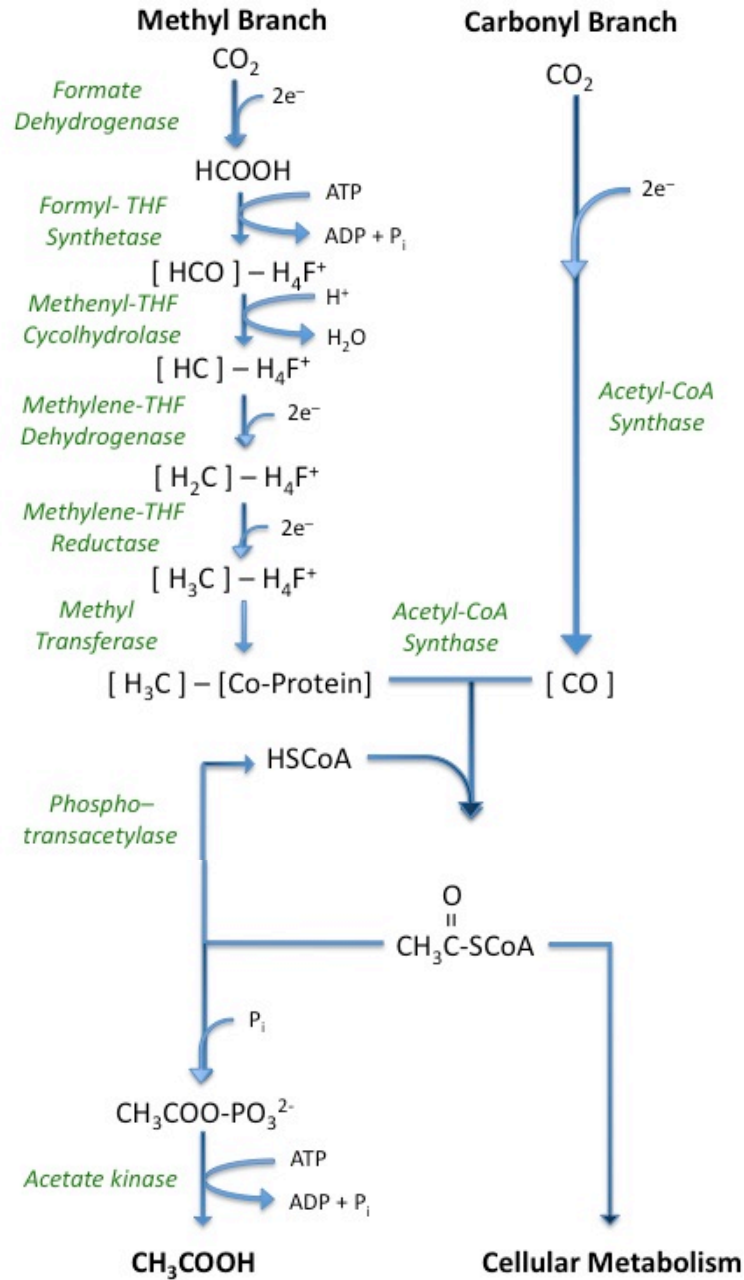


Figure 1.2. The acetyl-CoA pathway from *Moorella thermoacetica* (adapted from Drake *et al.*, 2008). Enzymes are italicized and in green.

conservation is achieved through the formation of a H⁺ or Na⁺ gradient across the cell membrane. Acetogens that form a proton gradient use electron carriers such as menaquinone and cytochromes (Drake, 1994). Some acetogens, such as *Acetobacterium woodii*, use the Wood-Ljungdahl pathway to create a sodium gradient (Müller *et al.*, 1990). This gradient is then used by a Na⁺-translocating F₁ F₀ ATP synthase to generate energy (Müller *et al.*, 2008).

1.5.2 Acetogenic Metabolite Switching

Acetogens produce several different end products depending on the specific organism. These include acids (acetate, butyrate, and in some cases, small amounts of lactate and acetoin) (Drake *et al.*, 2008; Rogers *et al.*, 2013), solvents (ethanol, butanol, acetone and 2-propanol) (Dürre, 2008; Lee *et al.*, 2008b) and fine chemicals (cysteine, corrinoids) (Koesnandar *et al.*, 1991a; Koesnandar *et al.*, 1991b). Most acetogens are capable of producing an acid and at least one solvent (Figure 1.3) (Drake, 1994). Variation in compound production is due to metabolic shifts during growth that are induced by environmental cues (Bahl *et al.*, 1986; Drake, 1994; Drake *et al.*, 2008; Wong and Bennett, 1996; Woods, 1993). These cues include a decrease in pH, excess fatty acid, excess CO or H₂ gas, and addition of electron shuttles, such as methyl viologen (Kim *et al.*, 1988; Woods, 1993). These changes cause acetogens to switch from acidogenesis to solventogenesis (Figure 1.3). Acetogens produce primarily fatty acids during exponential growth (Andersch *et al.*, 1983; Hartmanis and Gatenbeck, 1984). Solvent production occurs in stationary phase and allows the cell to survive for sporulation to occur (Dürre, 2005).

Figure 1.3: Metabolite Switching Between Acidogenic and Solventogenic Phases in *C. acetobutylicum*

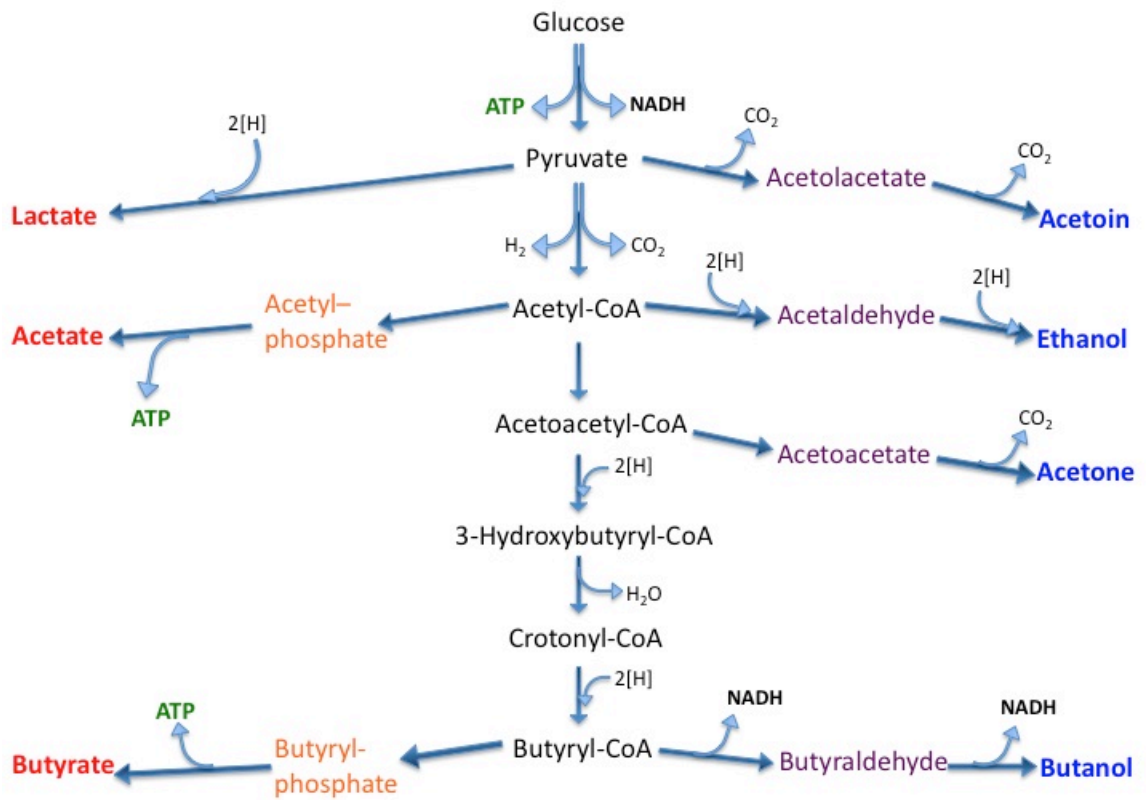


Figure 1.3. The flow of carbon and electrons toward acidogenic (left) or solventogenic (right) phases in *Clostridium acetobutylicum* (adapted from Dürre, 2008). The most common acid products are in red and the most common solvent products are in blue.

Solventogenesis coincides with a change in gene expression with Spo0A acting as the transcriptional regulator (Alsaker *et al.*, 2004; Dürre *et al.*, 1987; Dürre, 2005; Ullmann and Dürre, 1998). For example, a decrease in pH causes an undissociated acid (i.e. an acid molecule that is associated with a proton or salt ion) to diffuse across the cell membrane into the more alkaline cytoplasm where it dissociates again into salts and protons (Woods, 1993). The net increase of protons in the cytoplasm dissipates the chemiosmotic potential that the cell uses for energy conservation (Woods, 1993). In response, the cell reincorporates the acids to produce aldehyde compounds, which are then converted to solvents (Woods, 1993). The partial pressure of H₂ is another regulator of the switch between acidogenesis and solventogenesis.

1.5.3 Hydrogenases: Vital for Hydrogen Metabolism

The oxidation of H₂ is catalyzed by hydrogenases. *In vitro*, the reaction is reversible, but *in vivo* the reaction occurs primarily in one direction (Vignais *et al.*, 2001). H₂ uptake is coupled to the reduction of electron acceptors, while H₂ production occurs by proton reduction coupled to the oxidation of electron carriers.

The metal content of the catalytic center of hydrogenases is used for enzymatic classification (Eberly and Ely, 2008; Hedderich and Forzi, 2005; Heinekey, 2009; Jenney and Adams, 2008). The two main types of hydrogenases are the [Fe-Fe] hydrogenases (Meyer, 2007) and [Ni-Fe] hydrogenases (Casalot and Rousset, 2001; Frey, 1998). There are a number of alternative hydrogenases recently discovered, which will be covered more in-depth below. The [Ni-Fe]-

hydrogenases are widespread throughout the Bacteria and the Archaea, but are not found in the Eukarya. The range of [Fe-Fe]-hydrogenases is narrow since only a few anaerobic bacteria and eukaryotes possess them and they are absent from archaea (Meyer, 2007; Pütz *et al.*, 2006; Vignais *et al.*, 2001). There is no sequence similarity in the catalytic subunits of [Fe-Fe] hydrogenases and [Ni-Fe] hydrogenases. [Fe-Fe] hydrogenases function primarily to reduce protons to H₂ (Adams, 1990; Nicolet *et al.*, 2002; Vignais *et al.*, 2001) while the function of the [Ni-Fe]-hydrogenases varies depending on their class.

There are four classes of [Ni-Fe] hydrogenases that are differentiated by the subunits that contain Fe-S clusters and transfer electrons to and from the catalytic [Ni-Fe] center (Shima and Thauer, 2007). Class I [Ni-Fe] hydrogenases are respiratory enzymes that couple the oxidation of H₂ to the reduction of a terminal electron acceptor (Vignais and Colbeau, 2004). Class II [Ni-Fe] hydrogenases are H₂ sensors (Gebler *et al.*, 2007), while Class III hydrogenases are cytoplasmic enzymes. The cytoplasmic [Ni-Fe]-hydrogenases are only capable of H₂ oxidation and are found in archaea (Ma and Adams, 2001a) and bacteria (Viganis and Colbeau, 2004). Class IV [Ni-Fe] hydrogenases are membrane-bound and are found across bacteria and archaea (Mnatsakanyan *et al.*, 2004; Sapro *et al.*, 2003).

1.5.4 Potential for Hydrogen Production

Hydrogen production by acetogens and other fermentative bacteria is used as an electron sink. While the theoretical maximum for H₂ production from 1 mole of glucose is 12 moles of H₂, the actual maximum is 4 moles of H₂ per glucose due to

the need for concomitant acetate and ATP production (Verhaart *et al.*, 2010). Under standard conditions (1 M reactants, 25°C, pH 7.0, 1 atm), the complete oxidation of glucose to CO₂ and H₂ has a Gibbs energy (ΔG°) of +3.2 kJ/mol. This means the reaction cannot proceed without the input of extra energy. To this end, acetogens obtain two ATP/glucose from the Embden-Meyerhof pathway, and then produce two additional ATP/glucose by acetate kinase. Energy production by generating acetate thus lowers the potential H₂ yield from glucose (and other hexoses). Furthermore, in order for the 4 H₂/glucose to be achieved by mesophiles, the H₂ partial pressure must be kept low (< 0.022 kPa) or else H₂ formation is inhibited (Schink and Stams, 2006).

Regardless of their type, hydrogenases use different electron carriers as electron donors. Under standard conditions, the mid-point redox potential of the H⁺/H₂ couple is -414 mV while the mid-point redox potentials of the two most common electron carrier pairs are -320 mV for NAD⁺/NADH and -398 mV for ferredoxin (Fd_{ox}/Fd_{red}) (Thauer *et al.*, 1977). Thus, while the use of ferredoxin is more energetically favorable, the formation of other end products like ethanol and lactate is more feasible thermodynamically. Indeed, in mesophilic fermenters, H₂ is only produced as a last resort electron sink.

While acetogens are well studied and offer a good starting point for biohydrogen production, there are a number of issues with their practical application in an industrial setting. The majority of acetogens that have been studied are mesophiles, which are easily outcompeted by contaminants in high-carbon environments. This leads to the frequent shut down of fermentors to clean the

equipment or replace the cultures, which in turn leads to inefficiency and cost increases (Blumer-Schuetz *et al.*, 2008). Currently, to cut down on contamination, the waste stream is heat-treated, sometimes multiple times.

1.6 Biohydrogen and Biofuel Production by Thermophiles and Hyperthermophiles

Thermophiles are those microorganisms with an optimal growth temperature between 45°C and 80°C and have been widely investigated for H₂ production for multiple reasons (see Pawar and van Niel, 2013 for a review). First, increasing the growth temperature lowers the Gibbs energy (Stams, 1994) thus allowing for faster metabolic turnover and growth (Tijhuis *et al.*, 1993). If this effect is combined with a low H₂ partial pressure, then ambient H₂ concentrations need to be 10³-fold higher to inhibit H₂ formation at thermophilic temperatures relative to mesophilic temperatures (Verhaart *et al.*, 2010). Furthermore, increased temperatures make it more likely for H₂ production from NADH by reversed electron transport (Boiangiu *et al.*, 2005). Finally, the energetically more favorable oxidation of ferredoxin can be used to push the less favorable production of NADH because of the higher temperatures (Boiangiu *et al.*, 2005).

1.6.1 Benefits and Limitations of Thermophilic Biohydrogen Production

The use of ferredoxin in place of NADH combined with higher H₂ production rates are the primary reasons why thermophilic mixed cultures have already been shown to produce nearly 4 H₂/glucose, doubling the H₂ production efficiency of mesophiles (Ibrahim *et al.*, 2013; Verhaart *et al.*, 2010). Using thermophilic

organisms for food waste degradation results in a higher H₂ production potential and specific H₂ production rates (Shin *et al.*, 2004). Recent technological advances allow heat recovery in the fermentation step such that the additional heat demand required in thermophilic fermentation does not incur significantly higher costs when compared to mesophilic fermentation (Ljunggren and Zacchi, 2010; Pawar and van Niel, 2013).

There are still several limits to the use of thermophiles. In order for any biohydrogen production to be economically feasible, H₂ yields should surpass the theoretical limit of 4 H₂/glucose (Hallenbeck and Ghosh, 2009). H₂ production from pure culture thermophiles has approached – but not exceeded – this limit at 3.8 mol/glucose that was produced independently by *Caldicellulosiruptor sacchrolyticus* on wheat straw (Ivanova *et al.*, 2009) and *P. furiosus* on cellulobiose (Chou *et al.*, 2007). To further optimize H₂ production from thermophiles, several strategies must be examined for increased H₂ yield (mol/hexose), hydrogen production rate (volumetric productivity in mmol L⁻¹ h⁻¹), and specific production rate (mmol gCDW⁻¹ h⁻¹). Experimental and reactor design can help to increase these values to some extent (Hallenbeck, 2009; Nath and Das, 2004; Wang and Wan, 2009). Thermophilic consortia may also be useful in place of pure cultures (Bagi *et al.*, 2007; Brenner *et al.*, 2008; Zeidan and Van Niel, 2009). Indeed, mixed thermophilic cultures have achieved as much as 4.85 mol H₂/glucose (Ibrahim *et al.*, 2013). However, these mixed cultures often are not optimized for H₂ yield on a particular substrate and up to 43% of H₂ produced can be consumed by homoacetogenic processes (Saady, 2013). Therefore, with the right starting cultures and further optimizations, the H₂

yield may be even higher.

Another factor inhibiting the use of thermophiles is the cost of feedstock for growth media remains inhibitory in part because yeast extract and semi-refined sugars are required for growth (Ljunggren and Zacchi, 2010; Pawar and van Niel, 2013). Cell lysis also tends to occur when substrate concentrations are too high (Ljunggren *et al.*, 2011a; Ljunggren *et al.*, 2011b). Thus, low substrate concentrations in the medium require larger reactors along with larger facility and consequently will demand more water and energy. The use of microorganisms that can grow at temperatures higher than those of thermophiles may alleviate some of these issues.

1.6.2 Hyperthermophiles

Hyperthermophiles are those microorganisms whose optimal growth temperatures exceed 80°C and possess several potential benefits for industrial uses (Stetter, 1996; Stetter, 2003). For example, the heat-treatment step in a waste treatment plant can be consolidated with the growth step of hyperthermophiles thereby decreasing costs while removing pathogens and breaking down wastes (Angenent *et al.*, 2004; Bertoldo and Antrankikian, 2011; Blumer-Schuetz *et al.*, 2008; Bougrier *et al.*, 2008; Girguis and Holden, 2012; Wiegel *et al.*, 1985). If hyperthermophiles were used for agricultural waste treatment, then this would drastically cut down on contamination issues, since the extreme reactor conditions would limit the possible microorganisms capable of contaminating the reactor (Abe and Horikoshi, 2001; Blumer-Schuetz *et al.*, 2008; Wiegel *et al.*, 1985). Also,

operating at hyperthermophilic temperatures means the viscosity of the waste is lowered and there is no need for a reactor cooling step (Wiegel *et al.*, 1985). Moreover, hyperthermophiles have faster metabolisms than thermophiles (Tijhuis *et al.*, 1993) thus increasing the amount of waste remediated and biofuel produced per unit of time. Finally, the constraints on waste concentration with thermophiles due to osmolarity issues may not necessarily apply across all clades of hyperthermophiles because of differing cell wall composition and salinity tolerances.

1.6.3 Hyperthermophile Hydrogen Production Models

Hyperthermophiles are found in both the Bacteria and the Archaea, although archaeal hyperthermophiles are far more diverse. There are four main hyperthermophilic or extremely thermophilic (optimal temperatures 65-80°C) model organisms: the bacteria *Caldicellulosiruptor saccharolyticus*, *Thermoanaerobacter tengcongensis*, and *Thermotoga maritima*, and the archaeon *Pyrococcus furiosus* (Verhaart *et al.*, 2010). All of these organisms use carbohydrates for growth, and all but *T. tengcongensis* possess a wide variety of hydrolases and transferases (Vanfossen *et al.*, 2008). Although each organism produces H₂, they possess different pathways for sugar catabolism. *C. saccharolyticus* and *T. tengcongensis* both use the Embden-Meyerhof pathway and generate NADH as the primary reducing equivalents to produce H₂. Both species lack the NADH:ferredoxin oxidoreductase genes found in mesophiles (Boiangiu *et al.*, 2005; Van de Werken *et al.*, 2008) and instead possess an NADH-dependent hydrogenase that produces H₂

only at low H₂ partial pressures (Soboh *et al.*, 2004). As a result, *C. saccharolyticus* uses NADH to produce lactate and *T. tengcongensis* uses NADH to produce mainly ethanol (Soboh *et al.*, 2004).

Hydrogen production in *T. maritima* also generates reducing equivalents by the Embden-Meyerhof pathway, but the way reducing equivalents are recycled differs. It possesses a trimeric Fe-only hydrogenase that uses both NADH and ferredoxin in a 1:1 ratio to produce H₂ (Schut and Adams, 2009). It does this by using the exergonic oxidation of ferredoxin to drive the unfavorable oxidation of NADH and maintains a ratio of 1:1 NADH:Fd via an Fd:NADH oxidoreductase (Schut and Adams, 2009). In the case of higher H₂ partial pressures, *T. maritima* switches to lactate production, although the function of the NADH:Fd bifurcating hydrogenase does not cease (Huber *et al.*, 1986). *T. maritima* also possesses the ferredoxin-dependent hydrogenase that is responsible for hydrogen production by *P. furiosus* (*mbh* operon; 13 genes) (Huber *et al.*, 1986; Silva *et al.*, 2000). *P. furiosus* is a representative member of the Thermococcales.

1.7 Introduction to the Thermococcales

The Thermococcales are a large order within the Euryarchaeota branch of the Archaea. It is composed of the genera *Thermococcus* (Achenbach-Richter *et al.*, 1988), *Pyrococcus* (Fiala and Stetter, 1986), and *Palaeococcus* (Takai *et al.*, 2000). All known Thermococcales species are slightly irregular spherical cells (0.5-2.5 μm) with flagella (Bertoldo and Antranikian, 2006). Most Thermococcales species are

obligate anaerobic organotrophic hyperthermophiles that either require or are stimulated by elemental sulfur for growth (Bertoldo and Antranikian, 2006).

Of the Thermococcales, species of the genus *Thermococcus* are the most widespread, having been isolated from terrestrial freshwater systems to offshore oil wells and deep-sea hydrothermal vents (Bertoldo and Antranikian, 2006). The genus *Thermococcus* is fairly large with over 30 isolates and is composed of obligate anaerobes that have optimal growth temperatures of 80-90°C and whose doubling times are 30-90 minutes (Bertoldo and Antranikian, 2006). *Thermococcus* species couple the oxidation of peptides and polysaccharides to the reduction of elemental sulfur (S⁰) and protons, although protein-based substrates are generally preferred for growth (Bertoldo and Antranikian, 2006). Representative of its genus, *Thermococcus* sp. ES1 has a salinity tolerance of 0.96-6.46% total salt (Bertoldo and Antranikian, 2006). *Thermococcus* and *Pyrococcus* species are the best studied of the Thermococcales, with many of their enzymes being investigated for PCR and industrial applications (Bertoldo and Antranikian, 2006).

Pyrococcus species are thus far only isolated from marine environments and are all associated with the hydrothermal vent environment (Bertoldo and Antranikian, 2006). With both higher ranges of growth (70-105°C) and optimal growth temperatures (circa 100°C) than *Thermococcus*, *Pyrococcus* species tend to prefer more complex organic substrates (Bertoldo and Antranikian, 2006). Representative of its genus, *P. furiosus* has a salinity tolerance of 0.5-5.0% total salt (Bertoldo and Antranikian, 2006).

Based on 16S sequence, it is believed that *Palaeococcus* is the oldest lineage of the Thermococcales and diverged prior to the formation of the *Thermococcus* and *Pyrococcus* genera (Takai *et al.*, 2000). It is also the smallest genera of the Thermococcales. *P. ferrophilus* (Takai *et al.*, 2000), *P. pacificus* (Zeng *et al.*, 2013), and *P. helgesonii* (Amend *et al.*, 2003) are currently the only identified species. All *Palaeococcus* species are barophilic (optimum 30MPa) and have temperature optima closer to that of *Thermococcus* species (80-83°C). The presence of sulfur is required for growth.

The complete genomes of several Thermococcales species have been determined. Among the *Pyrococcus* spp., these include *P. furiosus* (Robb *et al.*, 2001), *P. abyssi* (Cohen *et al.*, 2003), *P. horikoshii* (Kawarabayasi *et al.*, 1998), *P. yayanosii* (Jun *et al.*, 2011), *Pyrococcus* sp. NA2 (Lee *et al.*, 2011), and *Pyrococcus* sp. ST04 (Jung *et al.*, 2012b). Among the *Thermococcus* spp., these include *T. kodakarensis* (Fukui *et al.*, 2005), *T. barophilus* (Vannier *et al.*, 2011), *T. gammatolerans* (Zivanovic *et al.*, 2009), *T. onnurineaus* (Lee *et al.*, 2008a), *T. sibiricus* (Mardanov *et al.*, 2009), *Thermococcus* sp. 4557 (Wang *et al.*, 2011), and *Thermococcus* sp. CL1 (Jung *et al.*, 2012a). As part of this dissertation, an additional *Thermococcus* complete genome sequence was determined for *T. paralvinellae* (Jung *et al.*, 2014). All of these genomes consist of a single circular chromosome 1.72-2.09 MB in length.

Although most Thermococcales require sulfur for growth, the species used in this study do not have this requirement. Some Thermococcales are capable of producing noticeable amounts of H₂ in the absence of sulfur (Bertoldo and Antranikian, 2006; Osowski *et al.*, 2011). *P. furiosus* is the best studied of the

Thermococcales and is one of the model organisms used in the dissertation. It does not require sulfur for growth and produces H₂ from a wide variety of substrates (Adams *et al.*, 2001; Fiala and Stetter, 1986). It possesses various sugar and peptide hydrolases and transferases enabling it to grow on several types of feedstock (Vanfossen *et al.*, 2008). It is aerotolerant enough to be used in large-scale industry, as shown by its current use in the desulfurization of tire rubber (Bredberg *et al.*, 2001). Moreover, a genetic system recently became available for *P. furiosus* (Basen *et al.*, 2012; Lipscomb *et al.*, 2011). A survey of 19 *Pyrococcus* and *Thermococcus* spp. in the Holden lab culture collection identified two *Thermococcus* strains (CL1 and ES1, renamed *T. cleftensis* and *T. paralvinellae* respectively) that produce a large proportion of H₂ even when grown with sulfur (Oslowski *et al.*, 2011). These strains were included as model organisms in this dissertation.

1.8 Metabolism in the Thermococcales

1.8.1 Modifications to the Embden-Meyerhof-Parnas Pathway

P. furiosus and other members of the Thermococcales differ from the other three model organisms mentioned above in that they possess a modified Embden-Meyerhof pathway (Kengen and Stams, 1994; Verhees *et al.*, 2003). First, the hexokinase and fructose-6-phosphate kinase steps in the pathway are ADP dependent instead of ATP dependent (Figure 1.4). Second, the glyceraldehyde-3-phosphate dehydrogenase and phosphoglycerate kinase steps are replaced by glyceraldehyde-3-phosphate:ferredoxin oxidoreductase. This replacement means that the oxidation of glyceraldehyde-3-phosphate uses ferredoxin instead of NAD⁺

Figure 1.4: Modified Embden–Meyerhof Pathway Present in *P. furiosus*

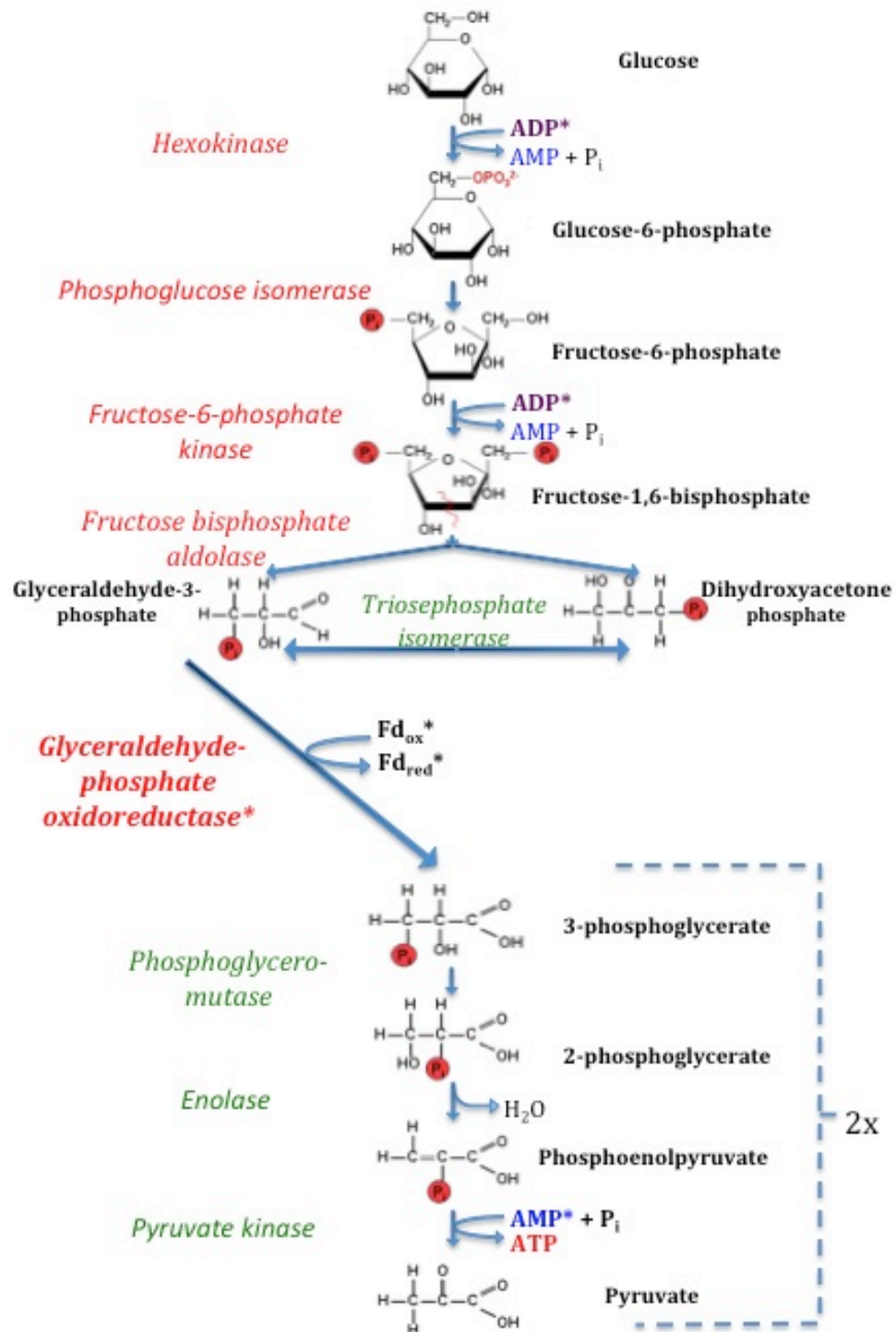


Figure 1.4. Adapted from (Kengen, 1994) and (Sato and Atomi, 2011). Enzymes are italicized and in green or red (if the enzyme sequence is unique to archaea). * denotes modifications from the traditional Embden-Meyerhof pathway. F_{d_{ox}} is oxidized ferredoxin and F_{d_{red}} is reduced ferredoxin.

as the electron acceptor, is no longer P_i -dependent, and does not involve the intermediate 1,3-bisphosphoglycerate (Kengen *et al.*, 1996). However, this also means that ATP is not formed by substrate-level phosphorylation by the phosphoglycerate kinase (Kengen *et al.*, 1996). Thus, there is no net gain of ATP during glycolysis in *P. furiosus* and the organism must gain additional ATP through other means.

1.8.2 Hydrogen Production by *P. furiosus*

Pyruvate oxidation to acetyl-CoA and CO_2 in *P. furiosus* is catalyzed by pyruvate:ferredoxin oxidoreductase, leading to the production of additional reduced ferredoxin. As a result, *P. furiosus* generates 8 moles of reduced ferredoxin per mole of glucose instead of the 4 moles of reduced ferredoxin and two moles of NADH per mole of glucose often found in fermentative bacteria. *P. furiosus* has a membrane-bound hydrogenase complex that accepts electrons from ferredoxin directly (Sapra *et al.*, 2000) and has a high H_2 production activity relative to other hydrogenases. This transmembrane hydrogenase complex also functions as a proton pump to generate a proton motive force, which drives ATP synthesis via oxidative phosphorylation (Sapra *et al.*, 2003).

In addition to the membrane-bound, ferredoxin-dependent hydrogenase, *P. furiosus* also has two cytoplasmic hydrogenases that use NAD(P)H as the electron donor and catalyze the NADH-dependent reduction of elemental sulfur to H_2S . However, these hydrogenases are not thought to be key for energy generation since they cannot use reduced ferredoxin and their activities in the cell are low. When H_2

partial pressure is high, *P. furiosus* can use a NAD(P)H:ferredoxin oxidoreductase to transfer electrons from NADH to ferredoxin or polysulfide. All of these mechanisms combine to make *P. furiosus* the most consistent hyperthermophilic producer of high H₂ yield across waste types (2.6-3.8 H₂/glucose) (Kengen and Stams, 1994; Chou *et al.*, 2007). This high H₂ yield may extend across other members of the Thermococcales, since a number of alternative hydrogenases have been discovered recently.

1.8.3 Alternative Hydrogenases in the Thermococcales

Originally studied in *T. onnurineus* NA1, some members of the Thermococcales family possess alternative hydrogenases to the canonical *Mbh* complex of *P. furiosus*. Several *Thermococcus* species are capable of oxidizing formate with the concomitant production of H₂ to support growth (Kim *et al.*, 2010). This growth is dependent on formate:H₂ lyase systems that are composed of formate dehydrogenase genes (*fdh*) clustered with membrane-associated hydrogenase genes (either *mfh*, *mnh*, *sulf*), which can then be coupled to ATP generation (Kim *et al.*, 2010). These membrane hydrogenases are members of the Hyg4-I and Hyg4-III clusters (Kim *et al.*, 2010) and most are organized into the first tripartite gene cluster known in members of the Thermococcales (Lim *et al.*, 2010). Specifically, the gene clusters are arranged such that the first gene encodes an oxidoreductase, the second a multimeric membrane-bound hydrogenase and the third a cation/anion antiporter (Lim *et al.*, 2010). *T. onnurineus* contains several distinct clusters of these genes and has been shown to grow on formate, as has *T.*

gammatolerans, *T. barophilus*, and *Thermococcus* sp. DT-4 (Kim *et al.*, 2010). Other *Thermococcus* species thus far have been shown to either not possess these genes or be incapable of growth on formate (Kim *et al.*, 2010). In this thesis, we shown that a close relative of *T. barophilus*, *T. paralvinellae* also possesses these genes.

Additionally, some *Thermococcus* strains (namely, *T. onnurineus* NA1 and *T. gammatolerans*) are the only known microorganisms aside from methanogenic archaea to possess the F₄₂₀-reducing hydrogenase, a Hyg4-III hydrogenase (Lee *et al.*, 2008a; Zivanovic *et al.* 2009). Although further study is required, it has been proposed that, in *Thermococcus* species, these genes may be essential to maintain redox balance during one-carbon substrate growth (Moon *et al.*, 2012).

In depth examination of *T. onnurineus* also revealed growth on CO and electron balance via H₂ production through a number of CO dehydrogenases (*cooS* and the ferredoxin-like *cooF*) and CO-induced hydrogenase clusters, together known as Coo-type hydrogenases (Moon *et al.*, 2012). These are the first known Coo-type hydrogenases in archaea (Lim *et al.*, 2010), belong to the Hyg4-II cluster (Moon *et al.*, 2012), and are distinguished from mesophilic or thermophilic bacteria by the presence of a Na⁺/H⁺ antiporter (Kim *et al.*, 2013). *Thermococcus* strain AM4 has also been shown to grow on CO (Sokolova *et al.*, 2004) and, based on genome sequence, it is believed that *T. barophilus* should also possess this capability (Lim *et al.*, 2010).

The presence of many types of hydrogenases allows *T. onnurineus* NA1, as well as potentially other *Thermococcus* species, to produce relatively high amounts of H₂ from a diversity of compounds. Moreover, when genetically engineered to be

under a strong promoter, *T. onnurineus* NA1 was capable of the highest H₂ production rate among CO-dependent H₂-producing prokaryotes by an order of magnitude (123.5 mmol liter⁻¹ hr⁻¹) (Kim *et al.*, 2013). Thus, the possible waste streams which *Thermococcus* species can use to produce high amounts of biohydrogen include a wide range of substrates. However, the environmental cues that allow this H₂ production are not well understood.

1.8.4 Metabolite Switching by *P. furiosus* in the Absence of Sulfur

In the presence of sulfur, *P. furiosus* produces H₂S instead of H₂ (Fiala and Stetter, 1986). Metabolite switching in *P. furiosus* has mostly been examined through comparing the physiology of the cell in the presence and absence of sulfur (Adams *et al.*, 2001; Chou *et al.*, 2007; Ma *et al.*, 1994; Ma *et al.*, 1995; Schut *et al.*, 2003). Both cytoplasmic and membrane hydrogenase activities increase in *P. furiosus* in the absence of sulfur (Adams *et al.*, 2001). Typically, *P. furiosus* produces acetate (or some other fatty acid), H₂ and CO₂ as metabolic end products in the absence of sulfur (Kengen and Stams, 1994; Verhees *et al.*, 2003). Pyruvate:ferredoxin oxidoreductase and acetyl-CoA synthetase (*in lieu* of phosphotransacetylase and acetate kinase) convert pyruvate from glycolysis first to acetyl-CoA and CO₂ and passes electrons to ferredoxin, then the acetyl-CoA is converted to acetate with concomitant ATP production (Mai and Adams, 1996). However, *P. furiosus* can also dispose of electrons by converting pyruvate to alanine by alanine aminotransferase, which requires NADH for the glutamate dehydrogenase and the amination step (Ward *et al.*, 2000).

Theoretically, formaldehyde:ferredoxin oxidoreductase and aldehyde:ferredoxin oxidoreductases in *P. furiosus* could reduce acetate to acetaldehyde, and then this acetaldehyde could be further reduced to ethanol as another mechanism for electron disposal (Ma and Adams, 1999; Roy *et al.*, 2001). Alternatively, alcohol production could also occur directly from the acetyl-CoA produced by pyruvate:ferredoxin oxidoreductase, or pyruvate:ferredoxin oxidoreductase could act as a non-redox decarboxylase and directly produce an acetaldehyde and CO₂ (Mai and Adams, 1996; Osowski *et al.*, 2011). More research must be done to determine if these pathways are used by *P. furiosus* and other Thermococcales species and how they impact H₂ production when cultures are grown without sulfur. Furthermore, other Thermococcales may produce metabolites that *P. furiosus* cannot, such as ethanol by *Thermococcus paralvinillae* (Ma *et al.*, 1995).

1.9 Possibilities of Waste Remediation by Thermococcales

There are many agricultural and food wastes to consider for the production of H₂ from extreme thermophiles and hyperthermophiles. (Hyper)thermophilic H₂ production can result in a net gain of energy for the system in two ways. Ideally, a hot starting waste, such as grain stillage or brewery waste is used such that the heat input is required to maintain thermophilic temperatures is minimal (Alger *et al.*, 2008). Additionally, the combination of the hydrolysis and acidification steps, even with significantly raising the temperature of a different (colder) waste, has been shown previously to result in a net gain of energy with other waste types (Lee *et al.*,

2009). Therefore, most of the recovered H₂ should result in a net gain of energy over mesophilic processes.

To date, there are no reports of using *Pyrococcus* or *Thermococcus* for the remediation of agricultural and food wastes. The goal is to consolidate their growth into the heat treatment step that frequently accompanies waste remediation. This section will explore a few potential agricultural wastes that may be remediated by *Pyrococcus* and *Thermococcus* species.

1.9.1 Brewery Waste Remediation

Over the past few years, brewery and distillery wastes have become one of the foci of food waste remediation. Several companies in the U.S. and Australia have developed remediation methods for application in the pectin, brewery, and yeast manufacturing industries (Panda, 2011). Despite major improvements in managing brewery wastes, water consumption and wastewater disposal remain major issues (Fillaudeau *et al.*, 2006). The major components of brewery waste are lignin and maltose-laden spent grain waste at the end of the heat-treatment mash and boiling phases and the dead yeast waste at the end of the fermentative phase of brewing. Lignin is extremely difficult to degrade and currently only extracellular fungal enzymes are known to treat this type of waste. However, maltose and yeast extract are both growth substrates for *Pyrococcus* and *Thermococcus* (Osowski *et al.*, 2011).

1.9.2 Dairy Waste Remediation

Raw cow milk contains over 100 chemical components, but the major components are water (87.4%), lactose (4.8%), fat (3.7%), casein (2.8%), minerals

(0.7%), and whey protein (0.6%) (Goff and Hill, 1993; Wong *et al.*, 1988). When raw milk is processed into pasteurized milk, cheese, butter, milk powder, and condensate, each product results in its own characteristic waste. As a result, different industries repurpose these wastes in different ways. For example, salvaging whey during cheese manufacturing is desirable because of the high nutritional value of whey (Chandan, 1997). A relatively under-researched dairy waste is antibiotic-laden milk.

1.9.3.1 Mastitis and Antibiotic Treatment of Dairy Cows

When a dairy cow has an inflammation of its udder, or mastitis, it is most commonly caused by a *Streptococcus* spp. The cow is often given an antibiotic to treat the infection. This is a relatively new practice and has only been implemented since the 1940's (Smith-Howard, 2010). Although there is increasing public awareness of over-utilization of antibiotics, the antibiotics used by the dairy industry are easily attainable and many dairy farmers do not understand the risks of preventative or over-treatment of their cows (Smith-Howard, 2010).

The antibiotic most commonly used to treat mastitis is a cephalosporin. Cephalosporins are defined by their 7-aminocephalosporanic acid nucleus (consisting of a six-membered dihydrothiazine ring fused with a four-membered β -lactam ring) (Hornish and Katariski, 2002). The most common cephalosporin is Ceftiofur. Ceftiofur is a 3rd generation cephalosporin and was developed strictly for veterinary use, specifically to treat metritis, foot rot, and respiratory disease (Hornish and Katariski, 2002). Ceftiofur contains an oxyiminoaminothiazolyl group

at the dihydrothiazine ring and a furoic acid thioester substitution at the β -lactam ring. The β -lactam ring is essential for antibiotic activity and the cleavage of any part of the ring results in complete loss of antibacterial activity.

1.9.3.2 Antibiotic Activity on Cell Wall Synthesis

Like other β -lactam antibiotics, Ceftiofur and cephalosporins disrupt bacterial cell wall synthesis by binding to penicillin-binding proteins (PBP) (which include transpeptidases, endopeptidases, carboxypeptidases, and transglycosidases). Normally, these enzymes would catalyze the transpeptidation reaction, which cross-links two glycan-linked peptide chains to form the cell wall. However, cephalosporins bind these enzymes such that the transpeptidase reaction can no longer occur. Although the cell wall continues to be synthesized, because it is no longer cross-linked, the new wall cannot maintain its strength. Also, the antibiotic-PBP complex stimulates the release of autolysins, which begin to degrade the existing cell wall. Thus, eventually, turgor pressure lyses the cell.

Cephalosporins are most effective against Gram-positive aerobes, but are also active against certain Gram-negative aerobes and some anaerobic bacteria. Third-generation cephalosporins were designed to have enhanced activity against Gram-negative bacteria, while retaining their efficacy against Gram-positive bacteria. Although Ceftiofur is quickly metabolized by the cow's liver, the metabolites produced also function as cephalosporins, namely desulforylceftiofur (DFC) (Beconi-Barker *et al.*, 1996). DFC can bind to protein because its exposed sulfhydryl moiety can reversibly bind to cysteine and glutathione, thus allowing DFC

to remain in the milk excretions (Beconi-Barker *et al.*, 1996; Hornish and Katarski, 2002). Since cephalosporins can remain in the edible products of treated animals, the allowable amount of drug residue is strictly regulated to ensure human safety. Moreover, food animals are generally treated for short periods (on the order of days, instead of weeks). While only 0.1% of the initial dose is excreted in milk, the milk cannot be added to the food supply for five days after treatment (Hornish and Katarski, 2002).

While cephalosporins such as Ceftiofur are extremely effective against bacteria, it has little to no effect on archaea because of differences in cell wall structure. Most bacteria have cell walls composed of peptidoglycan, a polysaccharide composed of two sugar derivatives – N-acetylglucosamine and N-acetylmuramic acid – and a small number of special amino acids, including L-alanine, D-alanine, D-glutamic acid and either lysine or diaminopimelic acid (DAP). These components connect to form the repeating unit in peptidoglycan, the glycan tetrapeptide (Figure 1.5). The glycan chains are connected by tetrapeptide cross-links between the muramic acids. The glycosidic bonds connecting the sugars, together with these bonds cross-linking the amino acids, are what provide the bacterial cell wall with rigidity. Archaea, however, lack peptidoglycan; specifically, the sugar N-acetylmuramic acid and the amino acid DAP. Instead, archaeal cell walls are composed of polysaccharide, pseudomurein, protein or glycoprotein (Figure 1.6), but the most common cell wall type is the paracrystalline surface layer (S-layer) (Figure 1.7).

Like all other Thermococcales for which the cell wall is determined, *P. furiosus* possesses an S-layer (Albers and Meyer, 2011). The cell membrane of Thermococcales species consists of a cytoplasmic membrane covered by a bilayer cell envelope with an inner periplasmic space and an external S-layer (Bertoldo and Antranikian, 2006). The S-layer is made up of protein or glycoprotein and tends to have a hexagonal symmetry, although the exact symmetry is dependent on the number and structure of the protein or glycoprotein subunits of which the layer is composed. Because archaeal cell walls lack peptidoglycan, archaea are resistant to the action of lysozyme and some antibiotics, such as β -lactams.

1.9.3.3 Disposal of Waste Milk

As mentioned above, the milk from a cow treated with Ceftiofur cannot be used for processing for five days after treatment. Since a normal dairy cow can produce 15-32 L of milk per day and must be milked daily, this means 90-160 L of milk per treated cow is produced that cannot enter the market. On a farm of 1,000 head of dairy cattle, there are on average 2-3 Ceftiofur-treated cows per week. Therefore, this farm is producing 7,800 to 25,000 L of unusable milk per year.

Dairy farmers currently have four primary means of disposal of this milk: they can feed it to neonatal calves, they can send it to the wastewater treatment plant, they can leave it in an open-air silo to be diluted by rainwater, or they can spray it on their fields. This milk actually is nutritionally poor and is not a good food source for calves (Moore *et al.*, 2009). As mentioned above, an increasing number of

Figure 1.5: Bacterial Cell Wall Structure

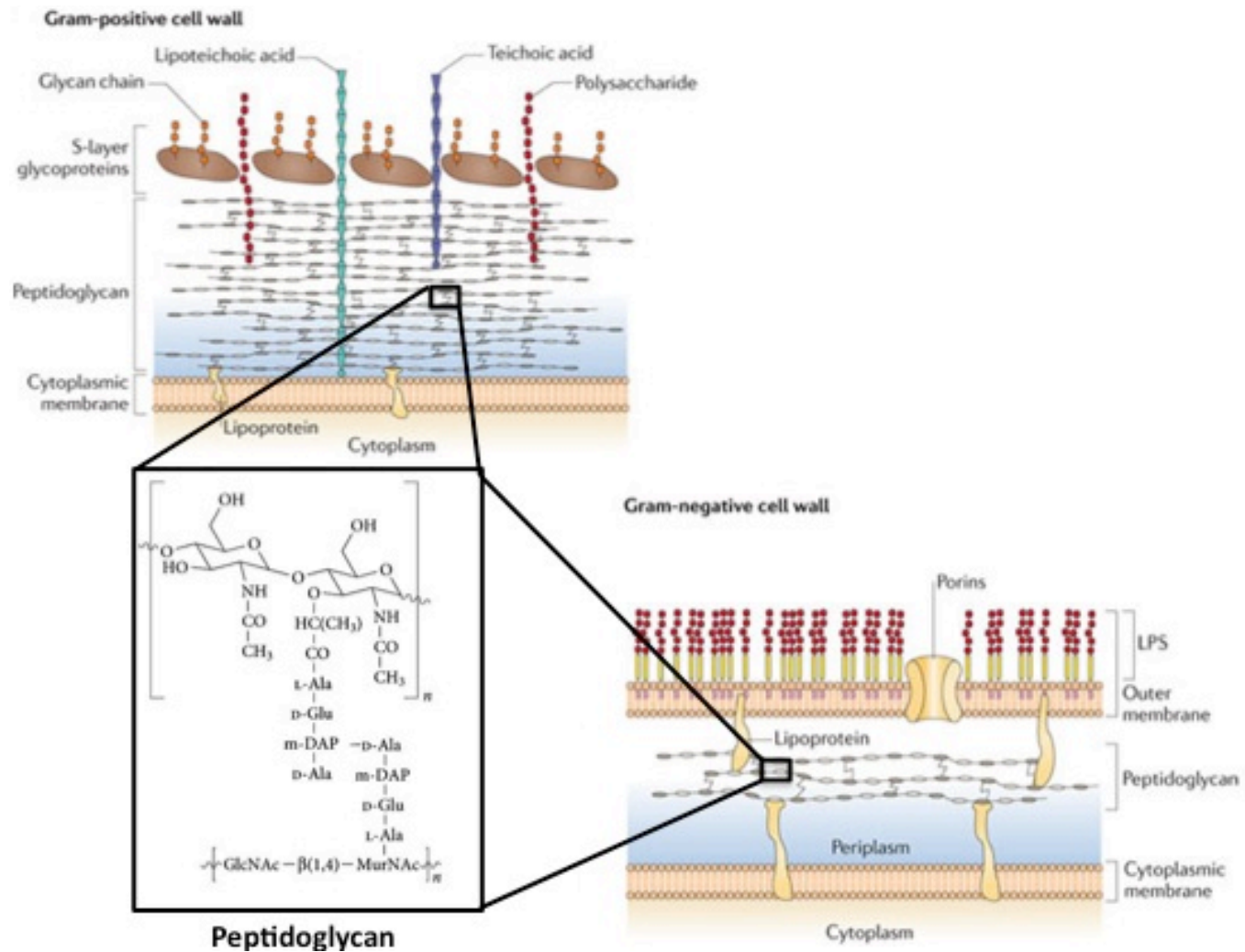


Figure 1.5. Adapted from (Albers and Meyer, 2011).

Figure 1.6: Archaeal Cell Wall Structure

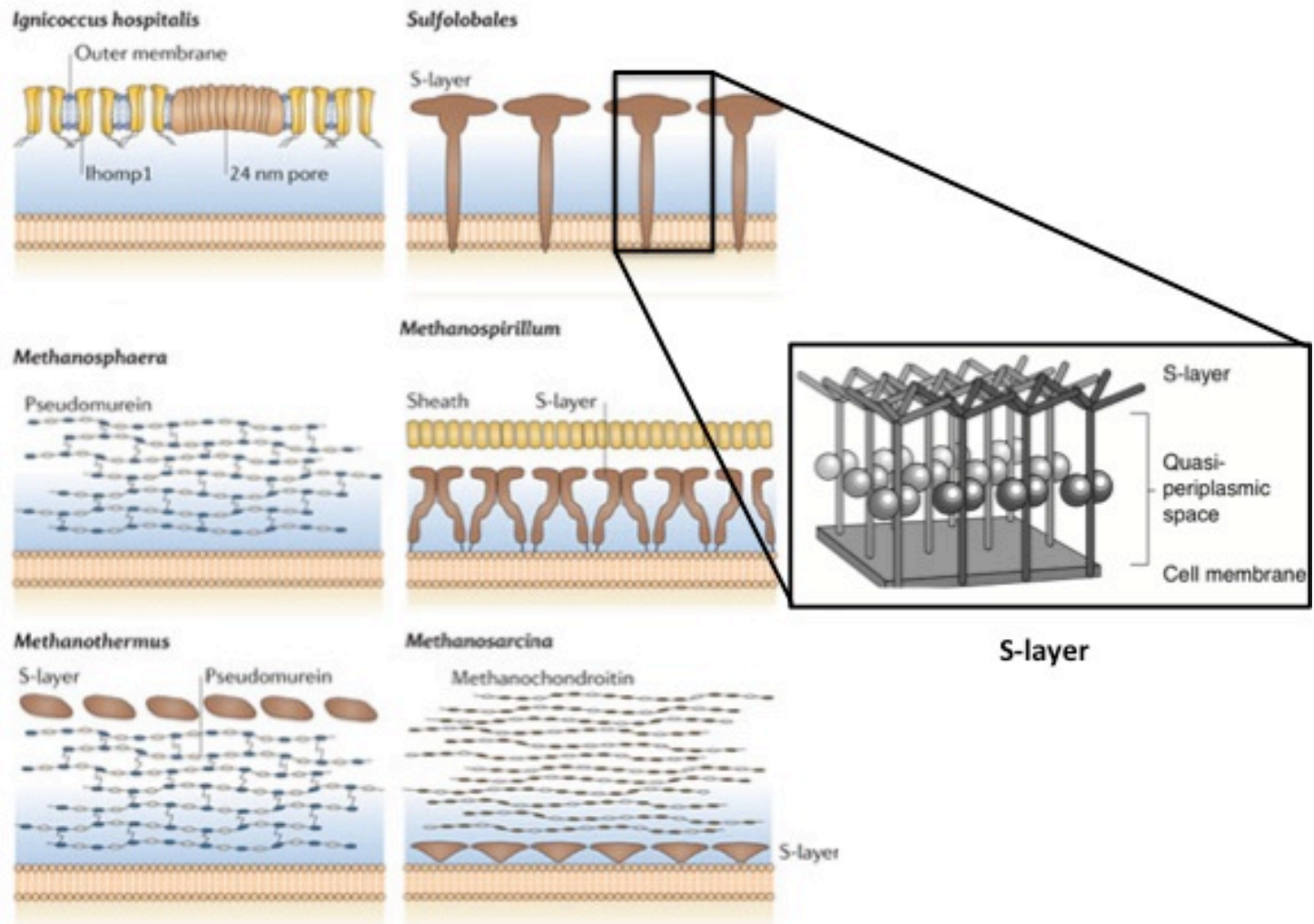


Figure 1.6. Adapted from (Albers and Meyer, 2011).

Figure 1.7: Distribution of Cell Wall Physiologies Among Archaea

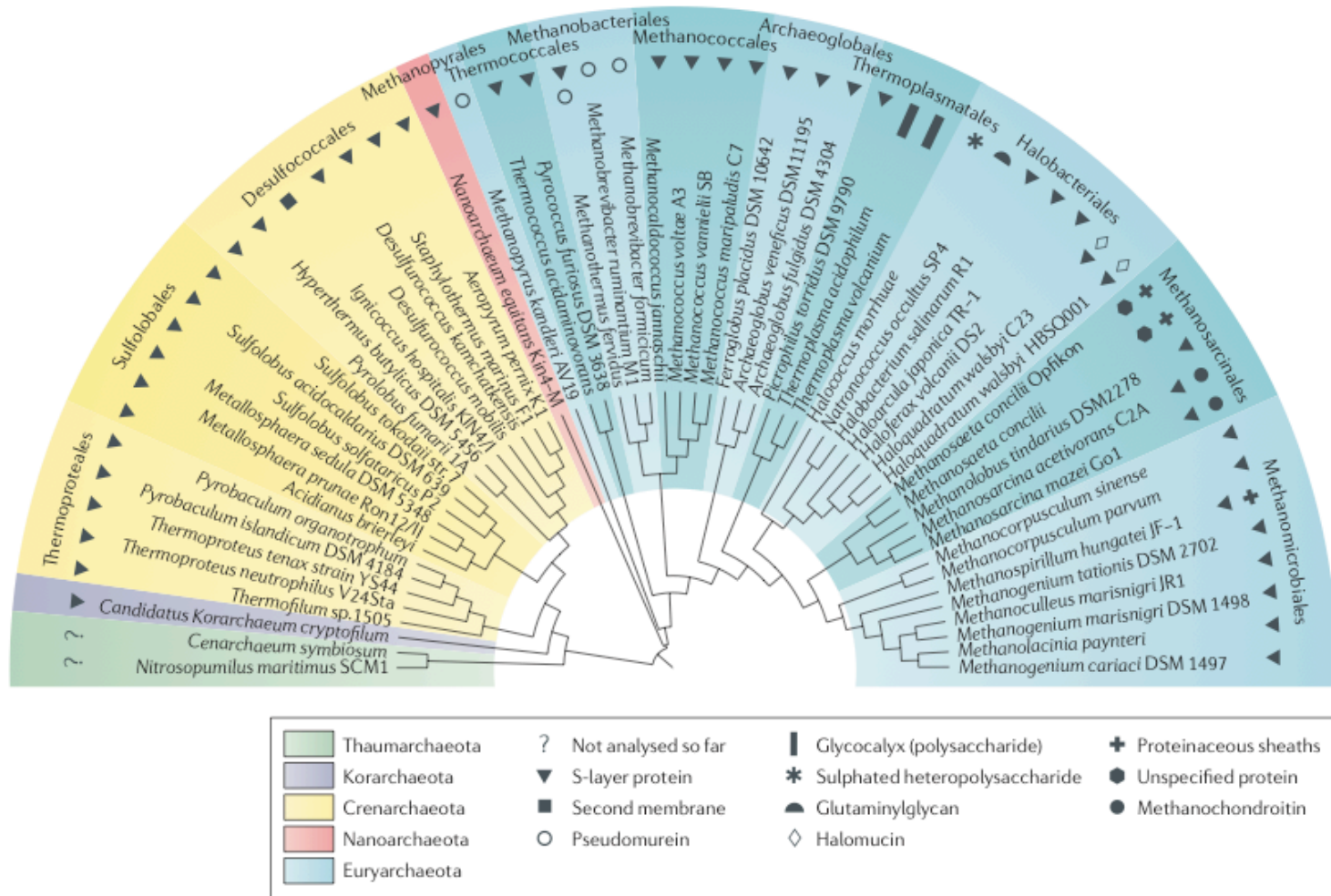


Figure 1.7. Adapted from (Albers and Meyer, 2011). Evolutionary distances unspecified.

wastewater treatment plants refuse to accept this waste. Moreover, the open-air silos attract mosquitos and other insects and pests. Thus, farmers generally prefer to spray the milk on their fields because it does not attract unwanted pests and replenishes carbon in the soil. Despite the fact that in some areas this practice is illegal, most farmers, especially in regions where wastewater disposal restrictions are increasing, dispose of their antibiotic-contaminated milk this way. This presents its own set of problems since the antibiotic concentration is low enough in the milk to not eradicate pathogenic microbes in the soil and is low enough to encourage the development of antibiotic resistance genes in native soil populations (Matthew *et al.*, 2007).

Thus, there is an increasingly urgent need to develop a system by which small businesses and farmers can lower the carbon content of their liquid waste without incurring undo costs or harm to the environment. Biological pre-treatment of large organic molecules by Thermococcales could lower the high carbon load in waste, provide the fermentative microbes in anaerobic digesters with more accessible forms of nutrients, lower wastewater treatment costs, and produce offset costs (Angenent *et al.*, 2004; Ntaikou *et al.*, 2010; Wang and Wan, 2009).

1.9.3.4 Lactose and Protein Transporters in Thermococcales

Lactose, the primary organic component of milk, is a dimer of glucose and galactose with a β -1,4 linkage. As it is only produced by lactating mammals, it is unlikely that Thermococcales possess a lactose-specific transporter. However, Thermococcales are capable of growth on a wide range of carbohydrate substrates

(Osłowski *et al.*, 2011; Vanfossen *et al.*, 2008) and some species possess the components of the lactose-degrading pathway (see Ch. 3 of this study). For example, all 20 strains of *Pyrococcus* and *Thermococcus* tested in the Holden lab culture collection were able to grow on cellobiose, which is chemically similar to lactose (i.e., a glucose dimer connected by a β -1,4 linkage) (Osłowski *et al.*, 2011). Furthermore, β -glucosidase, which cleaves β -1,4 linkages between sugars, is common in many *Pyrococcus* and *Thermococcus* strains, including *P. furiosus*.

The protein content of milk is 80% casein. This accounts for 24-28 gC/L milk and is comprised of α_{S1} -casein (12-15 gC/L milk), α_{S2} -casein (3-4 gC/L of milk), β -casein (9-11 gC/L milk), κ -casein (3-4 gC/L milk), and γ -casein (1-2 gC/L milk) (Robin *et al.*, 1993). Casein is a known organic source for *Pyrococcus* and *Thermococcus* species, even in the absence of sulfur (Osłowski *et al.*, 2011). The rest of the protein content of milk (5-7 gC/L milk) is collectively known as whey protein and is comprised of β -lactoglobulin, α -lactoglobulin, bovine serum albumin, immunoglobulins, and proteose peptones. Thus far, *P. furiosus* has not successfully been adapted to growth on pure whey protein, although *T. maritima* obtained 10^8 cells/mL (Remmereit and Thomm, 2008).

1.10 Summary of Thesis

As farm production increases, more waste is generated, which can lead to antibiotic build-up in waste and eutrophication of surrounding areas. To combat this, farms are required to remove waste to waste treatment facilities, but often this waste must be carbon-depleted before it is accepted by the facilities. Thus, we have

begun to develop a consolidated process capable of sanitizing and removing carbon in waste generated by these farms while still providing energy to partially offset the cost of waste treatment.

In exploring this process, we have determined that different environmental conditions are causing metabolic shifts in archaeal hyperthermophilic heterotrophs. The rate of H₂ production and the media preference for optimal H₂ production varies drastically between the different artificial growth conditions supplied to both *P. furiosus* and *T. paralvinellae*. Genomic data indicate that a wide variety of substrate types can be used by the Thermococcales and that all species have the genetic components for the pathways outlined in this paper with the exception of alcohol and formate dehydrogenases and formate:hydrogen lyase.

CHAPTER 2

COMPLETE GENOME SEQUENCE OF THE HYPERTHERMOPHILIC ARCHAEON

THERMOCOCCUS PARALVINELLAE

2.1 Summary

Thermococcus paralvinellae (formerly known as *Thermococcus* sp. strain ES1) is an anaerobic, hyperthermophilic archaeon from a hydrothermal vent that catabolizes sugars and peptides and produces H₂S from S⁰, H₂, acetate and CO₂ as its primary metabolites. We present the complete genome sequence of this strain (1,957,742 bp) with a focus on its substrate utilization and metabolite production capabilities. The sequence will contribute to the development of heterotrophic archaea for bioenergy production and biogeochemical modeling in hydrothermal environments.

2.2 Genomic Analysis of *Thermococcus paralvinellae*

Thermococcus paralvinellae is a hyperthermophilic archaeon isolated from a *Paralvinella* sp. polychaete worm collected from a hydrothermal vent on the Endeavour Segment in the northeastern Pacific Ocean (Pledger and Baross, 1989). It is an obligate anaerobe and catabolizes organic compounds such as maltose, cellobiose and tryptone and produces H₂S in the presence of elemental sulfur and H₂ in its absence (Pledger and Baross, 1989; Osłowski *et al.*, 2011). A decrease in the amount of S⁰ in the growth medium leads to enhanced production of H₂, ethanol,

butanol, and formate at the expense of H₂S and acetate production (Ma *et al.*, 1995). Aldehyde ferredoxin oxidoreductase, 2-ketoisovalerate ferredoxin oxidoreductase, and alcohol dehydrogenase have been purified and characterized from *T. paralvinellae* (Heider *et al.*, 1995; Heider *et al.*, 1996; Ma *et al.*, 1995; Ying *et al.*, 2009). Here we present the complete genome sequence of *T. paralvinellae* and identify genes for sugar catabolism and metabolite production.

The genome sequence of *T. paralvinellae* was acquired using Roche 454 GS FLX Titanium and Illumina Hiseq 2000 (Macrogen, Korea) for hybrid sequencing and Newbler 2.3 assembler for genome assembly. This resulted in three scaffolds, and the gaps between the scaffolds were closed by polymerase chain reactions. GeneMarkS (Besemer *et al.*, 2001), Glimmer 3.02 (Delcher *et al.*, 2007), and FgenesB (Softberry, Inc., Mount Kisco, NY) were used to predict open reading frames (ORFs). Their functions were verified using BLASTP (Altschul *et al.*, 1990) and InterProScan (Zdobnov and Apweiler, 2001). tRNAs and rRNAs were predicted using tRNAscan-SE and RNAmmer, respectively (Lagesen *et al.*, 2007; Lowe and Eddy, 1997). CRISPRFinder and SignalP were used to determine CRISPR repeats and extracellular proteins (Grissa *et al.*, 2007; Petersen *et al.*, 2011).

The complete genome of *T. paralvinellae* consists of a circular chromosome of 1,957,742 bp with no extra chromosome. It contains 2,090 ORFs and 24 pseudogenes with a GC content of 40.8%. The genome encodes 46 tRNAs and one rRNA operon consisting of two 5S rRNA genes, one 16S rRNA gene, and one 23S rRNA gene (Table 2.1). It has three CRISPR loci consisting of CRISPR-associated *cas* genes, as well as 17, 33 or 34 repeats, respectively.

Table 2.1 *Thermococcus paralvinellae* Genome Statistics

Attribute	Value
Genome Size (bp)	1,957,742
DNA Coding Region (bp)	1,759,707
DNA G + C Content	40.8%
Number of Replicons	1
Extrachromosomal Elements	0
Total Genes	2,090
rRNA Genes	4
tRNA Genes	46
Protein Coding Genes	2,016
Pseudogenes	24
Gene with Predicted Function	1,223

Table 2.1. The complete genome is available at GenBank with accession number CP006965.

The *T. paralvinellae* genome encodes an archaeal Embden–Meyerhof glycolytic pathway (Verhees *et al.*, 2003) and enzymes that oxidize 2-keto acids to organic acids with concomitant reduction of ferredoxin and substrate-level production of ATP. It contains various α -glucan active enzyme encoding genes such as amylopullulanase (TES1_1662), neopullulanase (TES1_1658), glycogen branching enzyme (TES1_0044), maltose-forming α -amylase (TES1_0024), 4- α -glucanotransferase (TES1_1899), and cyclodextrin glucanotransferase (TES1_1436). For redox reactions, the genome includes one cytosolic H₂-dependent hydrogenase (TES1_0164-0167), one F₄₂₀-dependent hydrogenase (TES1_1498-1501), two membrane-bound hydrogenases (TES1_1451-1482), one membrane-bound carbon monoxide dehydrogenase (TES1_1197-1212), two formate hydrogen lyases (TES1_0096-0111, TES1_1484-1497), and four alcohol dehydrogenases (TES1_0121, TES1_0221, TES1_0639, TES1_0987). There is also a membrane-bound NADH oxidoreductase (TES1_0865-0877) and a V-type ATP synthase (TES1_1696-1704) for energy synthesis on the membrane.

2.3 Nucleotide Sequence Accession Number

The complete genome sequence of *T. paralvinellae* is now available in GenBank database under accession number CP006965.

CHAPTER 3

***THERMOCOCCUS PARALVINELLAE* SP. NOV. AND *THERMOCOCCUS CLEFTENSIS* CL1 SP. NOV., NEW SPECIES OF HYPERTHERMOPHILIC HETEROTROPHS FROM DEEP SEA HYDROTHERMAL VENTS**

3.1 Summary

Two heterotrophic hyperthermophile strains, ES1^T and CL1^T, were isolated from *Paralvinella* sp. polychaete worms collected from active hydrothermal vent chimneys in the northeast Pacific Ocean. Both are obligate anaerobes and produce H₂S in the presence of elemental sulfur and H₂. Complete genome sequences are available for both strains. 16S rRNA gene sequences are more than 97% identical to most other *Thermococcus* species, suggesting that these belong in the genus *Thermococcus*, but not adequately distinguishing if they are unique species. Therefore, overall genome relatedness index (OGRI) analyses were performed to establish that these strains are new species. For each analysis, strain ES1^T is most similar to *Thermococcus barophilus* MP^T while strain CL1^T is most similar to *Thermococcus* sp. 4557. Concerning these most-similar strains, average nucleotide identity (ANI) scores were 84% for strain ES1^T and 81% for strain CL1^T, genome-to-genome direct comparison (GGDC) scores were 23% for strain ES1^T and 47% for strain CL1^T, and the species identification (SpecI) scores were 89% for strain ES1^T and 88% for strain CL1^T. For each analysis, strains ES1^T and CL1^T were below the species delineation cutoff. Therefore, based on their whole genome sequences,

strains ES1^T and CL1^T are suggested to represent novel species of the genus *Thermococcus* for which the names *Thermococcus paralvinellae* sp. nov. and *Thermococcus cleftensis* sp. nov. are proposed, respectively. The type strains are ES1^T (=DSM 27261 =KACC 17923) and CL1^T (=DSM 27260 =KACC 17922).

The GenBank/EMBL/DDBJ accession number for the genomic sequence of strain ES1^T is CP006965 and for strain CL1^T is CP003651.

3.2 Growth Parameters of Strains ES1^T and CL1^T

The genus *Thermococcus* is composed of hyperthermophilic obligate anaerobes that couple the oxidation of peptides and polysaccharides to the reduction of elemental sulfur (S⁰) and protons (Bertoldo and Antranikian, 2006). In this study, the complete genome sequences of two strains of *Thermococcus*, strain ES1^T and strain CL1^T (Jung *et al.*, 2012a; Jung *et al.*, 2014), were used to establish the novelty of these strains. Both strains were isolated from *Paralvinella* sp. polychaete worms collected from active hydrothermal vent chimneys on the Juan de Fuca Ridge in the northeastern Pacific Ocean (Pledger and Baross, 1989; Holden *et al.*, 2001). Notably, in a survey of 20 *Thermococcus* and *Pyrococcus* species, both strains produced noticeable amounts of H₂ even when grown on S⁰ (Oslowski *et al.*, 2011).

In this study, strains ES1^T and CL1^T were adapted for growth without S⁰ at 82°C through serial transfers on 0.5% (wt vol⁻¹) each of maltose and tryptone medium as previously described (Adams *et al.*, 2001). The concentration of cells and H₂ were monitored in duplicate at certain time intervals by phase-contrast microscopy and gas chromatography. The growth rate of strain ES1^T was the same

rate despite the presence or absence of S^o (doubling times of 65 min and 72 min, respectively) (Figure 3.1.1) while strain CL1^T grew much slower without S^o relative to cultures with S^o (Fig 3.1.2). Both strains grew and produced 3.25-5.05 mmoles of H₂ per liter of medium without S^o, and produced < 100 μmoles of H₂ per liter of medium when grown with S^o (Figure 3.1).

Based on previous studies, strain ES1^T grows with S^o within the range of 50–91°C with an optimum at 82°C (Pledger and Baross, 1989), and its maximum growth temperature increases 2°C when grown at 22 MPa (Pledger *et al.*, 1994). When shifted from growth on 15 g l⁻¹ of S^o to 1 g l⁻¹ of S^o, strain ES1^T increases its production of H₂, formate, ethanol and butanol at the expense of H₂S and acetate (Ma *et al.*, 1995). There are concomitant increases in hydrogenase, formate dehydrogenase, and alcohol dehydrogenase specific activities in crude cell extracts (Ma *et al.*, 1995). Several enzymes have been characterized from strain ES1^T including aldehyde ferredoxin oxidoreductase (Heider *et al.*, 1995), 2-ketoisovalerate ferredoxin oxidoreductase (Heider *et al.*, 1996), and alcohol dehydrogenase (Ma *et al.*, 1995; Ying *et al.*, 2009). Additional growth parameters and physiological characteristics of ES1^T are found in Pledger and Baross (1989).

Strain CL1^T grows with S^o within the range of 55–94°C with an optimum at 88°C (Holden *et al.*, 2001). Due to its ability to grow on maltose and cellobiose (Oslowski *et al.*, 2011), our study was focused on the sugar catabolizing enzymes produced by strain CL1^T. It possesses a GH57 type amylase, a glycoside hydrolase that only recognizes maltose, which has dual hydrolysis activity toward α-1,4- and α-1,6-glycosidic linkages and is only found in some of the *Thermococcales*, but has

Figure 3.1: Growth of Strains ES1^T and CL1^T in the Presence and Absence of Elemental Sulfur

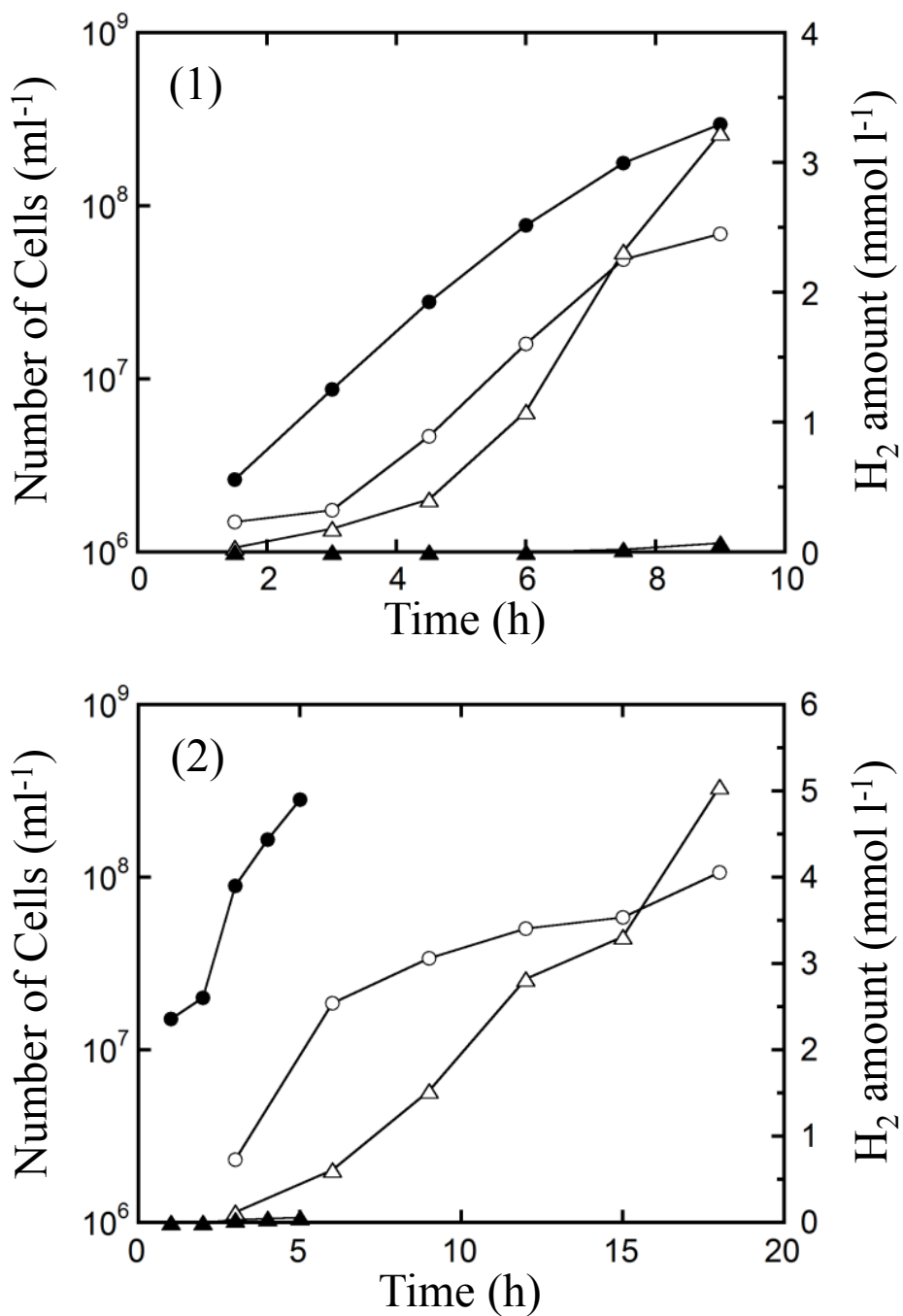


Figure 3.1. Cells per ml of medium (●,○) and mmoles of H₂ per liter (▲,△) for strain ES1^T (1) and strain CL1^T (2) when grown on 0.5% (wt vol⁻¹) each of maltose and tryptone with (filled symbols) and without (open symbols) 0.1% (wt vol⁻¹) elemental sulfur. Data points are averages of duplicate bottles.

never been shown in another microorganism (Jeon *et al.*, 2014). A cyclomalto-dextrinase also was purified and characterized from this organism (Lee *et al.*, 2013).

The phylogenetic relatedness of strains ES1^T and CL1^T to other *Thermococcus* spp. was determined using 16S rRNA gene sequences obtained from the Ribosomal Database Project (Wang *et al.*, 2007), as well as comparing them via megaBLAST (McGinnis and Madden, 2004). *Thermococcus* strain ES1^T shows 98.9% identity with *Thermococcus barophilus* MP^T, 97.9% identity with *Thermococcus kodakarensis* KOD1^T, and 97.7% identity with *Thermococcus* strain AM4. *Thermococcus* strain CL1^T shows 99.1% identity with *T. kodakarensis* KOD1^T and strain AM4, and 98.9% identity with *Thermococcus onnurineus* NA1^T and *Thermococcus* strain 4557. To resolve this, we aligned all *Thermococcales* species sequences using the default settings for CLUSTALW (Larkin *et al.*, 2007) in MEGA5 software (Tamura *et al.*, 2011). We constructed neighbor-joining phylogenetic trees in MEGA5 with the Jukes-Cantor model and bootstrap values obtained from 500 replicate trees (Figure 3.2). According to this alignment, the closest relatives to strains ES1^T and CL1^T are *T. barophilus* MP^T and *Thermococcus* sp. 4557, respectively.

3.3 Overall Genomic Relatedness Index Analyses

Since the 16S rRNA gene sequences in *Thermococcus* spp. generally show more than 97% identity across the genus (Figure 3.2), the complete genome sequences of strains ES1^T and CL1^T were compared with the complete genome sequences of its closest phylogenetic relatives and all other *Thermococcus* complete

Figure 3.2: 16S Phylogenetic Tree of Thermococcales Species with Strains ES1^T and CL1^T

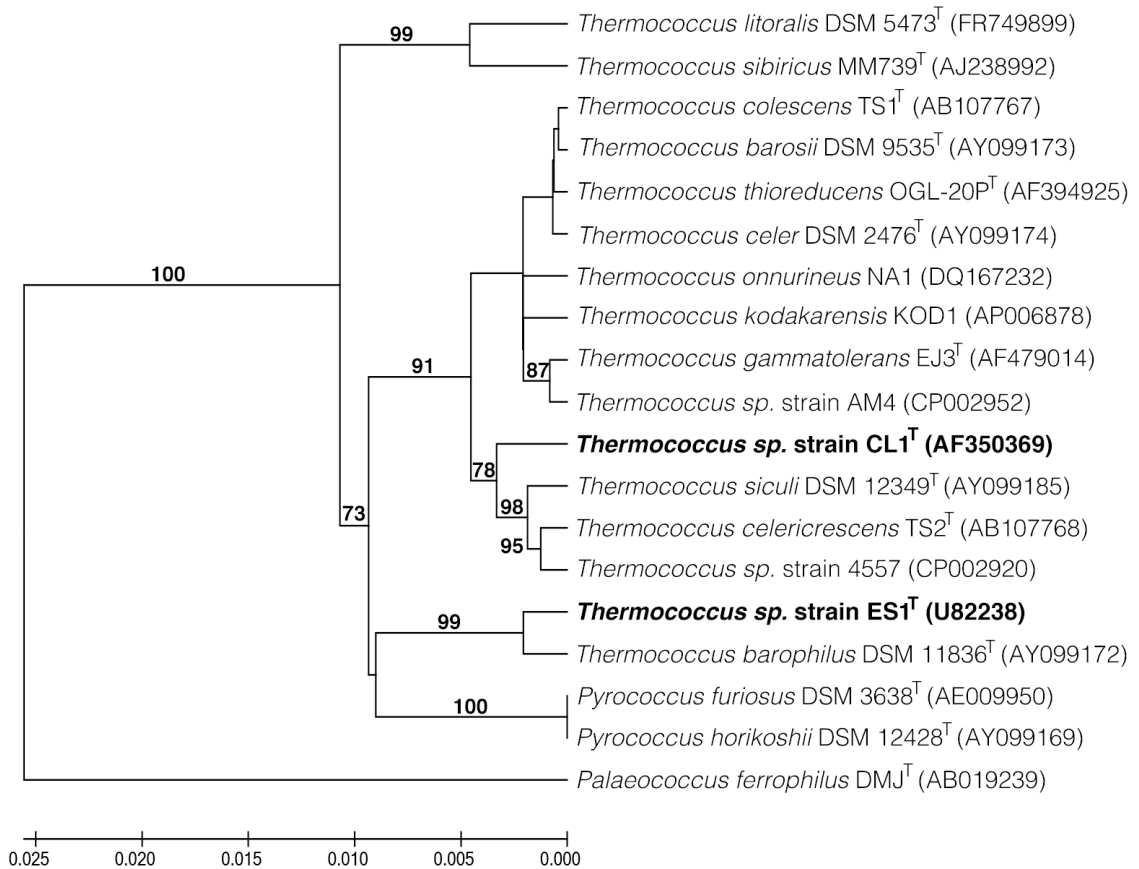


Figure 3.2. Neighbor-joining phylogenetic tree showing the position of strain ES1^T and strain CL1^T within the genus *Thermococcus* based on sequences of the 16S rRNA gene (1208 nt). GenBank accession numbers are included in parentheses. The topology of the tree was estimated by bootstraps based on 500 replications. The numbers at the branch points are the percentage support by bootstraps (bootstraps under 70% not shown). Bar, 2% sequence divergence.

sequences of its closest phylogenetic relatives and all other *Thermococcus* complete genome sequences using “overall genome relatedness index” (OGRI) analyses (Chun and Rainey, 2014). All genome sequences were obtained from the GenBank sequence database. We calculated the BLAST-based “average nucleotide identity” (ANI) score using the JSpecies program with the default parameters (Goris *et al.*, 2007; Richter and Rosselló-Móra, 2009). “Genome-to-genome direct comparison” (GGDC) analyses were performed using all three equations in the GGDC v. 2.0 program (Auch *et al.*, 2010). Forty marker genes were compared between strains ES1^T and CL1^T and their closest relatives using the “species identification” (SpecI) program (Mende *et al.*, 2013). BLASTZ (Schwartz *et al.*, 2003) and the “synteny mapping and analysis program” (SyMAP 4.0) (Soderlund *et al.*, 2011) were used to compute synteny blocks between strains ES1^T and CL1^T and all other *Thermococcus* genome sequences to determine which genes are present in ES1^T and CL1^T but missing from their closest relatives.

For each OGRI analysis, strain ES1^T was most closely related to *T. barophilus* MP^T. The ANI score for the strain ES1^T-*T. barophilus* MP^T comparison was 84%, which is below the 96% cut-off value for species determination by this approach (Table 3.1). GGDC calculations with BLAST+ for strain ES1^T and *T. barophilus* MP^T gave DNA-DNA homology (DDH) values of 23.2%, 34.6%, and 23.4% for GGDC1, GGDC2, and GGDC3 respectively, which are below the 60% cut-off for delineating species by this approach (Table 3.1). The SpecI analysis for strain ES1^T and *T. barophilus* MP^T gave an average percent identity of 89.1%, which is below the 96.5%

Table 3.1 Comparison of *in silico* ANIb and GGDC Analysis of Genomic DNA of *Thermococcus* sp. Strains ES1^T and CL1^T

Query Species	Comparison to <i>Thermococcus</i> sp. strain ES1				Comparison to <i>Thermococcus</i> sp. strain CL1			
	ANIb	GGDC DDH 1	GGDC DDH 2	GGDC DDH 3	ANIb	GGDC DDH 1	GGDC DDH 2	GGDC DDH 3
<i>Thermococcus barophilus</i>	84	23.2	34.6	23.4	68.37	13	18.2	13.3
<i>Thermococcus gammatolerans</i>	68.56	12.5	18.8	12.9	76.91	19.6	22.7	19.2
<i>Thermococcus kodakarensis KOD1</i>	68.61	12.6	18.1	13	75.67	18.7	21.4	18.3
<i>Thermococcus litoralis DSM 5473</i>	72.07	12.8	23.9	13.2	68.62	12.8	20.3	13.2
<i>Thermococcus onnurienus NA1</i>	69.97	12.9	30.8	13.3	76.94	27.1	20.9	24.7
<i>Thermococcus sibiricus</i>	71.31	12.6	21.3	13	66.76	12.8	19.1	13.2
<i>Thermococcus</i> sp. strain 4557	68.13	12.6	24.8	13	81.47	46.8	24.8	39.6
<i>Thermococcus</i> sp. strain AM4	68.18	12.5	17.7	12.9	77.5	21.3	22.9	20.5
<i>Thermococcus</i> sp. strain CL1	68.13	12.5	19.4	12.9	N/A	N/A	N/A	N/A
<i>Thermococcus</i> sp. strain ES1	N/A	N/A	N/A	N/A	68.11	12.5	19.4	12.9

Table 3.1. The ANIb score was calculated using the default BLAST parameters in JSpecies. The GGDC regression-based DDH estimates (%) are indicated for each algorithm using the default BLAST+ parameters is GGDC 2.0. Data in bold represent the closest relative to *Thermococcus* sp. strains ES1^T and CL1^T for each calculation type.

cut-off for delineating species by this approach, with all 40 gene homologies below the species cutoff (Table 3.2). Therefore, all three OGRI analyses indicated that strain ES1^T is a novel species.

SyMAP analysis showed that *T. barophilus* MP^T contains 83% of the open reading frames (ORFs) found in strain ES1^T. Among the genes found from strain ES1^T that are absent from *T. barophilus* MP^T are a second membrane hydrogenase operon, two formate:H₂ lyase operons, 12 glycosylases, and genes related to amino acid synthesis and transport (Table 3.3).

When compared to all *Thermococcus* and *Pyrococcus* genome sequences using BLASTp (Altschul *et al.*, 1990), strain ES1^T generally possesses more alcohol dehydrogenases (TES1_0121, TES1_0221, and TES1_0987) and acetyl-CoA synthetases (TES1_0746, TES1_1160, TES1_1231, and TES1_1345) than most *Thermococcus* species. It also possesses formate:H₂ lyases (TES1_0099-0103 and TES1_1488-93) that are absent in most *Thermococcus* and *Pyrococcus* species (Table 3.4).

For each OGRI analysis, strain CL1^T was most closely related to *Thermococcus* sp. 4557. The ANI score for the strain CL1^T-strain 4557 comparison was 81% (Table 3.1). GGDC calculations with BLAST+ for strains CL1^T and 4557 gave DDH values of 46.8%, 24.8%, and 39.6% (Table 3.1). The Specl analysis for strains CL1^T and 4557 gave an average percent identity of 87.8%, with all 40 gene homologies below the level of species cutoff (Table 3.2). Therefore, all three OGRI analyses indicated that strain CL1^T is a separate novel species.

Table 3.2 SpecI Analysis of *Thermococcus* sp. Strains ES1^T and CL1^T

COG	Strain ES1 vs. <i>T.</i> <i>barophilus</i>	Strain CL1 vs. Strain 4557	COG	Strain ES1 vs. <i>T.</i> <i>barophilus</i>	Strain CL1 vs. Strain 4557
COG0124	90.33	82.19	COG0099	93.29	94.44
COG0552	88.93	80.24	COG0098	86.58	92.51
COG0533	83.28	84.46	COG0215	88.28	84.81
COG0048	93.24	93.02	COG0197	86.37	92.71
COG0049	91.05	91.36	COG0094	90.04	92.39
COG0102	91.91	90.93	COG0097	90.99	90.45
COG0100	91.24	91.73	COG0096	90.08	94.91
COG0495	91.04	86.18	COG0091	92.36	91.51
COG0525	90.49	86.95	COG0090	89.31	91.81
COG0202	86.23	84.8	COG0093	91.95	91.78
COG0092	88.46	90.05	COG0201	83.08	86.93
COG0541	84.11	85.67	COG0088	91.28	93.49
COG0016	87.17	80.88	COG0186	91.67	96.13
COG0012	87.94	86.26	COG0185	96.24	92.54
COG0256	89.11	91.09	COG0184	90.57	91.89
COG0018	85.71	80.97	COG0080	91.52	92.68
COG0052	90.26	93.56	COG0081	91.40	93.24
COG0522	88.10	90.61	COG0087	91.93	92.34
COG0172	89.91	86.7	COG0085	90.14	88.01
COG0200	87.39	90.38	Average	89.09	87.79

Table 3.2. The percent homology of each COG between the reference species (either strain ES1^T or strain CL1^T) and its closest relative was calculated using the default parameters SpecI v 2.0. The data in bold represent the average percent homology of all COGs.

Table 3.3 ORFs Found in *Thermococcus* sp. Strains ES1^T Without Homologs in *Thermococcus barophilus*

Gene	Product	Gene	Product
ES1_0054	Hypothetical protein	ES1_0670	DNA topoisomerase VI subunit B
ES1_0055	Hypothetical protein	ES1_0671	DNA topoisomerase VI subunit A
ES1_0056	Pyruvate dehydrogenase subunit β	ES1_0672 to ES1_0674	All hypothetical proteins
ES1_0057	Pyruvate dehydrogenase subunit α	ES1_0675	GTP cyclohydrolase
ES1_0058	Hypothetical protein	ES1_0799 to ES1_0805	All hypothetical proteins
ES1_0059	Dihydropyridyllysine-residue acetyltransferase component	ES1_0805	Hypothetical protein
ES1_0060	Hypothetical protein	ES1_0806	Chromosome partitioning protein ParB-like protein
ES1_0061	Putative ATP-NAD/AcoX kinase	ES1_0807	Phosphoglycolate phosphatase
ES1_0062	Putative biotin/lipoate A/B protein ligase family protein	ES1_0808	Hypothetical protein
ES1_0063	Sodium-driven multidrug efflux pump protein	ES1_0809	Transcriptional regulator: ArsR family
ES1_0064	Phosphoenolpyruvate synthase	ES1_0810	Hypothetical protein
ES1_0077	Major facilitator superfamily permease	ES1_0811	Hypothetical protein
ES1_0078	Hypothetical protein containing β -lactamase-like domain	ES1_0893	Glycosyl transferase family protein 4
ES1_0079 to ES1_0081	All hypothetical proteins	ES1_0894	Glycosyl transferase family protein 5
ES1_0082	Hypothetical protein oxidoreductase molybdopterin-binding domain	ES1_0895	Hypothetical protein
ES1_0083	Hypothetical protein	ES1_0905	Hypothetical protein
ES1_0084	ABC-type iron(III) siderophore transport system: ATPase component	ES1_0906	Hypothetical protein
ES1_0085	ABC-type iron(III)-siderophore transport system: Permease component	ES1_0907	Threonyl-tRNA synthetase
ES1_0086	ABC-type iron(III)-siderophore transport system: periplasmic protein	ES1_0908	Hypothetical protein
ES1_0087 to ES1_0089	Hypothetical protein	ES1_0909	Hypothetical protein
ES1_0094	[NiFe] hydrogenase metallocenter assembly protein HypC	ES1_0910	DNA-directed RNA polymerase subunit L

Table 3.3 continued on next page

Table 3.3 continued

Gene	Product	Gene	Product
ES1_0095	Transcriptional regulator: TetR family	ES1_0911	Hypothetical protein
ES1_0096	Formate dehydrogenase subunit α	ES1_0912	Putative AP endonuclease
ES1_0097	Oxidoreductase 4Fe-4S ferredoxins	ES1_0913	Putative protease
ES1_0098	Hydrogenase 4 subunit D	ES1_0914	Hypothetical protein
ES1_0099	Hydrogenase 4: component B or formate; H_2 lyase subunit 3	ES1_0915	Hypothetical protein
ES1_0100	Hydrogenase 4: component C or formate; H_2 lyase subunit 4	ES1_0916	Hydrogenase expression/formation protein HypE
ES1_0101	Hydrogenase 4: component G or formate; H_2 lyase subunit 5	ES1_0917	Predicted ATPase: RNase L inhibitor (RLI) homolog
ES1_0102	Formate; H_2 lyase subunit 6	ES1_0918	ATP-dependent RNA helicase
ES1_0103	Hydrogenase 4: component I or formate; H_2 lyase subunit 7	ES1_0919	Hypothetical protein
ES1_0104	Hypothetical protein	ES1_0920	Hypothetical protein containing HAD-like domain
ES1_0105	Na^+/H^+ antiporter subunit MnhF	ES1_0921	Hypothetical protein
ES1_0106	Na^+/H^+ antiporter subunit MnhG	ES1_0922	Hypothetical protein
ES1_0107	Hypothetical protein	ES1_0923	Archaeal flavoprotein
ES1_0108	Na^+/H^+ antiporter subunit MnhB	ES1_1479	Na^+/H^+ antiporter subunit D
ES1_0109	Na^+/H^+ antiporter subunit MnhC	ES1_1480	Na^+/H^+ antiporter subunit E
ES1_0110	Na^+/H^+ antiporter subunit MnhE	ES1_1481	Na^+/H^+ antiporter subunit C
ES1_0111	Na^+/H^+ antiporter subunit MnhD	ES1_1482	Na^+/H^+ antiporter subunit MnhB
ES1_0112	Nucleotidyltransferase	ES1_1483	Hypothetical protein
ES1_0113	Vitamin B12 ABC transporter B12-binding component	ES1_1484	Na^+/H^+ antiporter subunit MnhG
ES1_0245	Ribonuclease P component 3	ES1_1485	Na^+/H^+ antiporter subunit MnhF
ES1_0246	Cystathionine γ -synthase	ES1_1486	Formate transporter
ES1_0247	Putative 5:10-methylenetetrahydrofolate reductase	ES1_1487	Hypothetical protein
ES1_0248	Hypothetical protein	ES1_1488	Hydrogenase 4: component I or formate; H_2 lyase subunit 7
ES1_0249	Hypothetical protein	ES1_1489	Formate; H_2 lyase subunit 6
ES1_0250	5-methyltetrahydropteroyltriglutamate	ES1_1490	Hydrogenase 4: component G or formate; H_2 lyase subunit 5
ES1_0251	Putative Aspartokinase	ES1_1491	Hydrogenase 4: component C or formate; H_2 lyase subunit 4
ES1_0252	Tryptophan synthase like subunit β	ES1_1492	Hydrogenase 4: component B or formate; H_2 lyase subunit 3

Table 3.3 continued on next page

Table 3.3 continued

Gene	Product	Gene	Product
ES1_0472	Putative pseudouridylate synthase	ES1_1493	NADH dehydrogenase (quinone)
ES1_0473	Hypothetical protein	ES1_1494	hydrogenase 4 subunit D
ES1_0474	3-octaprenyl-4-hydroxybenzoate carboxy-lyase	ES1_1495	4Fe-4S binding protein
ES1_0475	Pyrroline-5-carboxylate reductase	ES1_1496	Formate dehydrogenase subunit α
ES1_0476	Aspartate-semialdehyde dehydrogenase	ES1_1497	Formate dehydrogenase subunit FdhD
ES1_0477	Threonine synthase	ES1_1498	Coenzyme F420 hydrogenase subunit α
ES1_0478	Homoserine kinase	ES1_1499	Coenzyme F420 hydrogenase/dehydrogenase subunit β
ES1_0479	putative Aspartokinase	ES1_1500	Coenzyme F420 hydrogenase subunit γ
ES1_0480	Hypothetical protein	ES1_1501	Coenzyme F420 hydrogenase subunit α
ES1_0494	Hypothetical protein	ES1_1582 to ES1_1584	All hypothetical proteins
ES1_0495	Aminotransferase	ES1_1585	Type I restriction-modification enzyme: R subunit
ES1_0496	Putative Nitrogen regulatory protein P-II	ES1_1586	Hypothetical protein
ES1_0497	Ammonium transporter	ES1_1587	Type I restriction-modification enzyme: S subunit
ES1_0498	Argininosuccinate synthase	ES1_1588	Type I restriction modification enzyme: M subunit
ES1_0499	Argininosuccinate lyase	ES1_1589 to ES1_1591	All hypothetical proteins
ES1_0500	Carbamoyl phosphate synthase small subunit	ES1_1592	Integrase/recombinase
ES1_0501	Carbamoyl-phosphate synthase large subunit	ES1_1593 to ES1_1595	All hypothetical proteins
ES1_0502	Trans-homoaconitate synthase	ES1_1600	Leucyl aminopeptidase
ES1_0503	3-isopropylmalate dehydratase large subunit	ES1_1601	Putative hydantoin racemase
ES1_0504	3-isopropylmalate dehydratase small subunit	ES1_1602	Hypothetical protein
ES1_0505	3-isopropylmalate dehydrogenase	ES1_1603	Putative Asp/Glu racemase
ES1_0506	Lysine biosynthesis protein LysW	ES1_1604	Dipeptide transport system ATP-binding protein dppF
ES1_0507	Lysine biosynthesis protein LysX	ES1_1605	Dipeptide transport system ATP-binding protein dppF
ES1_0508	N-acetyl- γ -glutamyl-phosphate reductase	ES1_1606	Dipeptide transport system permease protein DppC
ES1_0509	Acetylglutamate/acetylaminoadipate kinase	ES1_1607	Dipeptide transport system permease protein DppB

Table 3.3 continued on next page

Table 3.3 continued

Gene	Product	Gene	Product
ES1_0510	Acetylornithine/acetyl-lysine aminotransferase	ES1_1608	Dipeptide-binding ABC transporter: periplasmic substrate-binding component
ES1_0511	Acetyl-lysine deacetylase	ES1_1609	Transcription regulator
ES1_0512	Hypothetical protein containing HAD-like domain	ES1_1610	Hypothetical protein
ES1_0528	Hypothetical protein	ES1_1611	Nitroreductase family protein
ES1_0529	Multiple sugar-binding transport ATP-binding protein	ES1_1612	Malate oxidoreductase
ES1_0530	Multiple sugar-binding transport inner membrane protein	ES1_1613	Succinyl-diaminopimelate desuccinylase (dapE)
ES1_0531	Multiple sugar-binding transport inner membrane protein	ES1_1614	Hypothetical protein
ES1_0532	Multiple sugar-binding transport solute-binding protein	ES1_1881	NDP-sugar dehydrogenase
ES1_0533	Transcriptional regulator	ES1_1882	NADH dependent dehydrogenase like protein
ES1_0534	Hypothetical protein	ES1_1883	Pyridoxal-phosphate-dependent aminotransferase
ES1_0535	Hypothetical protein	ES1_1884	Acetyl / acyl transferase-like protein
ES1_0536	Xylose isomerase-like protein	ES1_1885	Glycosyl transferase family protein 9
ES1_0537	Hypothetical protein	ES1_1886	Glycosyl transferase family protein 10
ES1_0538	Tungstate ABC transporter: periplasmic substrate-binding protein WtpA	ES1_1887	UDP-N-acetylglucosamine 2-epimerase
ES1_0539	Tungstate ABC transporter: permease protein WtpB	ES1_1888	Glycosyl transferase family protein 11
ES1_0540	Tungstate ABC transporter: ATP-binding protein WtpC	ES1_1889	Hypothetical protein
ES1_0556	CRISPR repeat Cas6-like RNA endoribonuclease	ES1_2028	Hypothetical protein
ES1_0557 to ES1_0559	All hypothetical proteins	ES1_2029	Hypothetical protein
ES1_0560	CRISPR-associated protein Cas5	ES1_2030	Putative glycosyl transferase
ES1_0561	Putative CRISPR-associated helicase Cas3	ES1_2031	Hypothetical protein
ES1_0571	Bipolar DNA helicase	ES1_2032	Glycosyl transferase family protein 12
ES1_0572	DNA double-strand break repair Mre11-like protein	ES1_2033	Glycosyl transferase family protein 13
ES1_0573	Chromosome segregation protein	ES1_2034	Glycosyl transferase family protein 14
ES1_0574	Single-stranded exonuclease	ES1_2035	Glycosyl transferase family protein 15

Table 3.3 continued on next page

Table 3.3 continued

Gene	Product	Gene	Product
ES1_0646 to ES1_0652	All hypothetical proteins	ES1_2036	Glycosyl transferase family protein 16
ES1_0665	SurE-like 5-nucleotidase	ES1_2037	NDP-sugar dehydrogenase
ES1_0666	Small neutral amino acid transporte	ES1_2038	Hypothetical protein containing oxidoreductase-domain
ES1_0667	Translation initiation factor IF-1A	ES1_2039	Pleiotropic regulatory protein: pyridoxal-phosphate-dependent aminotransferase
ES1_0668	Putative serine/threonine protein kinase: rio1 family	ES1_2040	Hypothetical protein containing Trimeric LpxA-like domain

Table 3.3. The presence of ORFs in strain ES1^T that were absent in *T. barophilus* was determined in SyMAP using the genome alignment function with default parameters.

Table 3.4 Comparison of ORFs Present in Select Thermococcales Species

	<i>Pyrococcus furiosus</i>	<i>Thermococcus sp. ES1</i>	<i>Pyrococcus sp. St04</i>	<i>Thermococcus sp. CL1</i>	<i>Pyrococcus abyssi</i>	<i>Pyrococcus horikoshii</i>	<i>Pyrococcus yayanosii</i>	<i>Pyrococcus sp. NA2</i>
Protein Catabolism								
alanine aminotransferase	PF1497	ES1_0366	Py04_1260	CL1_0451	PAB1810	PH1322	PYCH11820	PNA2_1901
glutamate dehydrogenase	PF1602	ES1_0048	Py04_1480	CL1_0542	PAB0391	PH1593	PYCH04880	PNA2_0178
Acid / Alcohol Production								
pyruvate oxidoreductase	PF0965-7 PF0971	ES1_1629-31 ES1_1635	Py04_1076-8	CL1_1243-5 CL1_1249	PAB1470, PAB1474-6	PH0678, PH0682, PH0684-5	PYCH06600-20, PYCH06660	PNA2_1292, PNA2_1296-8
2-ketoisovalerate oxidoreductase	PF0968-71	ES1_1632-35	Py04_1079-82	CL1_1246-9	PAB1470-3	PH0678-80	PYCH06630-60	PNA2_1292-5
formaldehyde:Fd oxidoreductase	PF1203	ES1_0748	Py04_1188	CL1_1348	PAB0798	PH1274	PYCH05360	PNA21850
aldehyde:Fd oxidoreductase	PF0346	ES1_1423	Py04_0091 Py04_0868	CL1_1347	PAB0647	PH1019	PYCH09430	PNA2_1543
acetyl-CoA synthetase	PF1540 PF1787	ES1_0772 ES1_1220 ES1_1296 ES1_1417	Py04_1410 Py04_1668	CL1_1587 CL1_0374	PAB0203, PAB1937	PH1739, PH1517	PYCH01760, PYCH07600	PNA2_0342, PNA2_0103
acyl-CoA synthetase	PF0532 PF1837	ES1_1122	Py04_0710 Py04_1719	CL1_1416 CL1_1666	PAB0226, PAB0854	PH0766, PH1787	PYCH01240, PYCH07060	PNA2_0392, PNA2_1406
alcohol dehydrogenase	PF0074 PF0075	ES1_0124 ES1_0229 ES1_1030	Py04_0301	-----	-----	-----	-----	PNA2_1382
formate dehydrogenase	PF1521	ES1_0097-100 ES1_1572-5	Py04_1234	CL1_0794	PAB1389 PAB2442	PH1353	PYCH11030	PNA2_1925 PNA2_1944

Table 3.4 continued on next page

Table 3.4 continued

	<i>Pyrococcus furiosus</i>	<i>Thermococcus sp. ES1</i>	<i>Pyrococcus sp. St04</i>	<i>Thermococcus sp. CL1</i>	<i>Pyrococcus abyssi</i>	<i>Pyrococcus horikoshii</i>	<i>Pyrococcus yayanosii</i>	<i>Pyrococcus sp. NA2</i>
Hydrogen Production								
formate:H ₂ lyase	-----	ES1_0102-6 ES1_1564-69	-----	-----	PAB1392-6	-----	PYCH11070-110	-----
NADH dehydrogenase	PF1441-53	ES1_0898-904	Py04_1295-307	CL1_0190-202	PAB0485-96	PH1446-56	PYCH11410-1530	PNA2_0032-44
hydrogenase, membrane	PF1423-36	ES1_1527-41 ES1_1542-54	Py04_1312-25	CL1_1129-42	PAB1884-95	PH1429-41	PYCH11230-360	PNA2_0015-28
hydrogenase I, cytoplasmic	PF0891-4	ES1_0094-5	Py04_0890-3	CL1_0141-5	PAB1784-7	PH1290-4	PYCH08370-400	PNA2_1665-8
hydrogenase II, cytoplasmic	PF1329-32	ES1_0172-5	Py04_1129-32	-----	PAB0638-41	-----	PYCH00020-50	PNA2_1551-5
Fd:NADH oxidoreductase	PF1327-8	ES1_1268-71	Py04_0009-10 Py04_0997-8 Py04_1133-4	CL1_0639-40	PAB1737-8	PH1873-4	PYCH00010, PYCH08330	PNA2_1556-7
ATP synthetase, membrane	PF0176-84	ES1_1787-94	Py04_0327-35	CL1_0928-36	PAB1181-6, PAB2378-9	PH1972-80	PYCH15690-760	PNA2_0831-8

Table 3.4. Putative genes encoding sugar and peptide catabolism and fermentation production in *Thermococcales spp.* Dashes indicate that no homologous gene was found. Homologs obtained through BlastP at NCBI.

SyMAP analysis showed that strain 4557 contains 81% of the open reading frames found in strain CL1^T. ORFs that appear in strain CL1^T but are absent in strain 4557 are largely hypothetical proteins but also include proteins utilized in saccharide catabolism (Table 3.5). The strain CL1^T genome sequence is distinct from other *Thermococcus* and *Pyrococcus* genomes in that it contains five clustered regularly interspaced short palindromic repeats (CRISPR) loci that are similar to, and yet distinct from, the two CRISPR-Cas systems in *Thermococcus kodakarensis* (Jung *et al.*, 2012a; Elmore *et al.*, 2013).

3.4 Description of *Thermococcus paralvinellae* sp. nov.

Thermococcus paralvinellae (par.al.vi.nel'lae. N.L. gen. n. *paralvinellae* referring to the polychaete *Paralvinella*).

Cells are flagellated irregular cocci and variable in size. Diameter 0.8–1.0 μm. Obligate anaerobe. Optimal growth occurs at 82°C (range 50°C to 91°C), pH 8.0 (range 5.0 to 8.3), and 3.23% total salt (range 0.96–6.46%). Elemental sulfur is not essential for growth, but stimulates growth and results in a higher growth yield. Hydrogen produced (> 2mM) at the absence of sulfur. Heterotrophic growth occurs on complex proteinaceous substrates (yeast extract, tryptone, casein), maltose, cellobiose, and a mixture of 20 amino acids when vitamins are present. No growth is observed by nitrate or sulfate reduction. 0.01% (wt vol⁻¹) yeast extract and vitamins are required for growth. Membrane lipids are composed of di- and tetraether phytanyl lipids. Resistant to chloramphenicol (100 μg/ml), streptomycin (100

Table 3.5 ORFs Found in *Thermococcus* sp. Strains CL1^T Without Homologs in *Thermococcus* sp. Strain 4557

Gene	Product	Gene	Product
CL1_0315 to CL1_0324	All hypothetical proteins	CL1_1087	Putative DNA-binding: iron metalloprotein endonuclease
CL1_0523 to CL1_0529	All hypothetical proteins	CL1_1088	Hypothetical protein
CL1_0530	Hypothetical protein containing PIN domain 13	CL1_1089	NAD kinase
CL1_0531	IS element ISTsi1 orfB trasposase	CL1_1090	Hypothetical protein
CL1_0532	Site-specific integrase-resolvase	CL1_1091	Hypothetical protein
CL1_0533	Hypothetical protein	CL1_1092	Nol1-nop2-sun family nucleolar protein III
CL1_0534	Hypothetical protein	CL1_1093 to CL1_1096	All hypothetical proteins
CL1_0535	Ribose-5-phosphate isomerase type A	CL1_1097	Putative transcription regulator: MarR family 2
CL1_0536	Hypothetical protein	CL1_1098	Hypothetical protein
CL1_0537	Threonine synthase 1	CL1_1099	Molybdopterin converting factor: subunit 1
CL1_0538	Hypothetical protein containing KH domain β -lactamase-domain protein	CL1_1100	Hypothetical protein
CL1_0539	Proteasome subunit β 1	CL1_1101	Hypothetical protein
CL1_0540	Hypothetical protein	CL1_1102	Molybdopterin converting factor subunit 2
CL1_0541	Hypothetical protein containing ion transport domain	CL1_1103	Hypothetical protein
CL1_0542	Glutamate dehydrogenase	CL1_1104	Hypothetical protein
CL1_0543	Sodium-dependent transporter	CL1_1105	Hypothetical protein containing adenosine specific kinase domain
CL1_0544	α -glucosidase related protein	CL1_1106	HamI-like protein
CL1_0545	Nitrogen regulatory protein P-II (lnB)	CL1_1107	Transcription regulator: AsnC family 2
CL1_0546	Glycogen branching enzyme	CL1_1108 to CL1_1114	All hypothetical proteins
CL1_0849	Hypothetical protein	CL1_1115	Hypothetical protein containing radical SAM domain
CL1_0850	Glycoside hydrolase family 57 protein	CL1_1170	Hypothetical protein

Table 3.5 continued on next page

Table 3.5 continued

Gene	Product	Gene	Product
CL1_0851 to CL1_0855	All hypothetical proteins	CL1_1171	Acylamino acid-releasing protein
CL1_0856	Glycosyl transferase family protein 2	CL1_1172 to CL1_1175	All hypothetical proteins
CL1_0857	Glycosyl transferase family protein 3	CL1_1176	SAM-dependent methyltransferase 1
CL1_0858	Lps biosynthesis rfbU-like protein	CL1_1177	Hypothetical protein containing peptidase_M19 domain
CL1_0859	Putative oligosaccharyl transferase: STT3 subunit 2	CL1_1178	Hypothetical protein
CL1_0860	Hypothetical protein	CL1_1179	Hypothetical protein
CL1_0875 to CL1_0879	All hypothetical proteins	CL1_1996	Putative pyridine nucleotide-disulfide oxidoreductase
CL1_0880	Hypothetical protein containing SAM domain 4	CL1_1997	Hypothetical protein containing isochorismatase domain
CL1_0881	Ribonuclease P protein component 2	CL1_1998	Glucose-1-dehydrogenase
CL1_0882	Glycogen synthase	CL1_1999	Putative deoxyhypusine synthase
CL1_0883	Putative transcription regulator: TrmB family	CL1_2001	Hypothetical protein
CL1_0884	Cyclomaltodextrinase	CL1_2002	Hypothetical protein
CL1_1062 to CL1_1070	All hypothetical proteins	CL1_2003	GNAT family acetyltransferase 5
CL1_1071	DNA-RNA helicase: superfamily II	CL1_2004	Hypothetical protein
CL1_1072 to CL1_1082	All hypothetical proteins	CL1_2005	Putative phosphohydrolase: HD superfamily
CL1_1083	Triosephosphate isomerase	CL1_2006 to CL1_2009	All hypothetical proteins
CL1_1084	Phosphopantetheine adenylyltransferase	CL1_2010	Molybdenum cofactor biosynthesis protein 2: MoeA
CL1_1085	Hypothetical protein	CL1_2011	Molybdenum cofactor biosynthesis protein MoeB
CL1_1086	Acyl-CoA synthetase (NDP forming): large subunit		

Table 3.5. The presence of ORFs in strain CL1^T that were absent in strain 4557 was determined in SyMAP using the genome alignment function with default parameters.

µg/ml), and vancomycin (100 µg/ml). G + C content is 40.8 mol% based on the total genome calculations. GenBank database accession number CP006965.

The type strain ES1^T (=DSM 27261 =KACC 17923) was isolated from a polychaete worm of the genus *Paralvinella* residing in a fragment of the black smoker, which was located at the depth of 2,200 m on the Endeavour Segment of the Juan de Fuca Ridge in the northeastern Pacific Ocean (47° 57' N, 129°06' W).

3.5 Description of *Thermococcus cleftensis* sp. nov.

Thermococcus cleftensis (cleft.en'sis. N.L. masc. adj. *cleftensis* referring to the Cleft segment of the Juan de Fuca Ridge).

Cells are irregular cocci. Diameter approximately 1 to 2 µm. Obligate anaerobe. Optimal growth occurs at 88°C within the range of 55–94°C. Elemental sulfur is not essential for growth, but significantly stimulates growth. Hydrogen (> 2mM) is produced in the absence of sulfur. Heterotrophic growth occurs on complex proteinaceous substrates (yeast extract, tryptone, casein), maltose, cellobiose, and a mixture of 20 amino acids when vitamins are present. 0.01% (wt vol⁻¹) yeast extract and vitamins are required for growth. G + C content is 55.8 mol% based on the total genome calculations. GenBank database accession number is CP003651.

The type strain CL1^T (=DSM 27260 =KACC 17922) was isolated from a polychaete worm of the genus *Paralvinella* residing in a fragment of black smoker, which was located at the depth of 2,350 m on the Cleft segment of the Juan de Fuca Ridge (44° 30' N, 130° 30' W).

CHAPTER 4

HYDROGEN PRODUCTION BY *PYROCOCCUS FURIOSUS* AND *THERMOCOCCUS PARALVINELLAE* ES1 GROWN ON SPENT BREWERY GRAIN AND RAW BOVINE MILK

4.1 Summary

Pyrococcus furiosus and *Thermococcus paralvinellae* grew without sulfur at 95°C and 82°C, respectively, and produced H₂ at rates of 5-36 fmol H₂ cell⁻¹ h⁻¹ on carbohydrate and peptide media with and without 10 mM acetate and low pH (pH 5), and on spent brewery grain and raw bovine milk. Thirteen enzyme activities were measured for redox reactions and ATP production from both organisms in five defined media and in 1% (vol/vol) milk. *P. furiosus* and *T. paralvinellae* produced H₂ *in vivo* at the same rates but methyl viologen-dependent membrane hydrogenase activities in *T. paralvinellae* were low compared with those in *P. furiosus* suggesting that *T. paralvinellae* may produce H₂ using different enzymes. Formate was detected in spent media while ethanol was not detected. Formate and alcohol dehydrogenase activities were very low to undetectable. After 100 hr, *P. furiosus* and *T. paralvinellae* produced up to 5.1 mmol of H₂ per liter of medium when grown on 0.1-10% (w/v) spent brewery grain and 0.1-10% (v/v) raw milk from cows undergoing treatment with the bacterial antibiotic Ceftiofur and from untreated cows. The amount of H₂ produced by *T. paralvinellae* increased with increasing waste concentrations, but decreased with *P. furiosus* above 1% concentrations. All mesophilic bacteria from

the un-incubated raw milk that grew on Luria Bertani, Sheep's Blood, and MacConkey agar plates were eliminated during incubation with the hyperthermophiles. The results demonstrate the potential of using hyperthermophilic heterotrophs for rapid agricultural waste remediation, pathogen removal, and biohydrogen production in a consolidated bioprocess.

4.2 Introduction

Nearly all food and agricultural waste in the U.S. enters landfills, making it the second largest contributor of material entering landfills (Levis *et al.*, 2010; Staley and Barlaz, 2009). It is increasingly being diverted to wastewater treatment facilities for anaerobic digestion to limit landfill growth (Diggelman and Ham, 2003; Lai *et al.*, 2009). The waste contains high concentrations of organic compounds and often harmful chemicals such as antibiotics and hormones (Bougrier *et al.*, 2007; Ntaikou *et al.*, 2010; Wang and Wan, 2009) that foul wastewater treatment equipment leading to increasing restrictions on entering waste content (Lee *et al.*, 2007). Biological pre-treatment of large organic molecules by fermentative organisms lowers the high organic carbon load in waste, lowers wastewater treatment costs, and can produce bioenergy to partially offset costs (Angenent *et al.*, 2004; Ntaikou *et al.*, 2010; Wang and Wan, 2009). Conceivably, hyperthermophilic heterotrophs could be used to consolidate wastewater heat treatment and organic remediation in a single step to decrease costs while removing pathogens and producing H₂ as an energy product (Angenent *et al.*, 2004; Bougrier *et al.*, 2007; Girguis and Holden, 2012).

Pyrococcus and *Thermococcus* species are commonly studied hyperthermophilic heterotrophs (Atomi *et al.*, 2011). They catabolize carbohydrates and peptides and produce acetate, CO₂, and H₂S from elemental sulfur. Some species, such as *Pyrococcus furiosus* and *Thermococcus paralvinellae*, produce significant amounts of H₂ in lieu of H₂S in the absence of sulfur (Fiala and Stetter, 1986; Hensley *et al.*, 2014). Complete genome sequences (Robb *et al.*, 2001; Jung *et al.*, 2014) and biochemical characterizations (Sapra *et al.*, 2003; Kim *et al.*, 2010) suggest these organisms produce H₂ on their cytoplasmic membrane and link this to the formation of an electrochemical gradient and ATP synthesis across the membrane. *T. paralvinellae* contains genes for putative CO-, formate-, and F₄₂₀-hydrogenases that are absent from *P. furiosus*, in addition to NADH- and ferredoxin-dependent hydrogenases in both organisms, suggesting the organisms have different pathways for H₂ generation. Hydrogenase, alcohol dehydrogenase, and formate dehydrogenase activities as well as H₂, ethanol, and formate concentrations increased in *T. paralvinellae* when cultures were shifted from growth on 15 g/l to 1 g/l of sulfur indicating the organism has multiple mechanisms for electron disposal in the absence of sulfur (Ma *et al.*, 1995).

While the catabolic and energy generation pathways of *P. furiosus* and *T. paralvinellae* are reasonably well established (Figure 4.1), their physiology under adverse bioreactor conditions (e.g., low pH, high acetate concentrations) are poorly understood. In this study, the growth and H₂ production rates, the production of other metabolites, and the activities of 13 redox and ATP synthesis enzymes were measured for these organisms on varying carbon sources and suboptimal reactor

Figure 4.1: Proposed Redox and ATP synthesis enzyme reactions in *P. furiosus* and *T. paralvinellae*.

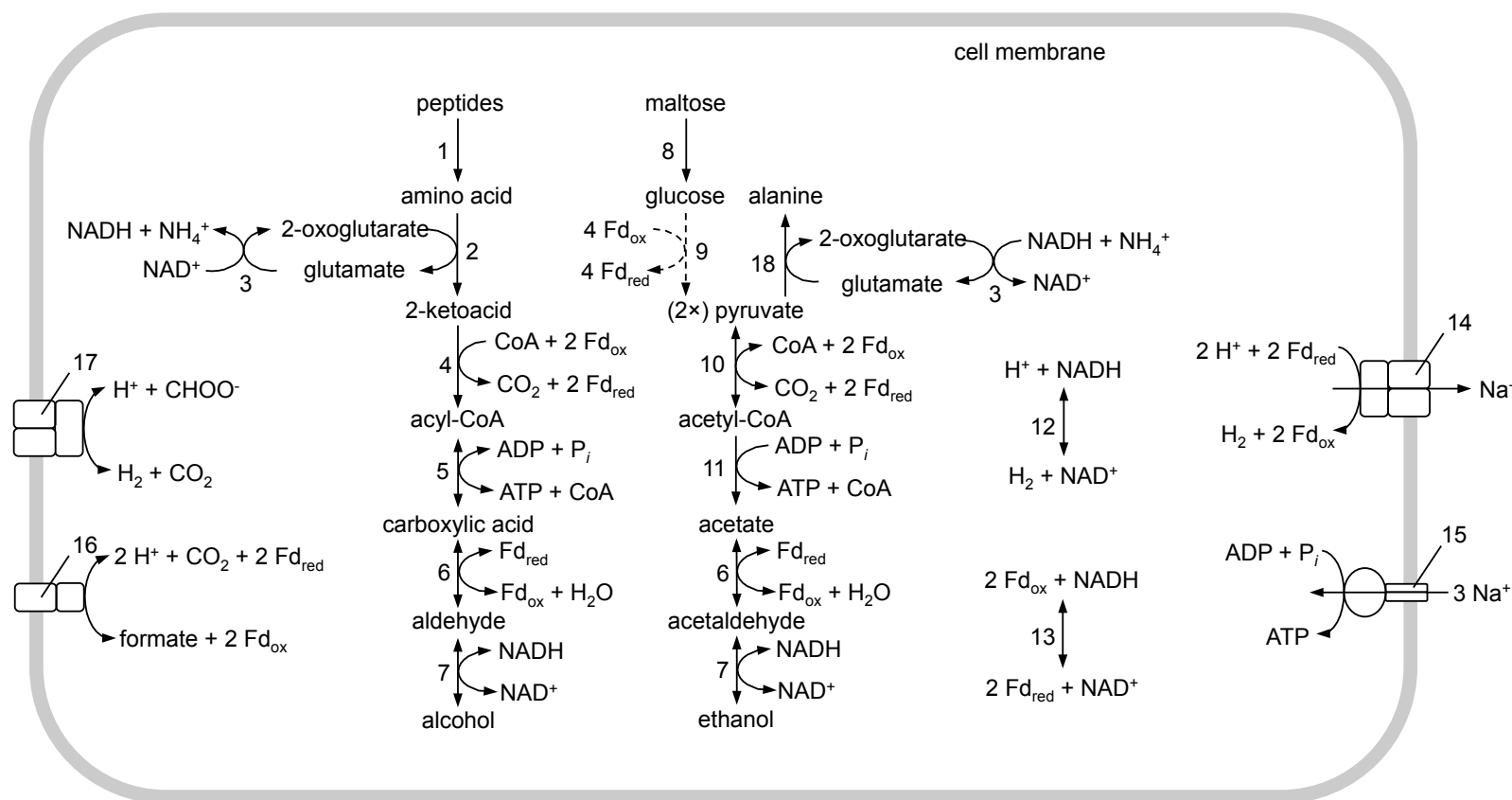


Figure 4.1. The enzymes are as follows: 1, membrane hydrogenase; 2, cytoplasmic hydrogenase; 3, membrane ATP synthase; 4, NADH:Fd oxidoreductase; 5, glutamate dehydrogenase; 6, alanine aminotransferase; 7, pyruvate:Fd oxidoreductase; 8, isovalderate:Fd oxidoreductase; 9, ADP-forming acetyl-CoA/acyl-CoA synthetase; 10, aldehyde:Fd oxidoreductase; 11, formaldehyde:Fd oxidoreductase; 12, alcohol dehydrogenase; 13, formate:Fd oxidoreductase (*T. paralvinellae* only). Fd, electron carrier ferredoxin.

conditions. These organisms were also grown on spent brewery grain and raw milk from cows treated with Ceftiofur and untreated cows. Ceftiofur is a heat-labile antibiotic used to treat mastitis in dairy cattle (Sunkara *et al.*, 1999), which we sought to remove from the milk during growth of the hyperthermophiles. This study also reports the rates of H₂ production by *P. furiosus* and *T. paralvinellae* when grown on these wastes and the efficacy of removing mesophilic bacteria, protein, and carbohydrates from the raw milk wastes. The results establish the feasibility of using these organisms for agricultural waste remediation with concomitant H₂ production.

4.3 Materials and Methods

4.3.1 Organisms used

Pyrococcus furiosus (DSM 3638) was obtained from the Deutsche Sammlung für Mikroorganismen und Zellkulturen (Braunschweig, Germany). *Thermococcus paralvinellae* ES1 (DSM 27261) was from the Holden lab hyperthermophile culture collection.

4.3.2 Growth conditions

The media for growth were modified from a medium used previously (Adams *et al.*, 2001). The base medium was composed of the following (per liter): 28 g of NaCl, 3.5 g of MgSO₄ • 7H₂O, 2.7 g of MgCl₂ • 6H₂O, 0.33 g of KCl, 0.25 g of NH₄Cl, 0.14 g of CaCl₂ • 2H₂O, 1 g of NaHCO₃, 0.1 ml of 100 mM Na₂WO₄ • 2H₂O, 1 ml of Adams

mineral solution (Adams *et al.*, 2001), 50 μ l of 0.5% (wt/vol) resazurin, 0.5 g of cysteine-HCl \cdot H₂O, and 0.5 g of Na₂S \cdot 9H₂O. For defined media experiments, different carbon sources were added to the base medium solution. The carbohydrate (C) medium contained 0.5% (wt/vol) maltose and 0.01% (wt/vol) yeast extract (enzymatic, Difco). The carbohydrate-acetate (C+A) medium contained 0.5% maltose, 0.01% yeast extract, and 10 mM sodium acetate. The peptide (P) medium contained 0.5% (wt/vol) casein hydrolysate and 0.01% yeast extract. The carbohydrate-peptide (C+P) medium contained 0.5% maltose, 0.05% casein hydrolysate, and 0.01% yeast extract. To examine growth at low pH, carbohydrate medium was pH balanced to 5.00 ± 0.05 at room temperature (C5 medium) before the addition of 1 mM potassium phosphate buffer (pH 5.0). All other media were pH balanced to 6.80 ± 0.05 at room temperature before the addition of 1 mM potassium phosphate buffer (pH 6.8). The defined media culture bottles each contained 20 mL of medium in a 60 mL serum bottle with 1 atm of N₂ in the headspace. Growth was also tested on 0.5% (wt/vol) lactose + 0.01% yeast extract in base medium as a follow-up to the raw milk growth experiments described below.

For the waste media experiments, one of three waste types was added as a carbon source to the base medium above. The milk medium contained 0.1%, 1% or 10% (vol/vol) raw bovine milk obtained fresh from a local dairy farm (Barstow Farms, Hadley, MA). The raw milk was from cows that had been treated with Ceftiofur within the previous 48 h and from untreated cows. The grain medium contained 0.1% 1% or 10% (wt/vol) spent brewery grain from a local brewery (Amherst Brewing Company, Amherst, MA). Initial COD of 10% waste was 357 ± 6 g

(mean \pm SE) in raw milk from untreated cows, 363 ± 3 g in raw milk from treated cows, and 334 ± 3 g in spent grain waste. Milk and grain that not used within 12 h was frozen at -20°C . The waste media bottle experiments contained 50 ml of medium in a 120 ml serum bottle with 1 atm of N_2 in the headspace.

All cultures were incubated in an oven without stirring at 95°C for *P. furiosus* and 82°C for *T. paralvinellae*. The serum bottles were inoculated with a logarithmic growth-phase culture that had been grown and transferred at least three successive times in bottles on the medium used so that cultures were adapted to that medium. For the defined media experiments, 12 serum bottles were inoculated concurrently and a pair of bottles was removed during growth until the cultures reached stationary growth phase. For the waste media experiments, triplicate bottles were inoculated and subsampled every 12 h for up to 100 h. Cell concentrations were measured using a Petroff-Hausser counting chamber and phase-contrast light microscopy. The specific growth rate (μ) of the culture was determined by a best-fit curve through the logarithmic portion of the growth data.

Cultures were also grown in duplicate in a 20-liter bioreactor for each defined media type and for 1% raw milk from Ceftiofur-treated cows. The media were flushed with $\text{N}_2\text{-CO}_2$ (80%:20%) at a flow rate of 60 ml/min, stirred at 120 to 150 rpm, and heated to $95^{\circ}\text{C} \pm 0.1^{\circ}\text{C}$ for *P. furiosus* and $82^{\circ}\text{C} \pm 0.1^{\circ}\text{C}$ for *T. paralvinellae*. With the exception of the low pH condition ($\text{pH } 5.0 \pm 0.1$), the pH of the bioreactor media at the incubation temperature was 7.2 and was maintained (± 0.1 pH unit) by the automatic addition of 5% (wt/vol) NaHCO_3 . Cells from the bioreactor were harvested when they reached late logarithmic growth phase. The

medium was drained from the bioreactor through a glass cooling coil bathed in an ice-water-slurry into a carboy. The cells were then concentrated to less than 2 liters by ultrafiltration using a hollow fiber cartridge (0.2- μm pore size; Amersham Biosciences), except cells grown on the milk due to flocculation in the medium, and further concentrated by centrifugation at $10,000 \times g$ for 45 min. The resulting pellets were resuspended in an anoxic chamber in < 5 ml of degassed 50 mM Tris buffer (pH 8.0) plus 2 mM of sodium dithionite (DT), sealed in a N_2 -flushed serum bottle, and frozen at -20°C .

4.3.3 Metabolite measurements

Metabolite measurements were only performed on bottle experiments. Aliquots (100 μl) of headspace from each bottle at each time point were used to measure the amount of H_2 present using a gas chromatograph (Shimadzu GC-8A) equipped with a TCD, a 60/80 Carboxen 1000 column (Supelco) and Ar as the carrier gas. Hydrogen yields per cell ($Y_{p/x}$) were determined by plotting H_2 concentrations against cell concentrations for each set of time points within a growth curve. Specific H_2 production rates (q) were calculated from $(Y_{p/x} \times \mu)/0.693$, and maximum H_2 production rates (r_{max}) were calculated from the product of q times the maximum cell concentration (cell_{max}). For defined media experiments, soluble metabolites were measured after 18 h of incubation using ultra-fast liquid chromatography (Shimadzu) and a refractive index detector. A 1.5 ml aliquot was transferred into an Eppendorf microfuge tube and spun at 14,000 rpm for 5 min. The supernatant was decanted and filtered through a 0.22 μm pore

size filter (13 mm diameter, GVPP, Millipore) and 100 μ l of 1 M H₂SO₄ was added to 1 ml of filtrate. Samples were run through an Aminex HPX-87H ion exclusion column (300 mm \times 7.8 mm, Bio-Rad) with guard column (BioRad microguard Cation H) with 5 mM H₂SO₄ as the mobile phase. The column was kept at 30°C with a 0.6 ml/min flow rate and a 30 min sampling time.

4.3.4 Protein fractionation

All sample transfers and manipulations were carried out in an anoxic chamber and buffers were degassed with N₂. Stored cells were allowed to warm to room temperature and 2 μ g ml⁻¹ of DNase I were added. The cell suspension was mixed for 30 min. The sample vial was then placed in an ice-water slurry and sonicated for 30 min (Fisher Scientific, Sonic Dismembrator 500). Phase-contrast microscopy confirmed cell lysis. The cell suspension was spun in a centrifuge at 100,000 $\times g$ for 45 min. The supernatant was removed as the soluble protein fraction and the pellet was resuspended in buffer after being homogenized with a glass tissue grinder. The suspension was spun at 100,000 $\times g$ for 45 min as before and resuspended three times to wash the pellet. After the final spin, the pellet was resuspended in 1 ml of buffer. This was used as the insoluble protein fraction. The protein concentrations of the soluble protein fractions were determined spectrophotometrically using the Bradford assay (Bradford, 1976). The protein concentrations of the insoluble protein fractions were determined using the DC Protein Assay kit (Bio-Rad). Bovine serum albumin was used as the standard for

both procedures. Protein fractions that were not used immediately for enzyme activity assays were flash frozen in liquid N₂ and stored at -80°C.

4.3.5 Enzyme assays

Enzyme activities are expressed as units where 1 U is equal to 1 μmol of substrate transformed min⁻¹. The buffer used for all assays was 100 mM EPPS buffer (pH 8.4) and the assay temperature was 80°C, unless otherwise noted. At least three technical replicates were run for each assay. For enzyme assays containing benzyl viologen (BV) or methyl viologen (MV), a trace amount of 2 mM sodium dithionite (DT) was added to slightly reduce the buffer. The amount of all reagents used is given as the final concentration in the reaction vial.

The following anaerobic enzyme activity assays were performed using the insoluble protein fraction and were contained in rubber stopper-sealed serum vials (8 ml volume) that had been degassed and flushed with N₂. Membrane-bound hydrogenase (H₂ase mem) (Sapra *et al.*, 2000) activity was determined by following the H₂ evolution rate in a discontinuous assay using 3 mM MV reduced with 30 mM DT as the electron donor. H₂ was measured by gas chromatography as described above. Membrane-bound ATP synthase (Pisa *et al.*, 2007) activity was determined by following the phosphate evolution rate in a discontinuous assay by adding 2.5 mM sodium ATP after 4 min of initial incubation to 100 mM MES-100 mM Tris buffer (pH 6.0) containing 5 mM MgCl₂ and 200 mM KCl. The reaction was stopped after 2, 4 and 6 min by placing the serum vial on ice. The concentration of the

inorganic phosphate produced was measured spectrophotometrically as described previously (Heinonen and Lahti, 1981).

The following anaerobic enzyme activity assays were measured spectrophotometrically using the soluble protein fraction and were contained in rubber stopper-sealed glass cuvettes that had been degassed and flushed with N₂. Cytoplasmic hydrogenase (H₂ase cyto) (Bryant and Adams, 1989; Ma *et al.*, 2000) activity was determined by measuring the reduction of 1 mM BV at 600 nm [$\epsilon = 7,400 \text{ (M}\cdot\text{cm)}^{-1}$] under an H₂-CO₂ (80:20) headspace. Pyruvate:ferredoxin (Fd) oxidoreductase (POR) (Blamey and Adams, 1993) and 2-ketoisovalerate:Fd oxidoreductase (VOR) (Heider *et al.*, 1996) activities were determined by measuring the reduction of 1 mM MV [$\epsilon = 12,000 \text{ (M}\cdot\text{cm)}^{-1}$] and 1 mM BV, respectively, in an assay mixture that contained 2 mM MgCl₂, 0.4 mM thiamine pyrophosphate (TPP), and 0.2 mM coenzyme A (CoA). Pyruvate (10 mM) and 5 mM 2-ketoisovalerate were used as the substrates, respectively. Aldehyde:Fd oxidoreductase (AOR) (Mukund and Adams, 1991) and formaldehyde:Fd oxidoreductase (FOR) (Roy *et al.*, 1999) activities were determined by measuring the reduction of 3 mM BV at 600 nm using 0.5 mM crotonaldehyde and 0.25 mM formaldehyde, respectively, as the substrate. Fd:NADH oxidoreductase (FNOR) (Ma and Adams, 2001b) activity was determined by measuring the reduction of 3 mM BV at 600 nm in 50 mM CAPS buffer (pH 10.3) using 0.4 mM NADPH as the substrate. Alcohol dehydrogenase (ADH) (Ma and Adams, 1999) was determined by measuring the reduction of 10 mM NADP⁺ at 340 nm [$\epsilon = 6,220 \text{ (M}\cdot\text{cm)}^{-1}$] using 0.1 mM ethanol as the substrate. Alanine aminotransferase (AlaAT) (Ward *et al.*, 2000) activity was determined by measuring

the pyruvate evolution rate in a discontinuous assay by adding sample after 4 min of initial incubation to 100 mM KCl, 20 mM 2-ketoglutarate, 50 μ M pyridoxal-5'-phosphate, and 50 mM L-alanine. The reaction was stopped after 2, 4, and 6 min by placing the serum vial on ice. The amount of pyruvate in each vial was determined aerobically at room temperature using a lactate dehydrogenase assay that contained 100 mM potassium phosphate (pH 7.0), 0.4 mM NADPH, and 50 U of LDH from rabbit muscle.

The following aerobic enzyme activity assays were performed using the soluble protein fraction and were measured spectrophotometrically in glass cuvettes. Glutamate dehydrogenase (GDH) (Robb *et al.*, 1992) activity was determined by measuring the reduction of 0.4 mM NADP⁺ at 340 nm [$\epsilon = 6,220$ (M \cdot cm)⁻¹] using 6 mM sodium glutamate as the substrate. ADP-forming acetyl-CoA synthetase (ACS) (Hutchins *et al.*, 2001; Bräsen and Schönheit, 2004) activity was determined by measuring the production of DTNB-CoA by adding sample to 100 mM MOPS buffer (pH 7.0), 0.25 mM DTNB, 5 mM MgCl₂, 1 mM ADP, 5 mM K₂HPO₄, and 0.2 mM acetyl-CoA.

4.3.6 Waste remediation

To determine which portion of the milk waste was degraded during growth of the hyperthermophiles, 1% raw milk from Ceftiofur treated cows and untreated cows were inoculated separately with each organism and incubated as before along with uninoculated triplicate controls. A 1.5 ml aliquot was removed from each serum bottle every 12 h for soluble protein and reducing sugar measurements. For

protein measurements, 1 ml of sample was filtered through a 0.22 µm pore size filter (13 mm diameter, GVPP, Millipore) and the protein in the filtrate was measured using the Bradford assay. For the reducing sugar measurements, 0.5 ml of sample and 0.5 ml of dinitrosalicylic acid solution (DNS) were heated to 100°C for 5 min, cooled in ice for 5 min, and then absorbance measured at 545 nm with lactose used as standard. The DNS was composed of the following (per liter): 7.06 g of 3,5-dinitrosalicylic acid, 13.2 g of sodium hydroxide, 204 g of Rochelle salt, 5.53 g of sodium metabisulfite, and 5.06 ml phenol (boiled). Uninoculated controls determined if indigenous microbes were effecting waste content or H₂ production.

To determine if pathogens were removed from the milk, 1% raw milk from Ceftiofur-treated cows and untreated cows that was less than 48 h old, as well as base medium without an additional carbon source, were plated via a dilution-to-extinction method onto Luria Bertani, Sheep's Blood, and MacConkey agar plates both prior to and after 100 h of incubation with *T. paralvinellae* at 82°C. Technical triplicates of each media, time point, and agar plate type were run. The number of colony forming units per ml of inoculum was determined for all plates. To determine if Ceftiofur was present in raw milk before and after incubation, samples of undiluted raw milk from treated and untreated cows, as well as samples of 1% raw milk media, were tested utilizing the SNAP beta-lactam ST test kit (Waldron, 2013) before and after 100 hr of incubation.

4.3.7 Statistical analysis

Results were subjected to statistical analyses in R (R Core Team, 2013). The enzyme activity, metabolite production, and colony-forming-unity yields were compared using analysis of variance (ANOVA) and Tukey's Honestly Significant Difference test ($\alpha = 0.05$). The mean of at least three replicates are reported as means \pm standard error (SE). For brevity, the results of the Tukey tests are presented in Appendix A.

4.4 Results

4.4.1 Growth and metabolite production in defined media

Both cultures grew and produced H₂ in all waste media (Figure 4.2) and defined media (Figure 4.3) tested, except in the 0.5% lactose +0.01% yeast extract medium for both organisms. For both cultures in defined media bottle experiments, the C+P medium produced the largest cell_{max} and r_{max} (Table 4.1). For *T. paralvinellae*, this condition also showed the largest q (specific H₂ production rate) ($F_4=330.6, p<0.001$). In contrast for *P. furiosus*, the C+A medium showed the largest q , which was only significantly higher than the C medium (Table 4.1; $F_4=14.8, p<0.01$).

When comparing between the two organisms, the culture with maximum H₂ production differed greatly when comparing defined and waste medias. That is to say, *P. furiosus* produced more H₂ than *T. paralvinellae* in defined medium (Figure 4.2), but *T. paralvinellae* seemed to out perform *P. furiosus* especially with the brewery waste (Figure 4.3). However, we only measured H₂ production on defined

wastes for a maximum of 18 hrs, where the cultures were not in stationary phase for an extended period of time. It is possible that the results would have differed drastically if we had allowed the cultures to remain in stationary phase on defined wastes.

While H₂ was the primary metabolite produced, both organisms also produced acetate and formate (Table 4.2). Acetate production was highest in C+P and C+A media for *P. furiosus* and in P medium for *T. paralvinellae*. Overall, *P. furiosus* produced more formate than *T. paralvinellae*. Other metabolites produced were succinate, butyrate, and isovalerate at much lower concentrations (Table 4.2). As expected, these were mostly detected when casein hydrolysate was provided as a growth substrate. Ethanol production was not detected in any medium tested for either organism.

4.4.2 Growth and H₂ production in waste media

Macroscopically, there was clarification of spent brewery grain and raw milk media following 100 h of incubation at 82°C with *T. paralvinellae*, but not in the uninoculated control bottle incubated at the same temperature (Figure 4.4). Microscopically, neither *P. furiosus* nor *T. paralvinellae* were preferentially associated with the cellulose fibers of the spent brewery grain (Figure 4.5). The cell could not be accurately counted when grown on the spent brewery grain, and cell counts were highly variable when grown on milk due to precipitation and clumping of the milk at high temperatures.

Figure 4.2: Hydrogen Production by *P. furiosus* and *T. paralvinellae* on Defined Wastes

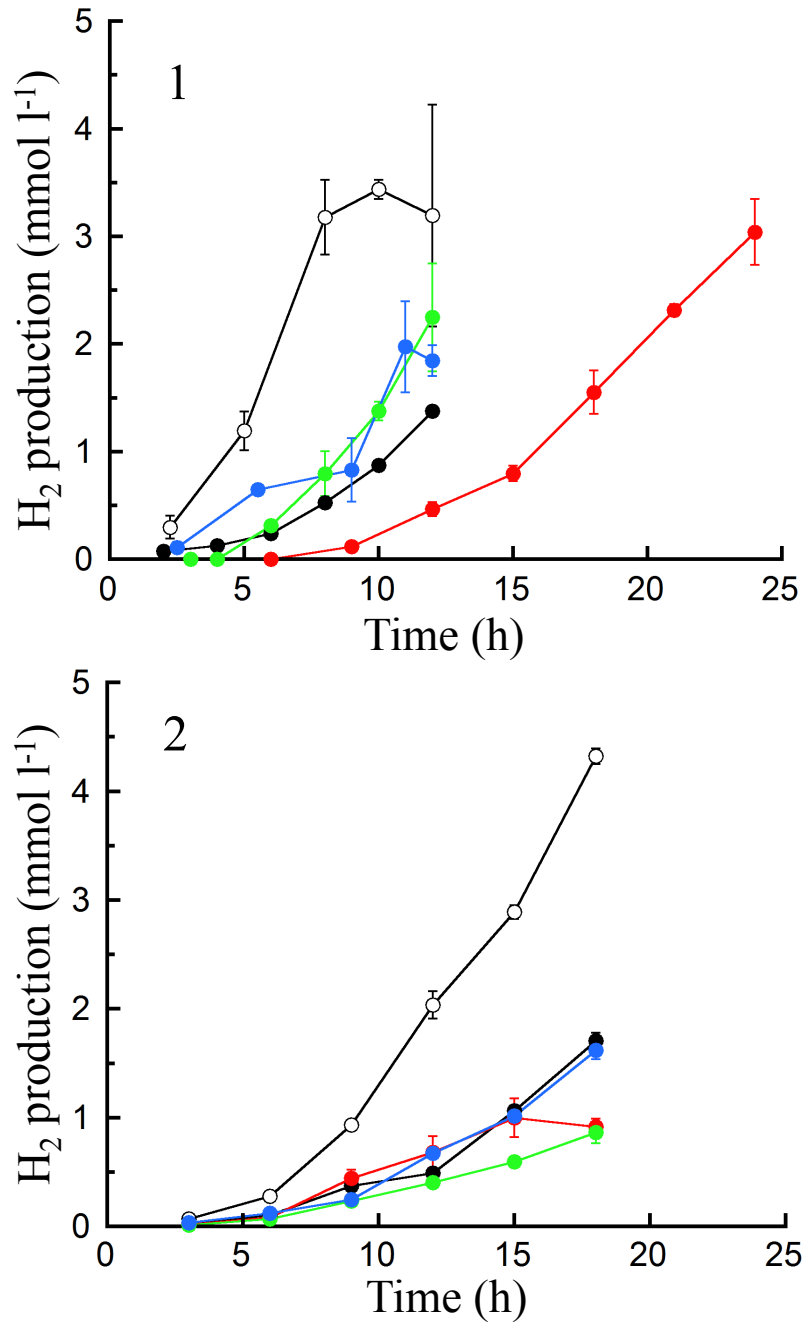


Figure 4.2. H₂ production by *P. furiosus* (1) and *T. paralvinellae* (2) in C medium (●), P medium (●), C+P medium (○), C+ A medium (●), and C5 medium (●). Error bars represent the standard error.

Figure 4.3: Hydrogen Production by *P. furiosus* and *T. paralvinellae* on Agricultural Wastes

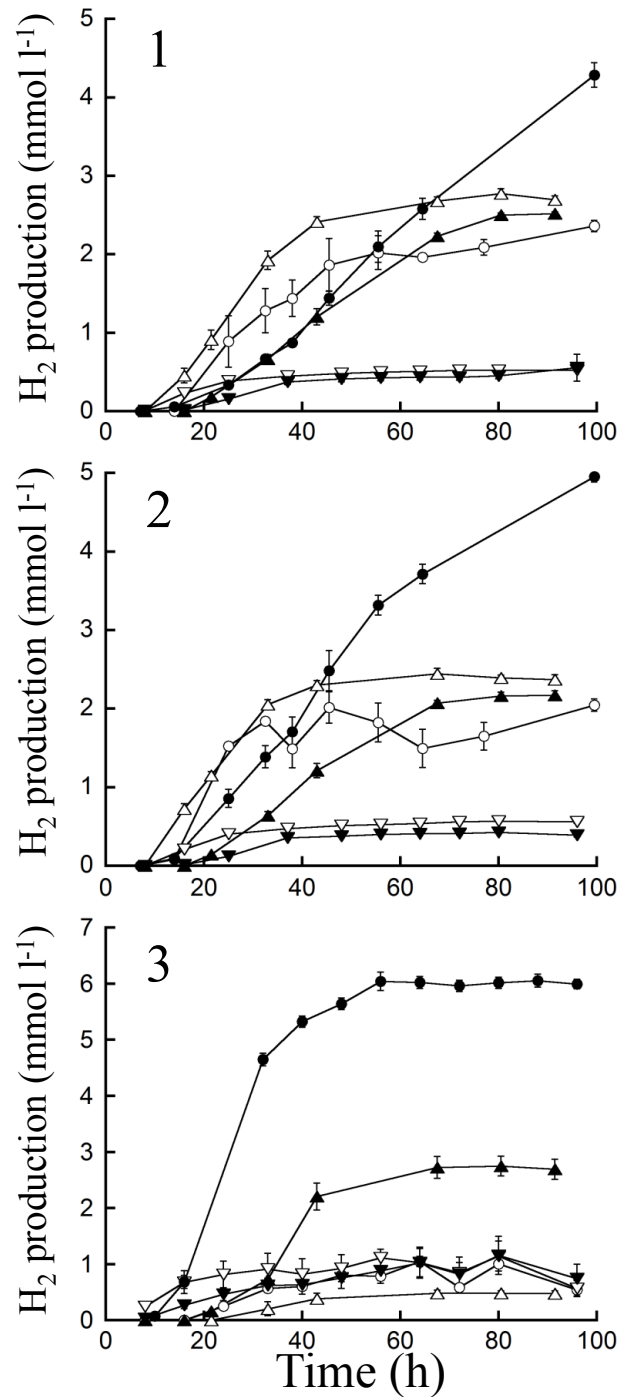


Figure 4.3: H₂ production by *P. furiosus* (open symbols) and *T. paralvinellae* (filled symbols) when grown on raw milk from cows treated with Ceftiofur (1), raw milk from untreated cows (2), and spent brewery grain (3). The concentrations of raw milk (vol/vol) and spent grain (wt/vol) used were 10% (○, ●), 1% (△, ▲), and 0.1% (▽, ▼).

Table 4.1 Kinetic Parameters for *P. furiosus* and *T. paralvinellae* on Various Defined Media (\pm 95% Confidence Interval)

Kinetic parameter ^z	C	P	C+P	C+A	C5	<i>p</i> -value
<i>P. furiosus</i> :						
μ (h ⁻¹)	0.43 \pm 0.05	0.31 \pm 0.07	0.49 \pm 0.12	0.54 \pm 0.11	0.39 \pm 0.08	NS
cell _{max} ($\times 10^8$, ml ⁻¹)	1.0 ^{a,b}	0.6 ^b	1.9 ^a	0.4 ^b	0.8 ^b	**
$Y_{p/x}$ (fmol H ₂ cell ⁻¹)	11 \pm 1 ^a	42 \pm 3 ^{a,b}	17 \pm 3 ^{a,b}	46 \pm 22 ^b	17 \pm 5 ^{a,b}	**
q (fmol H ₂ cell ⁻¹ h ⁻¹)	7 \pm 1 ^a	19 \pm 4 ^{a,b}	12 \pm 4 ^{a,b}	36 \pm 20 ^b	10 \pm 4 ^{a,b}	**
r_{max} (mmol H ₂ liter ⁻¹ h ⁻¹)	0.7 \pm 0.1 ^a	1.1 \pm 0.2 ^a	2.3 \pm 0.7 ^b	1.4 \pm 0.8 ^{a,b}	0.7 \pm 0.3 ^a	*
<i>T. paralvinellae</i> :						
μ (h ⁻¹)	0.45 \pm 0.08	0.35 \pm 0.08	0.34 \pm 0.07	0.37 \pm 0.05	0.35 \pm 0.07	NS
cell _{max} ($\times 10^8$, ml ⁻¹)	1.3 ^a	0.6 ^b	1.3 ^a	0.8 ^b	0.5 ^b	*
$Y_{p/x}$ (fmol H ₂ cell ⁻¹)	13 \pm 2 ^a	16 \pm 3 ^a	32 \pm 5 ^b	10 \pm 1 ^a	32 \pm 5 ^b	***
q (fmol H ₂ cell ⁻¹ h ⁻¹)	8 \pm 2 ^a	8 \pm 3 ^a	16 \pm 4 ^b	5 \pm 1 ^a	16 \pm 4 ^b	***
r_{max} (mmol H ₂ liter ⁻¹ h ⁻¹)	1.1 \pm 0.2 ^{a,b}	0.5 \pm 0.2 ^a	2.0 \pm 0.4 ^b	0.4 \pm 0.1 ^a	0.8 \pm 0.2 ^a	**

Table 4.1: ^z μ , specific growth rate; cell_{max}, maximum cell concentration; $Y_{p/x}$, product yield coefficient per cell; q , specific H₂ production rate; r_{max} , maximum H₂ production rate. * $p < 0.05$, ** $p < 0.01$, and *** $p < 0.001$. Tukey post-hoc test indicates groups whose members are not significantly different ^{a,b}. NS: no significance.

Table 4.2 Product Formation by *P. furiosus* and *T. paralvinellae* After 18 Hr of Growth on Defined Media

Product (mM)	C	P	C+P	C+A	C5	<i>p</i> -value
<i>P. furiosus</i>						
H ₂	2.00 ± 0.00 ^a	1.71 ± 0.08 ^a	4.92 ± 0.47 ^b	5.51 ± 1.18 ^b	3.71 ± 0.16	***
acetate	0.95 ± 0.05 ^a	0.06 ± 0.05 ^b	1.14 ± 0.27 ^a	1.66 ± 0.28	0.79 ± 0.06 ^a	**
formate	2.14 ± 0.08	0 ^a	0.01 ± 0.01 ^a	1.51 ± 0.25	0 ^a	***
isovalerate	0 ^a	0.46 ± 0.00 ^b	0.28 ± 0.28 ^b	0 ^a	0 ^a	***
succinate	0.14 ± 0.01 ^a	0.10 ± 0.00 ^a	0 ^b	0.22 ± 0.16 ^a	0 ^b	**
butyrate	0	0	0.01 ± 0.00	0	0	NS
<i>T. paralvinellae</i>						
H ₂	0.47 ± 0.04 ^a	0.76 ± 0.02	1.18 ± 0.00	0.29 ± 0.01 ^a	0.05 ± 0.01	***
acetate	0.20 ± 0.01 ^a	1.14 ± 0.09	0.30 ± 0.03 ^a	0.69 ± 0.00	0.01 ± 0.00	***
formate	0 ^a	0.54 ± 0.06	0 ^a	0 ^a	0	***
isovalerate	0 ^a	0.31 ± 0.00	0.02 ± 0.01	0 ^a	0 ^a	***
succinate	0 ^a	0.24 ± 0.01	0 ^a	0 ^a	0 ^a	***
butyrate	0 ^a	0 ^a	0 ^a	0.06 ± 0.00	0 ^a	***

Table 4.2: Mean product formation (mM) ± SE after 18 hr of incubation with the uninoculated control values subtracted out. * *p* < 0.05, ** *p* < 0.01, and *** *p* < 0.001. Tukey post-hoc test indicates groups whose members are not significantly different ^{a,b} NS: no significance.

For all waste types, *T. paralvinellae* produced higher amounts of H₂ with increasing concentration of waste (Figure 4.3). For *P. furiosus*, the amount of H₂ produced from 1% raw milk was higher than the amount for both 0.1% and 10% raw milk (Figure 4.3). *T. paralvinellae* produced significantly more H₂ on spent brewery grain than *P. furiosus* ($F_5=1298, p<0.001$) (Figure 4.3). *T. paralvinellae* produced more H₂ than *P. furiosus* in all waste conditions tested except 0.1% raw milk from Ceftiofur-treated cows and 1% raw milk from untreated cows. Growth and H₂ production did not significantly change for either microorganism between raw milk from cows treated with Ceftiofur and from untreated cows.

4.4.3 Remediation of raw milk waste

When 1% raw milk was incubated with *P. furiosus* and *T. paralvinellae*, the concentration of soluble protein decreased to undetectable concentrations for both organisms within 24 h for *P. furiosus* and within 48 h for *T. paralvinellae*, and was significantly lower than the soluble protein concentrations in uninoculated bottles for both *P. furiosus* ($F_3=7.12, p<0.01$) and *T. paralvinellae* ($F_3=5.29, p<0.05$) (Figure 4.6). Both organisms produced the same H₂ yield from the milk. The amount of reducing sugars in the milk (Figure 4.7) and the total COD decreased over time (Figure 4.8), but the concentrations were not significantly different from those in uninoculated bottles.

Dilution-to-extinction plating of 1% raw milk showed that milk from Ceftiofur-treated cows and untreated cows contain similar concentrations of bacteria prior to incubation (Table 4.3). The exception was that there were colony-

Figure 4.4: Clarification of Agricultural Waste Media with 100hr of Incubation

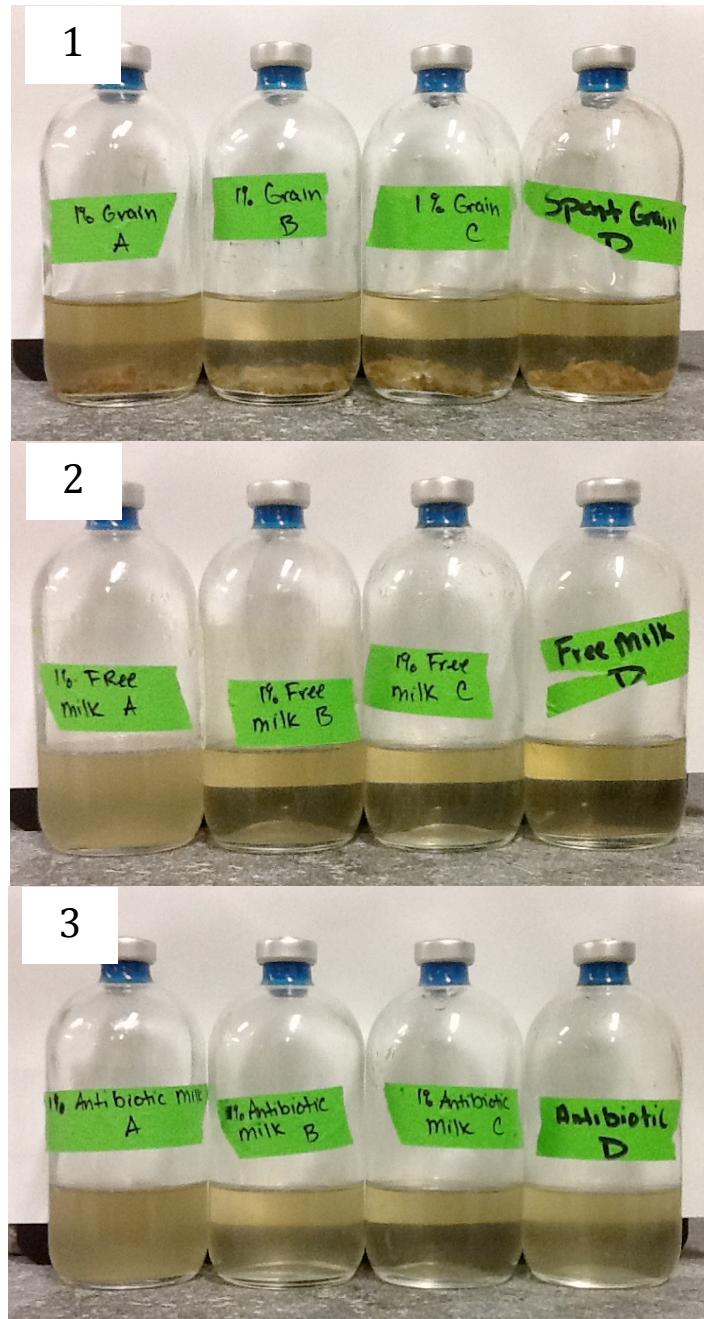


Figure 4.4: Clarification of media containing 1% (wt/vol) spent brewery grain 1% (1), (vol/vol) raw milk from untreated cows (2), and 1% (vol/vol) raw milk from cows treated with Ceftiofur (3) following 100 h of incubation at 82°C. Far left bottle was an uninoculated control, while the three remaining bottles were inoculated with *T. parvalvinellae* prior to incubation. Photos taken of shaken bottles.

Figure 4.5: Microscopy of *P. furiosus* and *T. parvalinellae* Cells in the Presence of Spent Grain

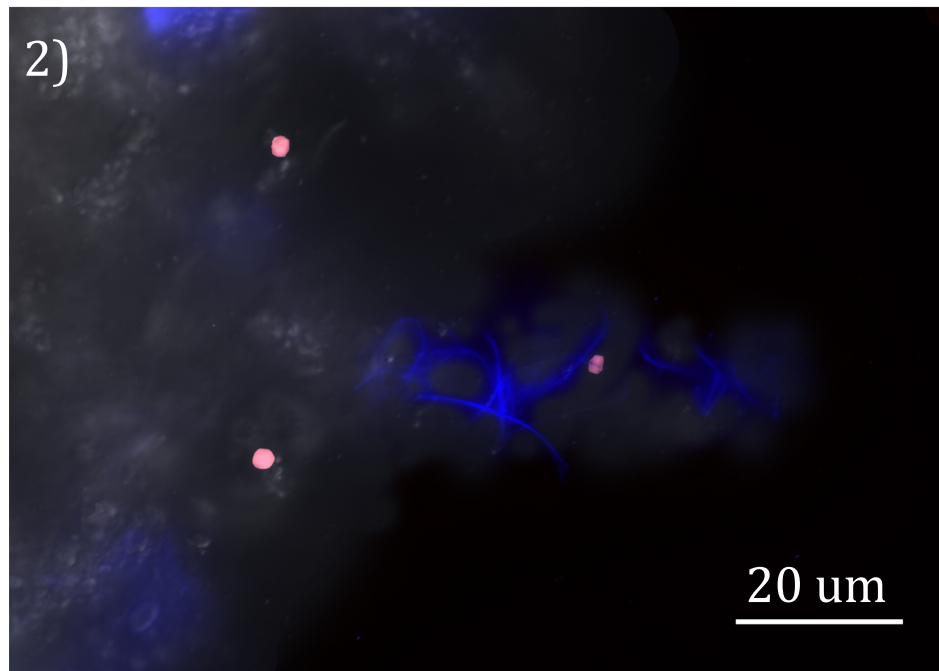
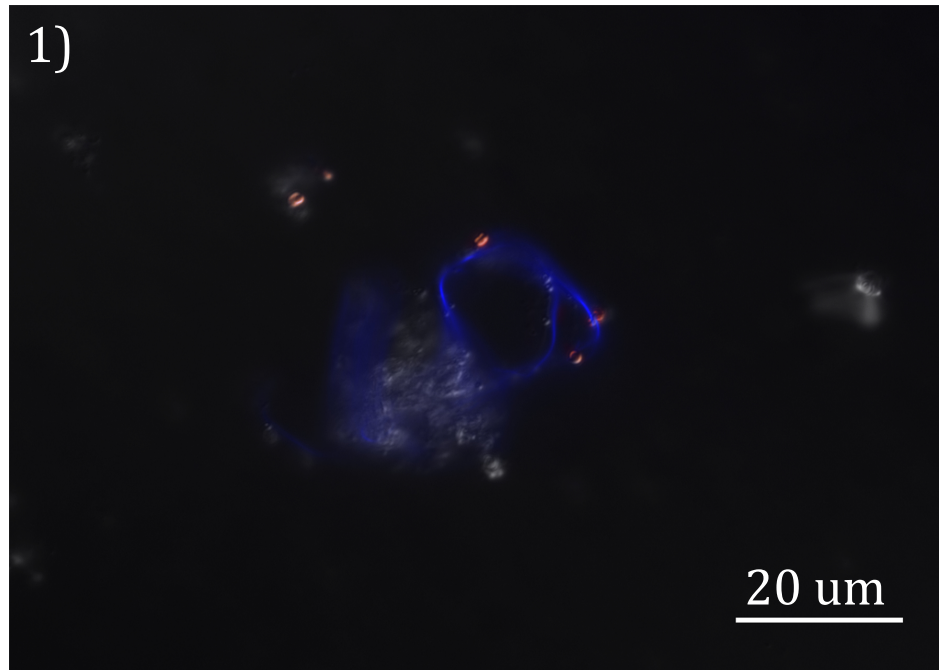


Figure 4.5: *P. furiosus* (1) and *T. parvalinellae* (2) cells at 100X magnification in a DIC field with 10% (w/vol) spent grain stained with CFW (blue). Selected cells are artificially highlighted with red. Scale bar is 20 microns.

Figure 4.6: Protein Degradation Concomitant with Hydrogen Production by *P. furiosus* and *T. paralvinellae* on 0.1% (vol/vol) Raw Milk Media

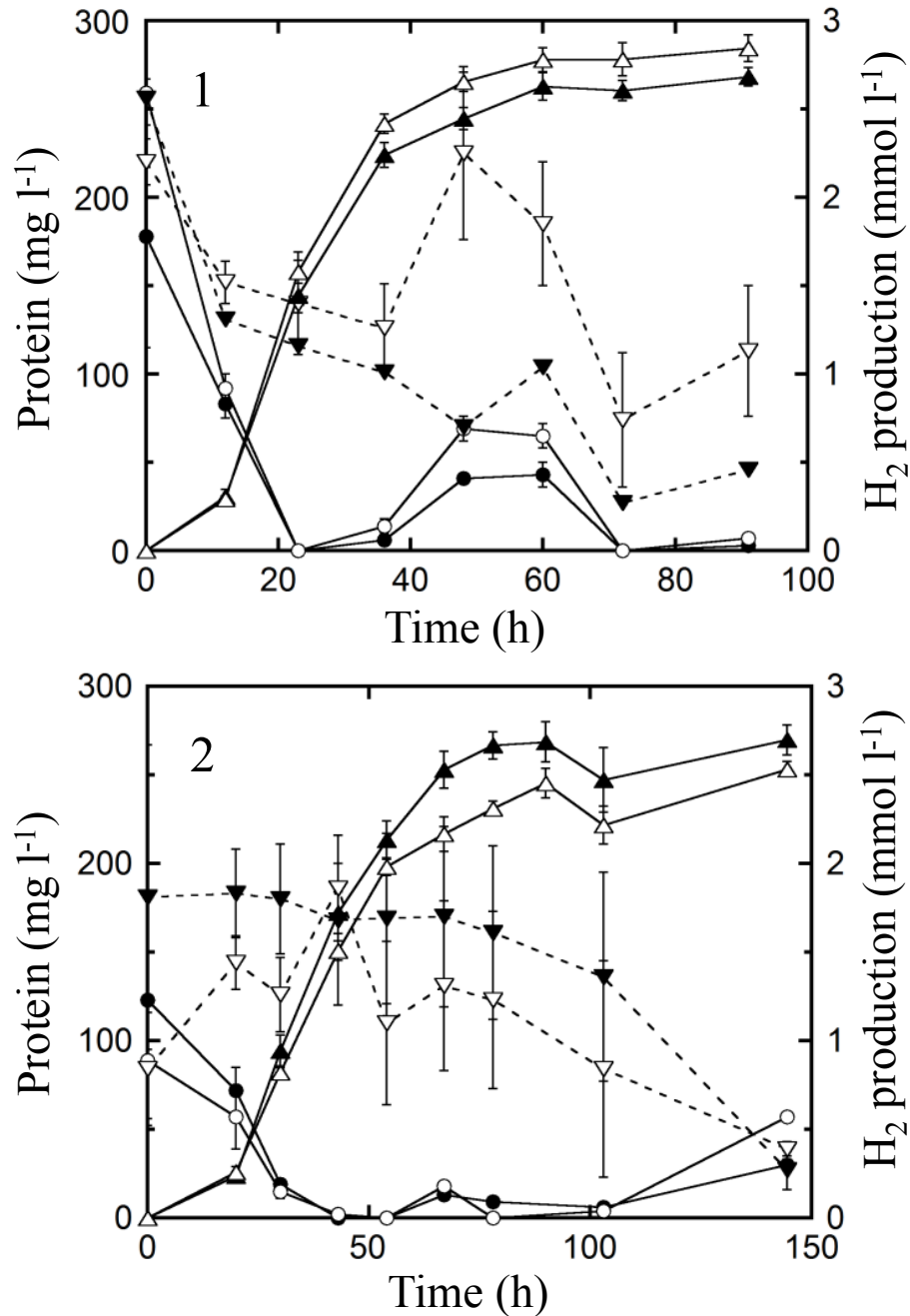


Figure 4.6: Protein degradation and H₂ production by *P. furiosus* (1) and *T. paralvinellae* (2) in 0.1% (vol/vol) raw milk from Ceftiofur-treated cows (open symbols) and untreated cows (filled symbols). The data show protein amounts from inoculated bottles (○, ●) and from uninoculated controls (∇, ▼) as well as H₂ amounts from inoculated bottles (Δ, ▲). There was no H₂ production in uninoculated bottles. Error bars represent the standard error.

Figure 4.7: Reducing Sugar Assay for *P. furiosus* and *T. parvalvinellae* on 0.1% (vol/vol) Raw Milk Media

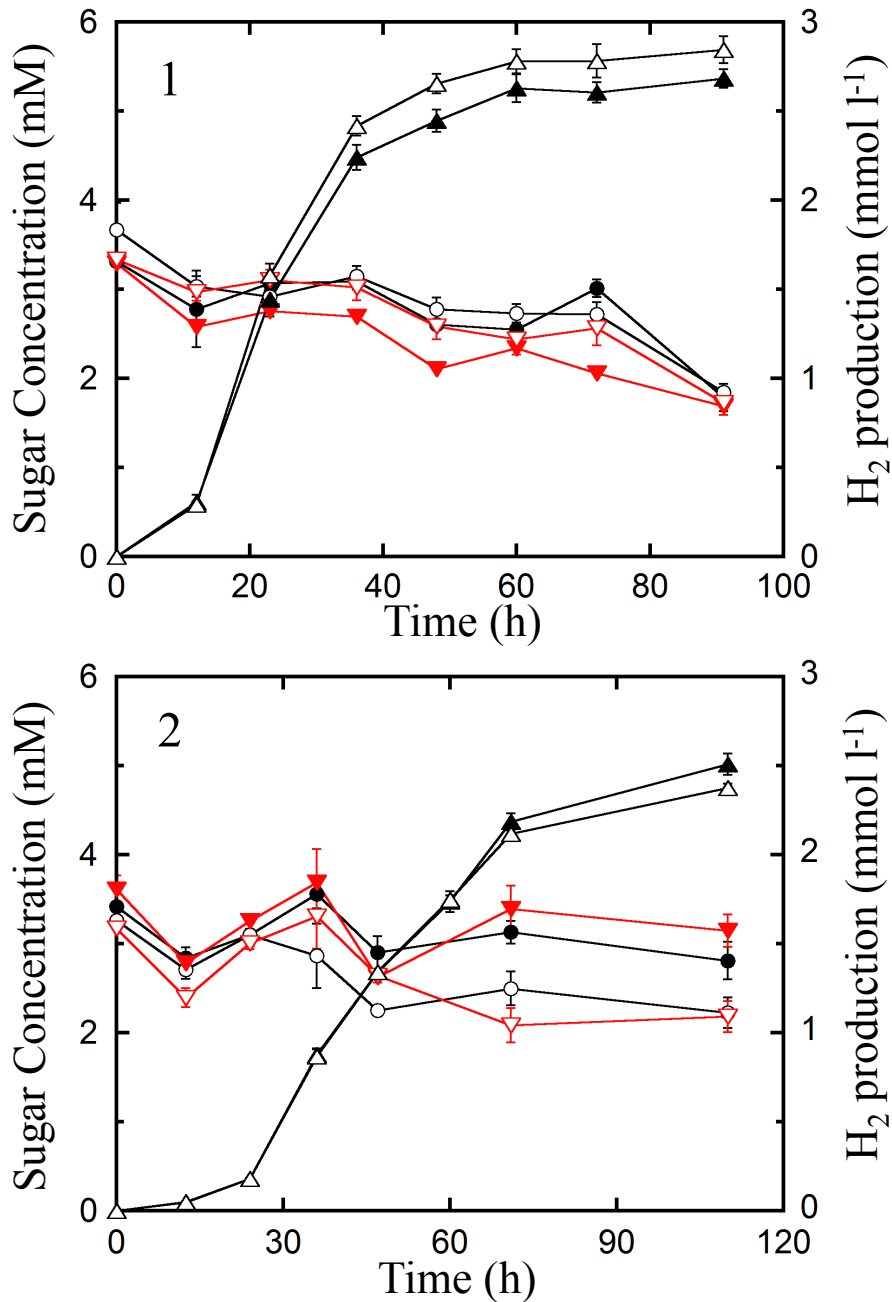


Figure 4.7: Sugar degradation and H₂ production by *P. furiosus* (1) and *T. parvalvinellae* (2) in 0.1% (vol/vol) raw milk from Ceftiofur-treated cows (open symbols) and untreated cows (filled symbols). The data show reducing sugar amounts from inoculated bottles (○, ●) and from uninoculated controls (∇, ▼) as well as H₂ amounts from inoculated bottles (Δ, ▲). There was no H₂ production in uninoculated bottles. Error bars represent the standard error.

forming units found on MacConkey agar plates from untreated cows that were completely absent from plates from cows treated with Ceftiofur. All plate types showed no colony forming units from medium that had been incubated with *T. paralvinellae* for 100 h at 82°C (Table 4.3). The plate experiment was only performed with *T. paralvinellae* since without contaminate growth at 82°C, it is highly unlikely that there will be contaminate growth at 95°C.

4.4.4 Growth in a 20-liter bioreactor

Specific growth rates of *P. furiosus* on each of the defined media increased significantly in the bioreactor relative to growth in serum bottles (Figure 4.9). For *T. paralvinellae*, specific growth rates increased in the bioreactor relative to bottles when the cultures were grown on C and P media. Otherwise, specific growth rates on the other three defined media were unchanged. As seen in the bottles, the growth rate in the bioreactor of *P. furiosus* on P medium was much lower than rates on C and C+P media, while there was no difference in the growth rates in these media with *T. paralvinellae* (Figure 4.10).

4.4.5 Enzyme activities

A summary and individual replicates of all specific enzyme activities are provided in Table 4.4 and Figure 4.11, respectively. Overall, enzymatic activities in both organisms changed the most when cells were grown under stressful conditions. *P. furiosus* and *T. paralvinellae* showed the largest dissimilarity in enzyme activities when grown on C+A medium (11 of 13 enzymes for both organisms) and C5 medium (6 of 13 activities for *T. paralvinellae* and 2 of 13

Figure 4.8: COD Measurements of *P. furiosus* and *T. parvalinellae* Grown on 0.1% (vol/vol) Raw Milk Media

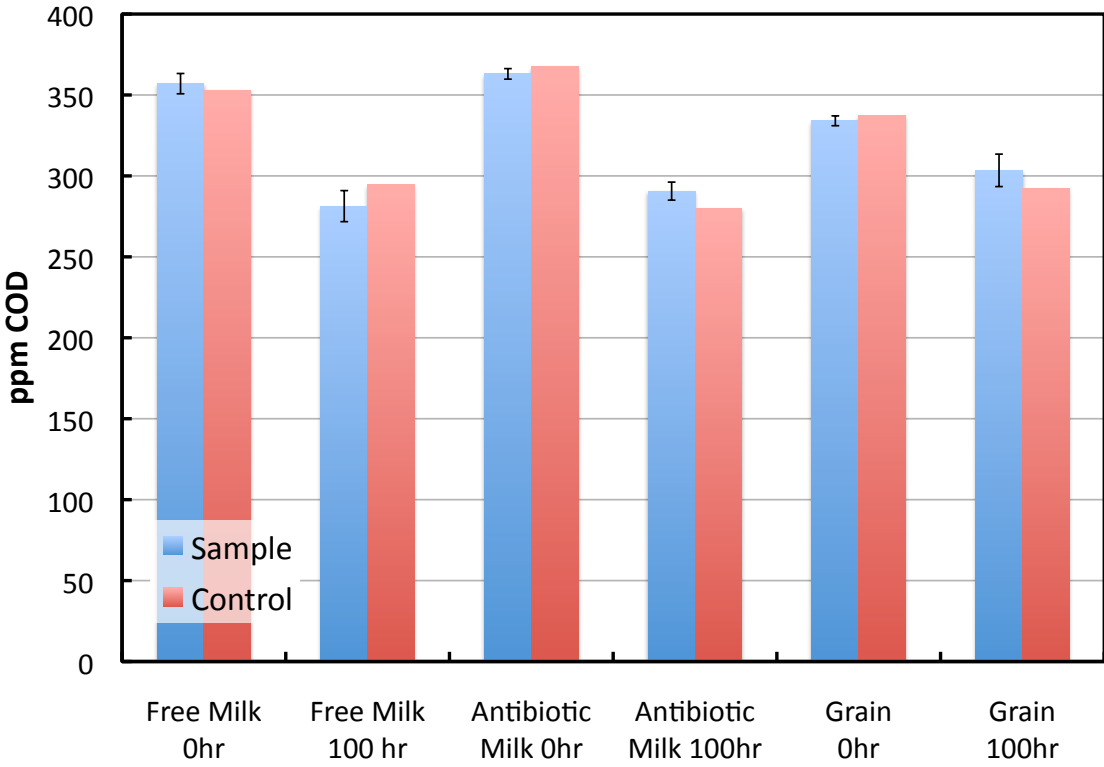


Figure 4.8: Samples were measured in triplicate and controls in duplicate. Error bars \pm SE. There were no significant differences between sample and control.

Table 4.3: Eradication of Culturable Microbes in 10% Raw Milk Media After 100hr of Incubation

Treatment	Luria Broth (x10 ³)	Sheep's Blood			MacConkey	
		α (x10 ²)	β (x10 ²)	λ (x10 ²)	Fermenter	Non- fermenter
0 h:						
Ceftiofur-treated	5.7 ± 4.2*	7.0 ± 3.0	2.0 ± 0.3	93 ± 77	0	0
Untreated	4.4 ± 3.7*	4.3 ± 3.8	4.6 ± 2.8	2.6 ± 1.2	3 ± 3	66 ± 56
Control	0	0	0	0	0	0
100 h:						
Ceftiofur-treated	0	0	0	0	0	0
Untreated	0	0	0	0	0	0
Control	0	0	0	0	0	0

Table 4.3: Mean colony forming units (\pm standard error, $n = 3$) per ml of fresh (< 2 h old) 1% (vol/vol) raw milk from Ceftiofur-treated and untreated cows in base medium, and base medium without a carbon source. * $p < 0.01$ compares ceftiofur-treated and untreated cows.

Figure 4.9: Growth Rates of *P. furiosus* and *T. parvalinellae* Grown in Bottles and 20-liter Bioreactors

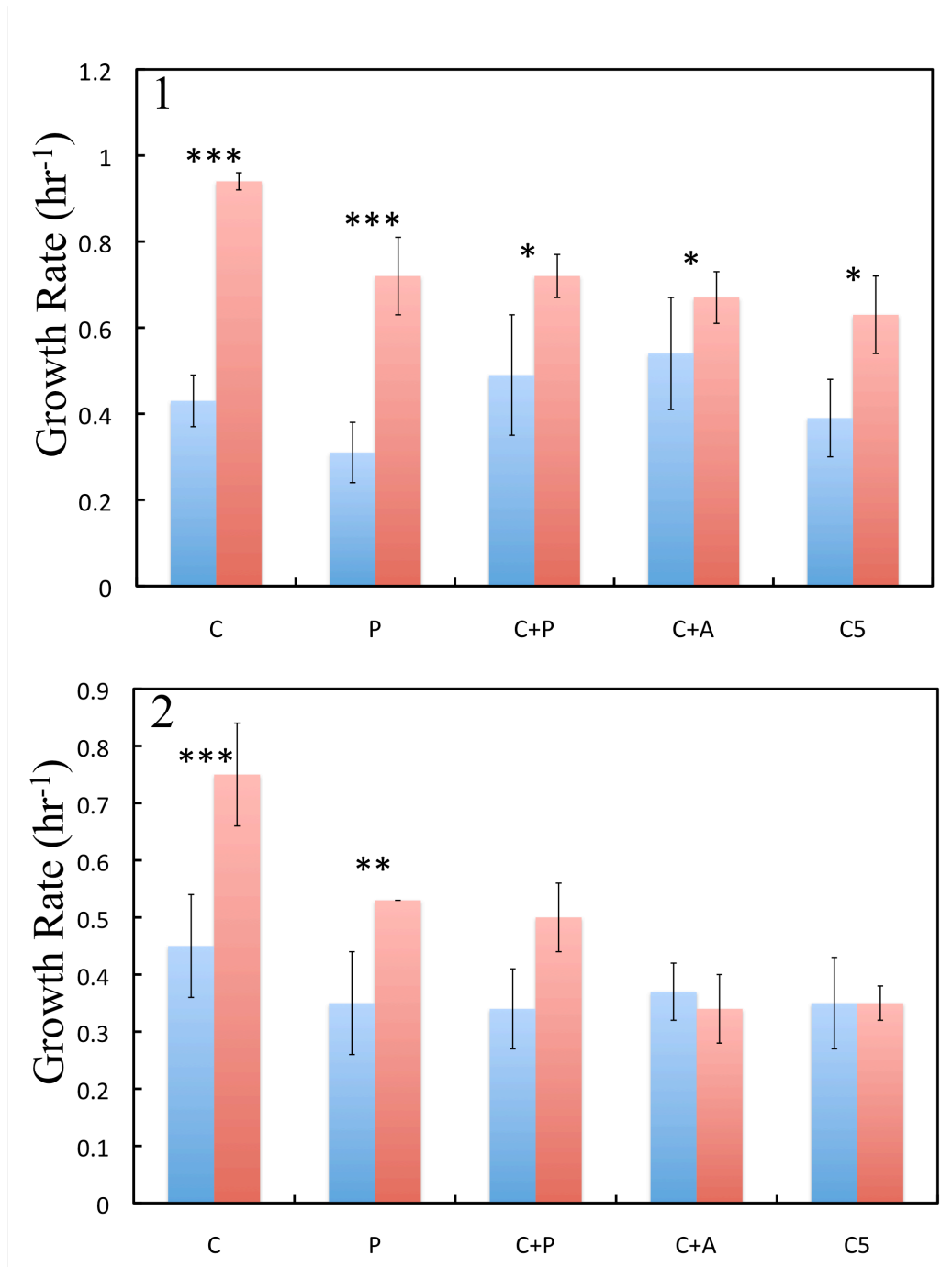


Figure 4.9: Growth rate (hr⁻¹) of *P. furiosus* (1) and *T. parvalinellae* (2) in 50 mL bottles (blue) and the 20-liter bioreactor (red) with the five defined media types. Error bars represent ± 1 SE. * $p < 0.05$, ** $p < 0.01$, and *** $p < 0.001$.

Figure 4.10: Growth of *P. furiosus* and *T. paralvinellae* in the 20-liter Bioreactor on Defined and Agricultural Media

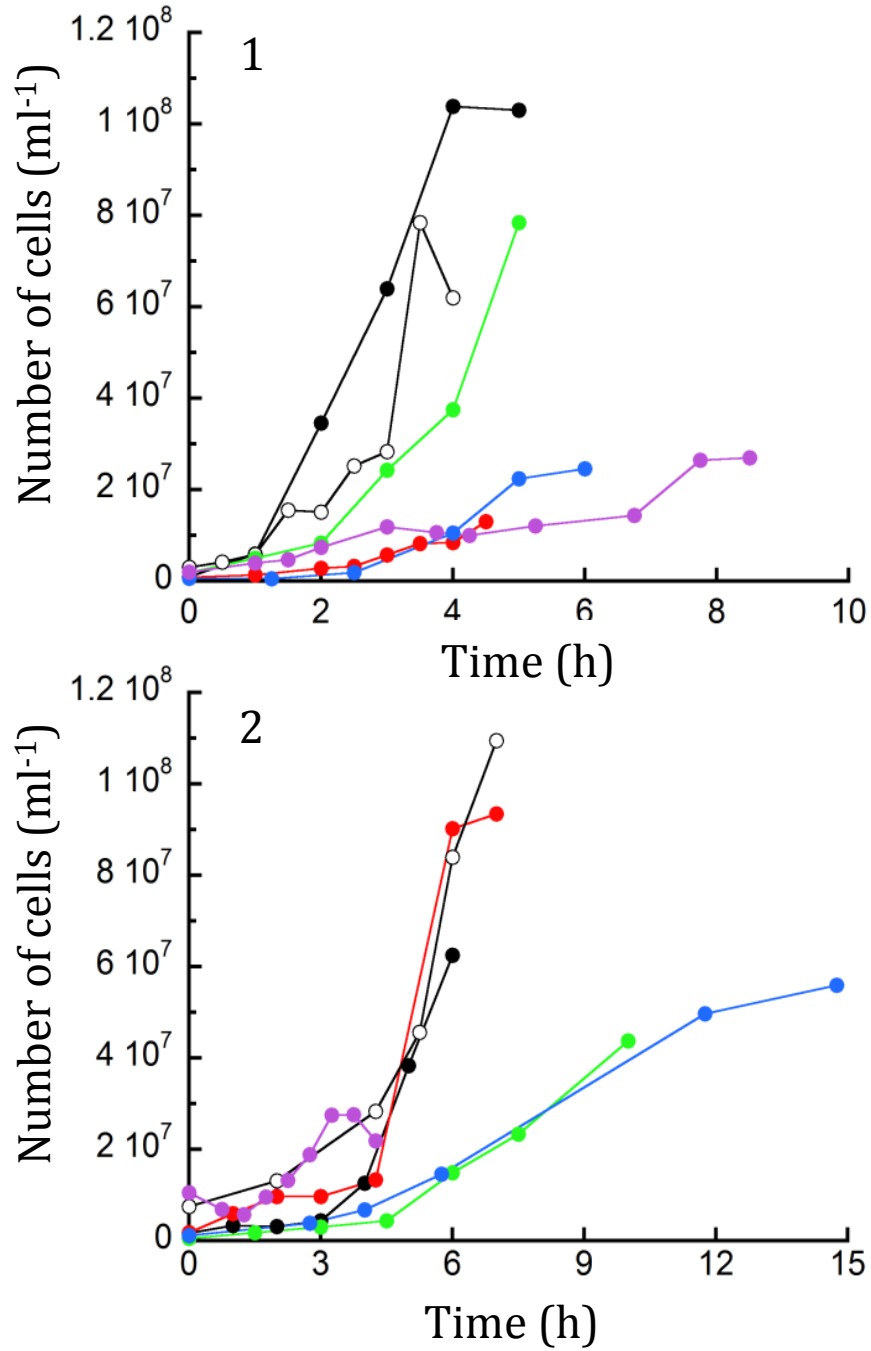


Figure 4.10: Growth of *P. furiosus* (1) and *T. paralvinellae* (2) in the 20-liter bioreactor in C medium (●), P medium (●), C+P medium (○), C+A medium (●), C5 medium (●), and 0.1% (vol/vol) raw bovine milk (●).

Table 4.4. *P. furiosus* and *T. parvalinellae* Specific Enzyme Activities

Enzyme	C	C+P	P	C+A	C5	1% raw milk	<i>p</i> -value
<i>P. furiosus</i>							
H ₂ ase (mem)	4.99 ± 0.31 ^a	12.74 ± 0.24 ^b	9.55 ± 0.50 ^{a,b}	11.42 ± 0.19 ^b	5.39 ± 0.40 ^{a,b}	ND	**
H ₂ ase (cyto)	1.27 ± 0.11 ^{a,b,c}	3.44 ± 0.49	0.73 ± 0.19 ^{a,c,d}	1.48 ± 0.29 ^{a,b,e}	0.15 ± 0.05 ^{d,f}	0.52 ± 0.023 ^{c,e,f}	***
ATP synthase	0.05 ± 0.00 ^a	0.70 ± 0.22	0.01 ± 0.01 ^a	0 ^a	0 ^a	ND	*
FNOR	6.10 ± 0.60 ^a	4.59 ± 0.48 ^a	3.90 ± 0.32 ^{a,b}	3.83 ± 0.47 ^{a,b}	0.31 ± 0.12 ^b	3.16 ± 1.59 ^{a,b}	***
GDH	1.85 ± 0.36 ^a	4.69 ± 0.42 ^b	9.90 ± 1.08 ^c	0.69 ± 0.08 ^a	0.91 ± 0.09 ^a	0.68 ± 0.16 ^a	***
AlaAT	0.54 ± 0.25	2.59 ± 1.76	3.05 ± 0.61	0.72 ± 0.14	0.36 ± 0.05	0.54 ± 0.29	NS
POR	2.27 ± 0.43	0.72 ± 0.03 ^a	0.93 ± 0.10 ^a	0.85 ± 0.09 ^a	0.30 ± 0.02 ^a	0.01 ± 0.01 ^a	***
VOR	1.88 ± 0.23 ^a	0.56 ± 0.12 ^{b,c}	2.01 ± 0.45 ^a	0.56 ± 0.06 ^{b,d}	1.35 ± 0.05 ^{a,b,d}	0.11 ± 0.05 ^{c,d}	***
ACSI+II	0.87 ± 0.09 ^{a,b,c}	1.15 ± 0.24 ^a	1.30 ± 0.12 ^b	0.68 ± 0.09 ^{a,c}	0.57 ± 0.04 ^{a,c}	0.44 ± 0.19 ^c	***
AOR	0.36 ± 0.04 ^a	0.24 ± 0.01 ^{a,b,d}	0.12 ± 0.03 ^{b,c,d}	0.26 ± 0.07 ^{a,c}	0.08 ± 0.02 ^d	0.06 ± 0.02 ^d	***
FOR	0.47 ± 0.08	0.36 ± 0.01	0.27 ± 0.06	0.45 ± 0.11	0.31 ± 0.09	0.47 ± 0.23	NS
ADH	0	0.01 ± 0.00	0	0	0	0.01 ± 0.01	NS
FDH	0.02 ± 0.00	0.02 ± 0.01	0.06 ± 0.02	0.01 ± 0.01	0.03 ± 0.01	0	NS

Table 4.4 continued on next page

Table 4.4 continued

Enzyme	C	C+P	P	C+A	C5	1% raw milk	<i>p</i> -value
<i>T. paralvinellae</i>							
H ₂ ase (mem)	3.34 ± 0.91	1.53 ± 0.31	4.62 ± 2.20	1.36 ± 0.29	0.18 ± 0.18	ND	NS
H ₂ ase (cyto)	0.21 ± 0.03 ^a	1.53 ± 0.15	0.54 ± 0.20 ^a	0.06 ± 0.01 ^a	0.05 ± 0.01 ^a	0.35 ± 0.14 ^a	***
ATP synthase	0.23 ± 0.04 ^{a,b}	0.39 ± 0.29 ^{a,c}	3.30 ± 0.44 ^d	4.41 ± 0.03 ^d	1.33 ± 0.20 ^{b,c}	ND	***
FNOR	0.21 ± 0.07 ^a	3.33 ± 0.60 ^{b,c}	3.42 ± 0.16 ^{c,d}	9.10 ± 1.02	1.84 ± 0.22 ^{a,b,d}	1.71 ± 0.22 ^{a,b,d}	***
GDH	12.09 ± 0.75 ^a	3.88 ± 1.26 ^b	9.03 ± 0.56 ^{a,c}	3.89 ± 0.91 ^b	8.31 ± 0.30 ^c	0.53 ± 0.14 ^b	***
AlaAT	1.21 ± 0.47 ^a	5.08 ± 1.27 ^{a,b}	5.80 ± 2.46 ^{a,b}	3.01 ± 0.11 ^{a,b}	8.00 ± 0.37 ^b	2.42 ± 0.45 ^{a,b}	*
POR	2.59 ± 0.13 ^a	1.29 ± 0.09	0.46 ± 0.10 ^b	0.41 ± 0.05 ^b	2.16 ± 0.40 ^a	0.18 ± 0.05 ^b	***
VOR	0.34 ± 0.07 ^a	0.44 ± 0.05 ^a	0.11 ± 0.03 ^b	0.02 ± 0.01 ^b	0.11 ± 0.03 ^b	0.14 ± 0.03 ^b	***
ACSI+II	0.34 ± 0.07 ^a	0.60 ± 0.03 ^b	0.52 ± 0.02 ^b	0.21 ± 0.02 ^{a,c}	0.60 ± 0.02 ^b	0.13 ± 0.06 ^c	***
AOR	0.35 ± 0.05 ^a	0.29 ± 0.05 ^a	0.48 ± 0.09 ^a	0.60 ± 0.10 ^a	1.55 ± 0.43	0.10 ± 0.03 ^a	***
FOR	0.28 ± 0.10 ^{a,b}	0.12 ± 0.03 ^a	0.62 ± 0.14 ^b	0.34 ± 0.13 ^{a,b}	0.46 ± 0.06 ^{a,b}	0.16 ± 0.02 ^a	**
ADH	0.03 ± 0.01 ^{a,b}	0.07 ± 0.03 ^a	0.02 ± 0.00 ^{a,b}	0 ^b	0.02 ± 0.01 ^{a,b}	0 ^b	**
FDH	0.06 ± 0.02 ^a	0.02 ± 0.00 ^{a,b}	0.03 ± 0.00 ^{a,b}	0.04 ± 0.01 ^{a,b}	0.02 ± 0.00 ^{a,b}	0.01 ± 0.01 ^b	*

Table 4.4. Specific activity (U/mg protein) are the averages of no less than three technical replicates and two biological replicates (\pm standard error). ND: a specific activity was not determined. *p*-values calculated from one-way ANOVA test comparing enzymatic activity across treatments. * *p* < 0.05, ** *p* < 0.01, and *** *p* < 0.001. Tukey post-hoc test indicates groups whose members are not significantly different ^{a,b,c,d,e,f}. NS: no significance.

Figure 4.11: Distribution of *P. furiosus* and *T. paralvinellae* Enzymatic Specific Activities

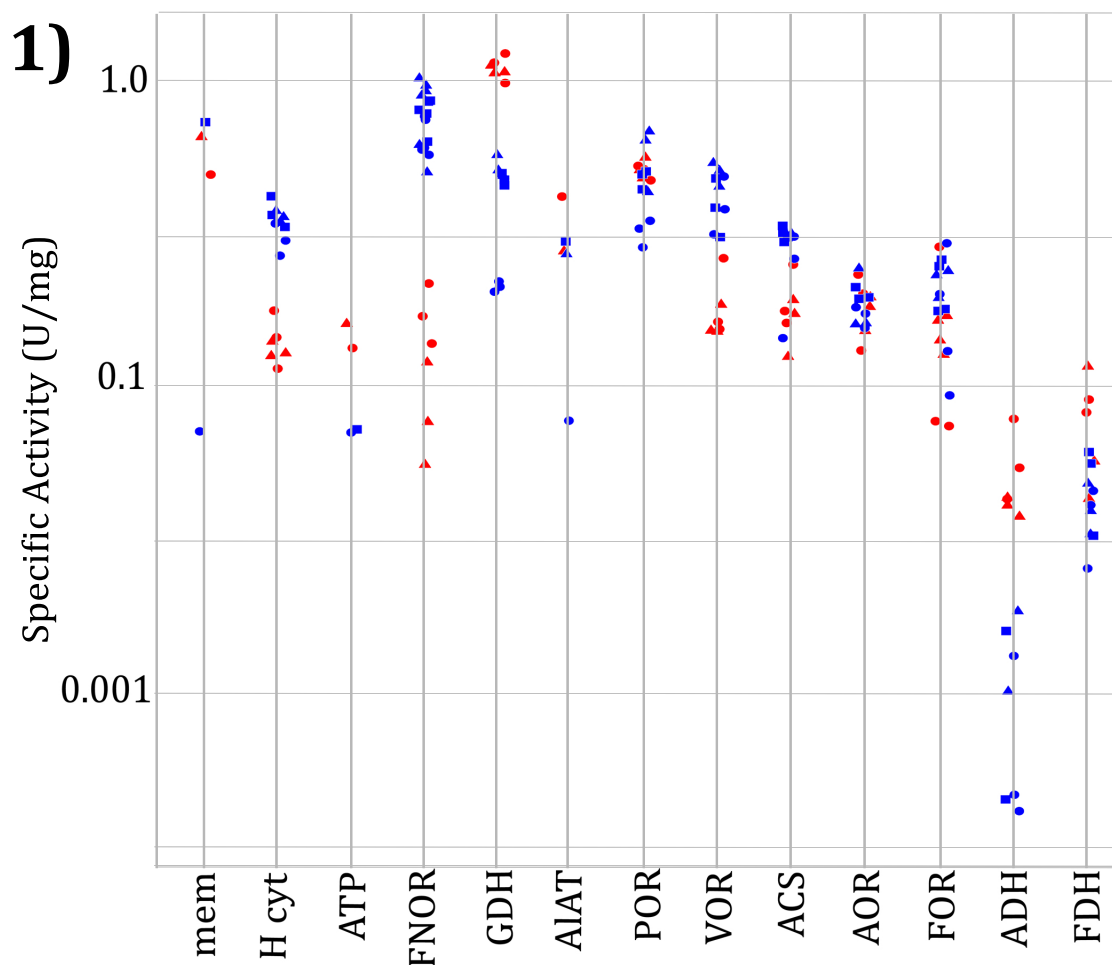


Figure 4.11 continued on next page

Figure 4.11 continued

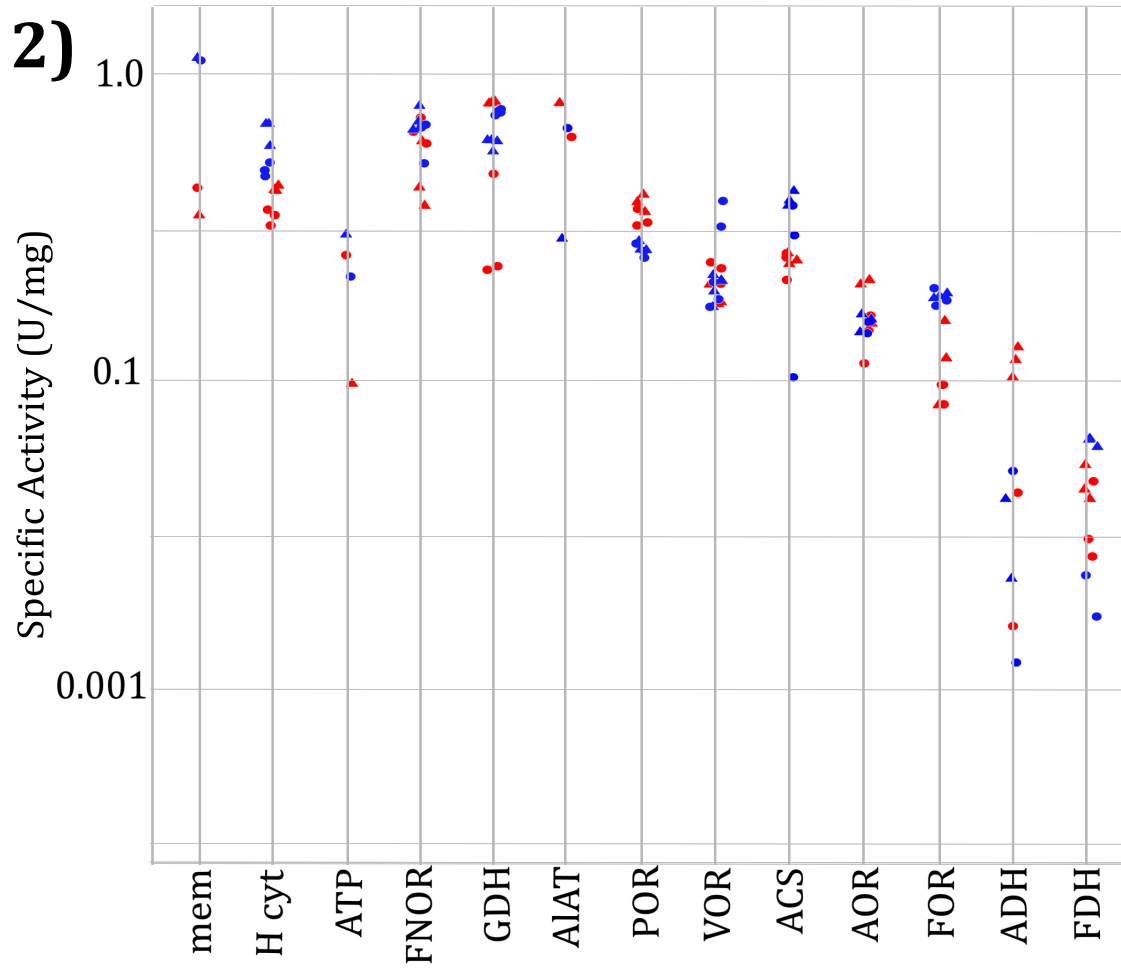


Figure 4.11 continued on next page

Figure 4.11 continued

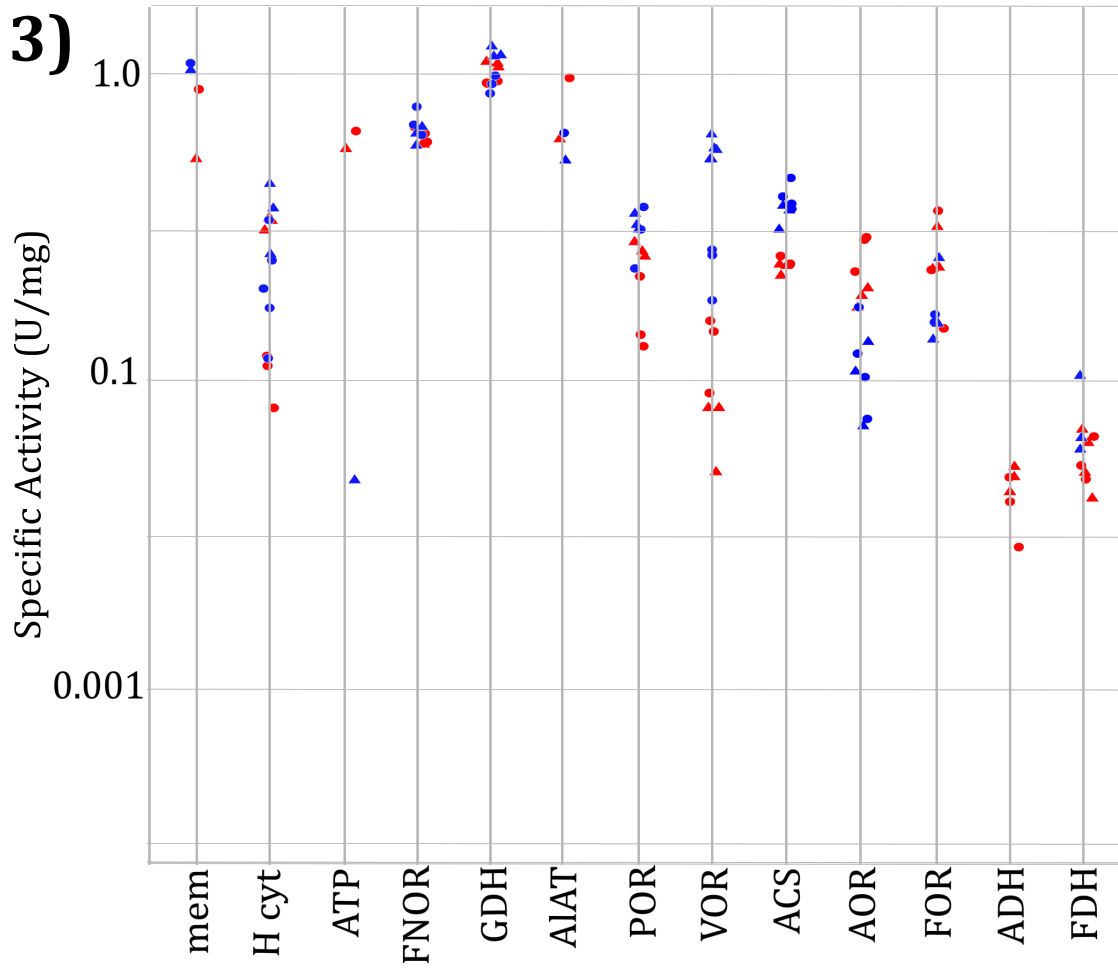


Figure 4.11 continued on next page

Figure 4.11 continued

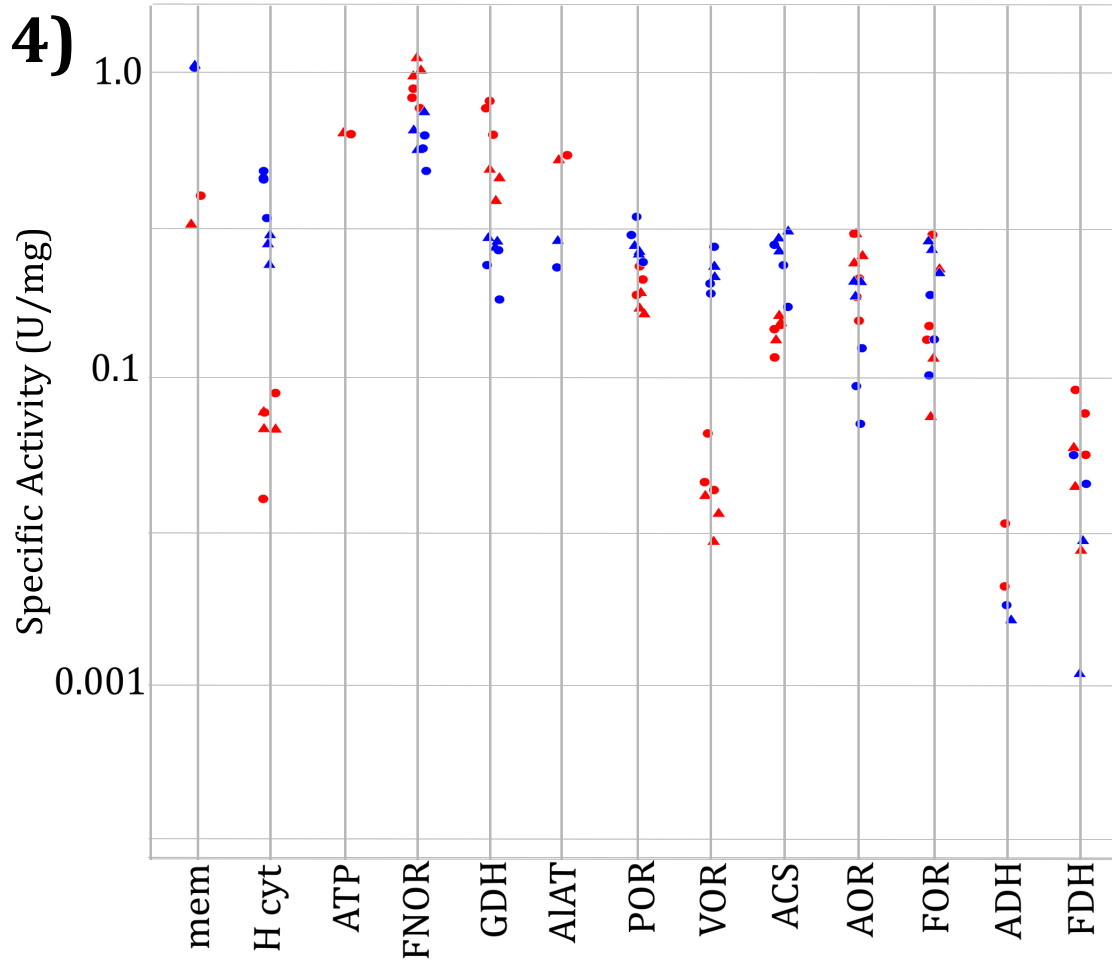


Figure 4.11 continued on next page

Figure 4.11 continued

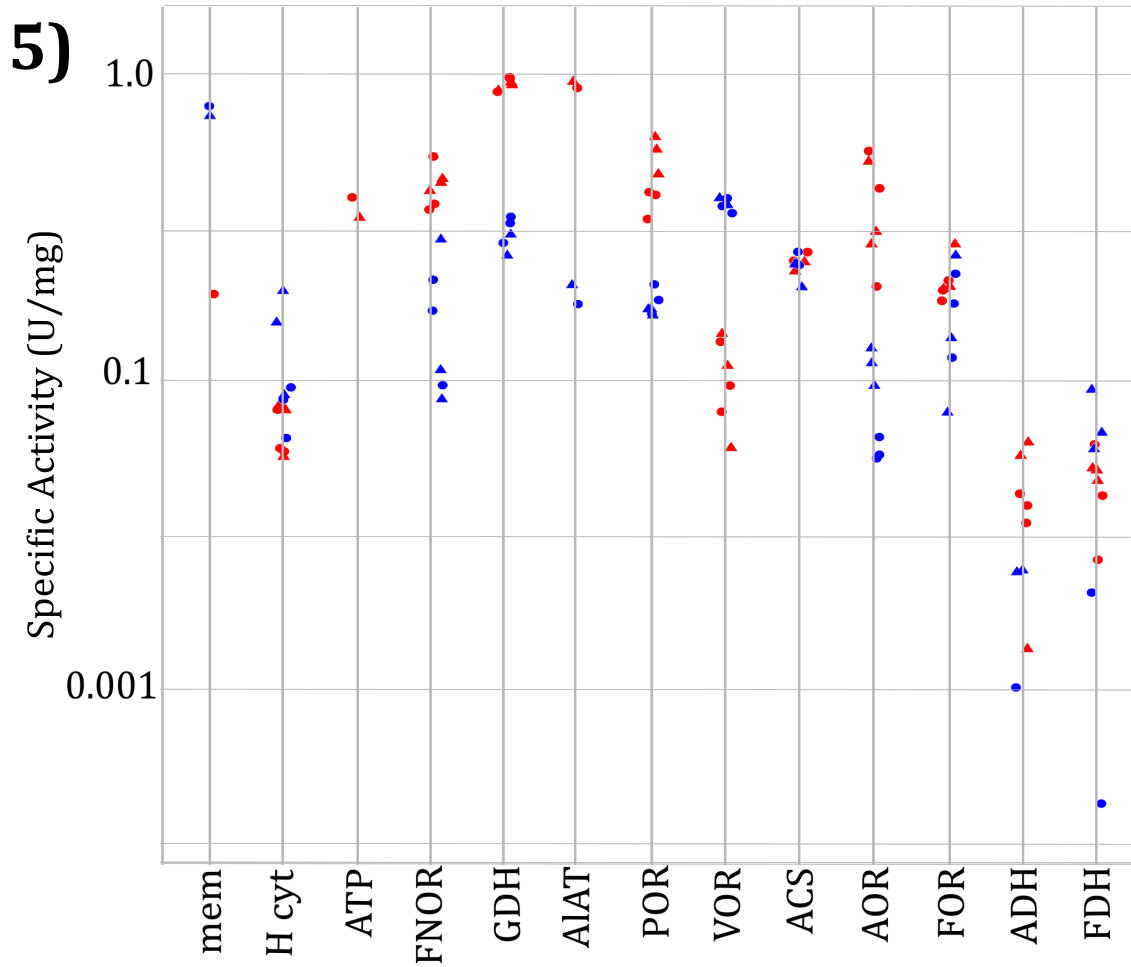


Figure 4.11 continued on next page

Figure 4.11 continued

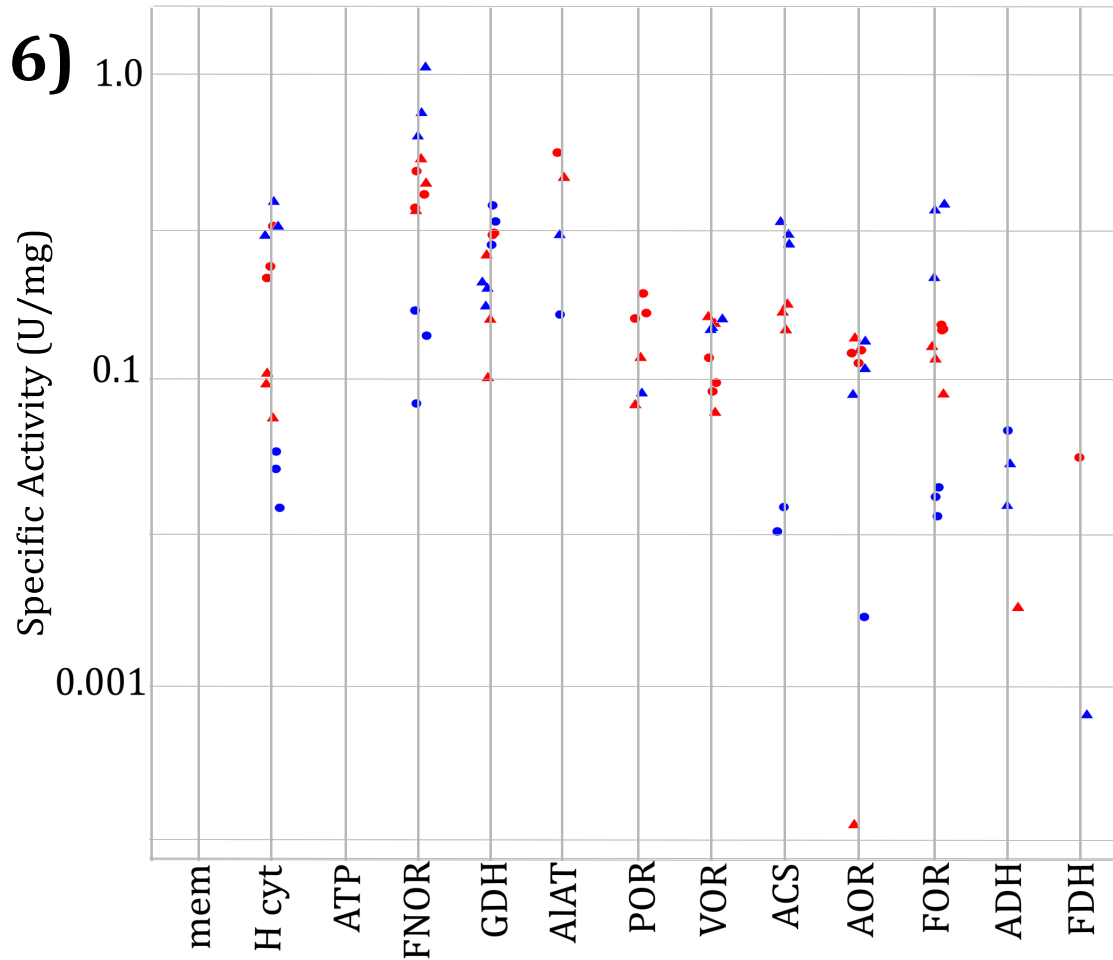


Figure 4.11: Each enzyme activity measured is individually represented by media. 1) C medium, 2) C+P medium, 3) P medium, 4) C+A medium, 5) C5 medium, 6) 1% raw milk. *T. parvalvinellae* (red) and *P. furiosus* (blue) enzyme activities are differentiated by biological replicate number (1 are circles, 2 are triangles and 3 are squares). Enzyme activities that were 0.000 are not represented.

enzymes for *P. furiosus*). For *P. furiosus*, membrane-bound hydrogenase activities were higher than any other enzyme activity for all defined media except for FNOR activity, which was higher when cells were grown on C medium ($F_{12}= 25.1$, $p < 0.001$). For *T. paralvinellae*, membrane-bound ATP synthase, GDH, and AlaAT activities were higher than all other enzyme activities ($F_{12}= 170.4$, $p < 0.001$).

Membrane-bound hydrogenase and ATP synthase activities could not be measured from cells grown on milk due to co-precipitation of insoluble cell fractions with heat curdled milk. Membrane-bound hydrogenase activity in *P. furiosus* cells grown in C+P medium was higher ($F_4= 12.05$, $p < 0.05$) than activities in cells from C and C5 media, and activity in cells from C+A medium was higher than that in cells from C medium. In contrast, the membrane-bound hydrogenase activities in *T. paralvinellae* did not show any significant change between the defined media. Membrane-bound hydrogenase activities in *P. furiosus* were higher than those in *T. paralvinellae* for cells grown on C+P ($F_1=798$, $p < 0.001$), C+A ($F_1=847$, $p < 0.005$), and C5 ($F_1=142.9$, $p < 0.01$) media. Cytoplasmic hydrogenase activities from C+P medium were higher in *P. furiosus* and *T. paralvinellae* cells than activities in cells from the other four defined media and 1% milk medium ($F_5=23.2$, $p < 0.001$). Cytoplasmic hydrogenase activities were higher in *P. furiosus* than in *T. paralvinellae* for cells grown on C ($F_1=66.7$, $p < 0.001$), C+P ($F_1=14.5$, $p < 0.01$), and C+A ($F_1=20.5$, $p < 0.01$) media. Membrane-bound ATP synthase activity in *P. furiosus* cells grown on C+P medium was higher than activities in cells from the other four defined media ($F_4=10.4$, $p < 0.02$). In *T. paralvinellae*, this activity was higher in cells grown on C+A and P media than on the other three defined media ($F_4=54.2$, $p < 0.001$). Membrane-

bound ATP synthase activity was higher in *T. paralvinellae* than in *P. furiosus* for cells grown on P ($F_1=57.0$, $p<0.02$), C+A ($F_1=2.1*10^4$, $p<0.001$), and C5 ($F_1=44.4$, $p<0.05$) media.

In *P. furiosus*, GDH activity was higher in cells grown on P medium than any of the other four defined media and 1% raw milk ($F_5=50.0$, $p<0.001$). POR activity was higher in cells grown on C medium than any of the other four defined media and 1% raw milk ($F_5=11.28$, $p<0.001$). In *T. paralvinellae*, AOR and FNOR activities were higher in cells grown on C+A medium than any of the other four defined media and 1% raw milk medium ($F_5=7.75$, $p<0.001$ and $F_5=37.72$, $p<0.001$, respectively). FNOR activity was lower in cells grown on C medium than on C+P and P media ($F_5=37.72$, $p<0.01$). VOR activity was higher in cells grown on C and C+P media than any other media ($F_5=14.45$, $p<0.05$), POR activity was higher in cells grown on C and C5 media than any other media ($F_5=30.32$, $p<0.05$), and GDH activity was higher ($F_5=28.8$, $p<0.02$) in cells grown on C medium than cells grown on C5, C+A, C+T, and 1% milk media. The other enzyme activities for both organisms either did not change with growth medium or did not show a consistent pattern in their differences.

4.5 Discussion

In the U.S., food waste management in composting facilities is nascent with only 3% of food waste composted in 2008 (Levis *et al.*, 2010). Diverting food waste to composting and biological treatment is considered promising to limit landfill growth and produce biofuels (Hermann *et al.*, 2011). Microorganisms that catabolize long-chain carbohydrates and polypeptides and produce an energy

product such as H₂, CH₄, and alcohols are ideal for these processes (Alper and Stephanopoulos, 2009; Angenent *et al.*, 2004). This study showed that the hyperthermophilic heterotrophs *P. furiosus* and *T. paralvinellae* grew and produced H₂ on carbohydrates and peptides, even at low pH and in the presence of 10 mM acetate, and on spent brewery grain and raw milk from cows treated with Ceftiofur and untreated cows. *T. paralvinellae* produced more H₂ and grew on higher feedstock concentrations relative to *P. furiosus*, but generally grew slower than *P. furiosus* on the wastes.

Raw bovine milk contains by weight 3% protein (mostly casein), 4% fat, and 5% carbohydrate (mostly lactose) (Wong *et al.*, 1988), while the solids in spent brewery grain are mostly carbohydrate (starch). In this study, *P. furiosus* and *T. paralvinellae* grew on defined media containing maltose (a hydrolysis product of starch) and casein hydrolysate, and soluble protein was removed from the milk by the organisms. Neither organism grew on lactose or removed it from the milk. They both possess genes for a putative β-galactosidase and grow on cellobiose (Osowski *et al.*, 2011), which chemically is similar to lactose. Therefore, it may be possible to adapt these organisms to grow on lactose.

Heat treatment and incubation with *P. furiosus* and *T. paralvinellae* also appears to remove culturable pathogens present in the waste and the Ceftiofur in milk from antibiotic-treated cows. While only 0.1% of the initial antibiotic dose is excreted in milk, the milk cannot be added to the food supply for five days after treatment (Hornish and Katariski, 2002). The half-life of Ceftiofur at 67°C is 6 h, which decreases with increasing temperature (Sunkara *et al.*, 1999). The U.S Food

and Drug Administration requires that the concentration of Ceftiofur in raw milk be less than 50 ppb (Samanidou and Nisyriou, 2008). There was no change in either growth rate or H₂ production for either organism when they were grown on milk from Ceftiofur-treated cows relative to milk from untreated cows. Ceftiofur is a β -lactam that inhibits peptidoglycan synthesis. Archaea lack peptidoglycan making them amenable to treatment of waste containing Ceftiofur.

P. furiosus produced up to 5 mmoles of H₂ per liter of medium for defined media. Although the H₂ production yields for defined media were not significantly different between the organisms, the membrane hydrogenase activity was lower in *T. paralvinellae* than in *P. furiosus* for most media. *T. paralvinellae* also produced larger amounts of H₂ than *P. furiosus* when grown on higher concentrations of wastes suggesting less H₂ inhibition in *T. paralvinellae*. These results may be due to differing H₂ production pathways in the two organisms. *T. paralvinellae* possesses genes for putative CO-, F₄₂₀- and formate-dependent hydrogenases that are lacking in *P. furiosus*, in addition to the ferredoxin- and NADH-dependent hydrogenases in both organisms (Jung et al., 2014). If active, they may ameliorate possible H₂ inhibition by having a more diverse electron carrier pool to draw from.

Mixed carbon media (i.e., maltose and peptides) improved H₂ production for both species rather than have no or a negative effect, as is the case with most mesophilic and thermophilic anaerobes (Kim et al., 2004; Pawar and Niel, 2013). Also unlike most other cultures, *P. furiosus* and *T. paralvinellae* tolerated a broad pH and nutrient concentration range. In many other H₂ producing organisms, as the pH decreases H₂ production becomes increasingly inhibited due to the effect of low pH

on hydrogenases (Dabrock *et al.*, 1992; Munro *et al.*, 2009). While pH 5 did decrease the specific activity of many enzymes in *P. furiosus* and *T. paralvinellae*, it did not decrease the growth or H₂ production rates relative to growth on maltose at pH 6.8.

This is the first time that H₂ production by hyperthermophiles has been investigated using agricultural waste as a feedstock. Prior to this study, the highest growth-temperature organism examined for H₂ production from agricultural waste was *Caldicellulosiruptor saccharolyticus* (Ivanova *et al.*, 2009). *C. saccharolyticus* is a thermophilic Gram-positive bacterium that grows optimally at 70°C and uses a wide range of sugars (Van de Werken *et al.*, 2008). It uses an NADH-dependent hydrogenase that produces H₂ only at low H₂ partial pressures (Soboh *et al.*, 2004). Like *P. furiosus*, the amount of H₂ production by *C. saccharolyticus* differed with the type of agricultural waste offered (Ivanova *et al.*, 2009). Unlike *P. furiosus*, *T. paralvinellae* produced increasing amounts of H₂ from both agricultural wastes types with increasing concentration and grew well at up to 25% waste concentration (data not shown). *T. paralvinellae* also grows over a lower temperature range than *P. furiosus*, which may give *T. paralvinellae* a cost advantage over *P. furiosus* due to lower reactor heating costs.

Enzyme activities and metabolite production in *P. furiosus* were largely as expected. Hydrogen:acetate ratios were approximately two when cells were grown on maltose, and increased when grown on peptides with isovalerate and (iso)butyrate also present. Formate concentrations equaled or exceeded those of acetate for cultures grown on maltose with and without added acetate for reasons that are unknown. GDH activity was significantly higher in cells grown on peptides

and POR activity was significantly higher in cells grown on maltose, which is expected for deamination of amino acids during peptide catabolism and growth on a hexose sugar, respectively (Figure 4.1), as observed previously (Adams *et al.*, 2001). Ethanol was undetectable and ADH activity was very low to undetectable suggesting that alcohol production is not a significant alternative pathway for electron disposal. Metabolite production and POR activity for *T. paralvinellae* was similar to *P. furiosus* with H₂:acetate ratios near two for most carbohydrate conditions, isovalerate present only in peptide media, and POR activity highest in carbohydrate media. AOR, VOR and GDH activities were significantly higher and FNOR lower in maltose-containing media suggesting that redox balance in *T. paralvinellae* involves factors not found in *P. furiosus*.

In conclusion, both *P. furiosus* and *T. paralvinellae* are amenable to the catabolism of carbohydrates and peptides with H₂ production over a range of pH and acetate concentrations with little impact on growth and H₂ production rates. For both organisms, H₂ production rates were highest on a mixture of carbohydrate and peptides. The organisms grew and produced H₂ on spent brewery grain and raw bovine milk, and mesophilic bacteria were eliminated from the wastes in the process, indicating that it is feasible to use hyperthermophilic heterotrophs in a single process step to reduce the organic load of food and agricultural wastes, generate H₂ as an energy byproduct, and remove pathogens.

CHAPTER 5

CONCLUSIONS

5.1 Direction and Future Work

This dissertation has presented three research projects with the goals of 1) elucidating the complete genome sequence of *Thermococcus paralvinellae*, 2) determining the taxonomic novelty of *T. paralvinellae* and *Thermococcus cleftensis* using overall genome relatedness index (OGRI) analyses while placing key features of their genomes in context of the rest of the Thermococcales, and 3) determining the effects of environmental conditions on the growth and enzymatic activity of *Pyrococcus furiosus* and *T. paralvinellae*, as well as their ability to degrade dairy and spent grain wastes. The first project found that *T. paralvinellae* possesses a formate:H₂ lyase, a H₂-producing carbon monoxide dehydrogenase, and an F420-dependent hydrogenase, in addition to multiple alcohol dehydrogenases. The second project showed that *T. paralvinellae* is, a close relative of *Thermococcus barophilus*, which also possesses a formate:H₂ lyase and is capable of growth on formate (Kim *et al.*, 2010). We also showed that *T. cleftensis* is a close relative of *Thermococcus sp. 4557*. The growth of both new species is enhanced by the presence of elemental sulfur, but neither require it for growth. The third and final project revealed that both *T. paralvinellae* and *P. furiosus* are able to degrade of dairy and spent grain wastes. However, *T. paralvinellae* grows better on spent grain than does *P. furiosus* while *P. furiosus* shows a decrease in H₂ production rate when tryptone is the only organic supplied for growth, unlike *T. paralvinellae*. The enzymatic

expression patterns revealed that *T. paralvinellae* and *P. furiosus* may possess different mechanisms for redox balance, as exemplified by the differential expression of AOR, FNOR, GDH, and VOR. Moreover, *T. paralvinellae* appears to be inhibited less by H₂ than *P. furiosus*.

We hope to continue these projects in different capacities. To continue the first and second projects, we'd like to examine *T. paralvinellae*, as well as *Pyrococcus abyssi* and *Pyrococcus yayanosii* to see if our predictions about their growth on formate hold true. Additionally, we'd like to determine a genetic system for *T. paralvinellae*, based on that of the negative selection system established in *T. barophilus* (Thiel *et al.*, 2014) and/or the upregulation of genes in *P. furiosus* using a naturally competent strain (Chandrayan *et al.*, 2012; Lipscomb *et al.*, 2011). We would utilize the established *T. paralvinellae* genetic system to examine the effects of overexpression of its many hydrogenases and alcohol dehydrogenases to see if we could develop a strain that has an increased H₂ production yield on agricultural wastes.

We would like to continue the third project in a plethora of ways, all with the end goal of applying hyperthermophiles to bioenergy production through the remediation of agricultural wastes. First, we'd like to create a reactor design that would produce the most amount of H₂. To do this, we will collaborate with the Civil and Environmental Engineering Department at the University of Massachusetts-Amherst. One of the things we would like to examine is whether a two-stage reactor design, where the hyperthermophilic culture degrades the waste and then the effluent is passed into a second, mesophilic reactor, where fermentative microbes

can degrade it further. The mesophilic culture could be a natural fermentative culture from the waste that has been adapted to high H₂ production. This not only has a potential for higher H₂ yield, but more complete COD removal.

While our collaborators are investigating more efficient pilot reactors, we would also like to examine the differences in enzymatic expression between log and stationary phase cultures. This is because of the preliminary differences observed with enzymatic expression between different biological replicates that were otherwise identical (Figure 4.5). Additionally, we'd like to examine differences in H₂ production between chemostat and batch cultures. Thus far, we have only operated our systems in batch mode, but chemostats completely remove possible H₂-production inhibitors accumulating in the media and therefore have the potential for greater H₂ yield.

Another of the short term goals we would like to accomplish in the future is to determine which potential waste sources would provide the best substrate for Thermococcales species. Although the wide range of amylases that some members of the Thermococcales possess means that a large range of sugar substrates may be utilized, complex protein substrates should provide good feedstock as well. Since our potential applications are therefore vast, we would probably start with feedstocks that have already been shown to work well with other thermophiles, such as fish (Remmereit and Thomm, 2008), fruit and vegetable waste (Ganesh *et al.*, 2014), and one-carbon compounds from steel mill waste (Kim *et al.*, 2013).

Finally, we'd like to select species that have minimum impact on the environment, as well as lower the salt content of our reactors. Thus, we'd like to

explore the salinity and percent waste tolerances of our Thermococcales species, as well as to determine whether freshwater fermentative-like hyperthermophiles represent good candidates for the degradation of the agricultural wastes. We may start with the screening of *Desulfurococcus* species, which are capable of hydrolysis and/or fermentation of a wide variety of polymeric and monomeric substrates (Perevalova *et al.*, 2005), as well as environmental sampling.

With the foundations laid by the work in this dissertation, we are well on our way to achieving our ultimate objective. The long-term goal of this research is to make a consolidated process wherein small businesses can reduce the carbon content of their waste while the maximum amount of hydrogen is produced. Thus, ideally, the small business owner or farmer can at least use the process to reduce waste in a self-sustaining manner and, hopefully, produce excess energy to help run their farm, thereby cutting down on costs.

BIBLIOGRAPHY

1. Abe F, Horikoshi K (2001) The biotechnological potential of piezophiles. *TRENDS Biotechnol* 19(3): 102–108.
2. Achenbach-Richter L, Gupta R, Zillig W, Woese CR (1988) Rooting the Archaeobacterial tree: The pivotal role of *Thermococcus celer* in Archaeobacterial evolution. *Sys Appl Microbiol* 10(3): 231-240.
3. Adams MWW (1990) The structure and mechanism of iron-hydrogenases. *Biochim Biophys Acta* 1020(2): 115–145.
4. Adams MWW, Holden JF, Menon AL, Schut GJ, Grunden AM, Hou C, Hutchins AM, Jenney Jr FE, Kim C, Ma K, Pan G, Roy R, Sapra R, Story SV, Verhagen MFJM (2001) Key role for sulfur in peptide metabolism and in regulation of three hydrogenases in the hyperthermophilic archaeon *Pyrococcus furiosus*. *J Bacteriol* 183(2): 716–724.
5. Alsaker KV, Spitzer TR, Papoutsakis ET (2004) Transcriptional analysis of *spo0A* overexpression in *Clostridium acetobutylicum* and its effect on the cell's response to butanol stress. *J Bacteriol* 189(7): 1959–1971.
6. Albers S-V, Meyer BH (2011) The archaeal cell envelope. *Nature Rev Microbio* 9(6): 414–426.
7. Alger MT, Garcia ML, Lee ES, Schlicher M, Angenent LT (2008) Thermophilic Anaerobic Digestion to Increase the Net Energy Balance of Corn Grain Ethanol. *Environ Sci Technol* 42: 6723–6729.
8. Alper H, Stephanopoulos G (2009) Engineering for biofuels: exploiting innate microbial capacity or importing biosynthetic potential? *Nature Reviews: Microbiology* 7: 715–723.
9. Altschul, SF, Gish W, Miller W, Myers EW, Lipman DJ (1990). Basic local alignment search tool. *J Mol Biol* 215(3): 403–410.
10. Amend JP, Meyer-Domabard DR, Sheth SN, Zolotova N, Amend AC (2003) *Palaeococcus helgesonii* sp. nov., a facultatively anaerobic, hyperthermophilic archaeon from a geothermal well on Vulcano Island, Italy. *Arch Microbiol* 179: 394-401.
11. Andersch W, Bahl H, and Gottschalk G (1983) Level of enzymes involved in acetate, butyrate, acetone and butanol formation by *Clostridium acetobutylicum*. *Eur J Appl Microbiol Biotechnol* 18: 327–332.

12. Angenent LT, Karim K, Al-Dahhan MH, Wrenn BA, Domínguez-Espinosa R (2004) Production of bioenergy and biochemicals from industrial and agricultural wastewater. *TRENDS Biotechnol* 22(9): 477–485.
13. Antoni D, Zverlov VV, Schwarz WH (2007) Biofuels from microbes. *Appl Microbiol Biotechnol* 77: 23–35.
14. Atomi H, Sato T, Kanai T (2011) Application of hyperthermophiles and their enzymes. *Curr Opin Biotechnol* 22(5): 618–626.
15. Auch AF, von Jan M, Klenk HP, Göker M (2010) Digital DNA-DNA hybridization for microbial species delineation by means of genome-to-genome sequence comparison. *Stand Genomic Sci* 2(1): 117–134.
16. Bagi Z, Acs N, Bálint B, Horváth L, Dobó K, Perei KR, Rákhely G, Kovács KL (2007) Biotechnological intensification of biogas production. *Appl Microbiol Biotechnol* 76(2): 473–482.
17. Bahl H, Gottwald M, Kuhn A, Andersch W, Gottschalk G (1986) Nutritional factors affecting the ratio of solvents produced by *Clostridium acetobutylicum*. *Appl Environ Microbiol* 52(1): 169–172.
18. Bartlett C (2010) Mapping waste in the food industry for Defra and the Food and Drink Federation. Oakdene Hollins, Research and Consulting. Reference number: DEFR01 235 summary.doc
19. Basen M, Sun J, Adams MWW (2012) Engineering a hyperthermophilic archaeon for temperature-dependent product formation. *mBio* 3(2): e00053–12.
20. Beconi-Barker MG, Roof RD, Vidmar TJ, Hornish RE, Smith EB, Gatchell CL, Gilbertson TJ (1996) Ceftiofur sodium: absorption, distribution, metabolism and excretion in target animals and its determination by HPLC. *ACS Symposium Series* 636: 70–84. DOI: 10.1021/bk-1996-0636.ch009
21. Bertoldo C, Antranikian G (2006) The order Thermococcales Prokaryotes. 3: 69–81. DOI: 10.1007/0-387-30743-5_5
22. Bertoldo C, Antranikian G (2011) Biotechnology of Archaea. *In: Encyclopedia of Life Support Systems* 9.
23. Besemer J, Lomsadze A, Borodovsky M (2001) GeneMarkS: A self-training method for prediction of gene starts in microbial genomes. Implications for finding sequence motifs in regulatory regions. *Nucleic Acid Res* 29(12): 2607–2618.

24. Blamey JM, Adams MWW (1993) Purification and characterization of pyruvate ferredoxin oxidoreductase from the hyperthermophilic archaeon *Pyrococcus furiosus*. *Biochim Biophys Acta* 1161: 19–27.
25. Blumer-Schuette SE, Kataeva I, Westpheling J, Adams MWW, Kelly RM (2008) Extremely thermophilic microorganisms for biomass conversion: Status and prospects. *Curr Opin Biotechnol* 19(3): 210–217.
26. Boiangiu CD, Jayamani E, Brügel D, Herrmann G, Kim J, Forzi L, Hedderich R, Vgenopoulou I, Pierik AJ, Steuber J, Buckel W (2005) Sodium ion pumps and hydrogen production in glutamate fermenting anaerobic bacteria. *J Mol Microbiol Biotechnol* 10: 105–119.
27. Bougrier C, Delgenes JP, Carrère H (2008) Effects of thermal treatments on five different waste activated sludge samples solubilisation, physical properties and anaerobic digestion. *Chem Engineer J* 139(2): 236–244.
28. Braber K (1995) Anaerobic digestion of municipal solid waste: A modern waste disposal option on the verge of breakthrough. *Biomass and Bioenergy* 9: 365–376.
29. Bradford MM (1976) A rapid and sensitive method for the quantitation of microgram quantities of protein utilizing the principle of protein-dye binding. *Anal Biochem* 72: 248–254.
30. Bräsen C, Schönheit P (2004) Unusual ADP-forming acetyl coenzyme A synthetases from the mesophilic halophilic euryarchaeon *Haloarcula marismortui* and from the hyperthermophilic crenarchaeon *Pyrobaculum aerophilum*. *FEBS Lett* 579: 477–482.
31. Bredberg K, Persson J, Christiansson M, Stenberg B, Holst O (2001) Anaerobic desulfurization of ground rubber with the thermophilic archaeon *Pyrococcus furiosus* – A new method for rubber recycling. *Appl Microbiol Biotechnol* 55(1): 43–48.
32. Brenner K, You L, Arnold FH (2008) Engineering microbial consortia: A new frontier in synthetic biology. *Trends Biotechnol* 26(9): 483–489.
33. Brodie HL, Carr LE, Condon P (2000) A comparison of static pile and turned windrow methods for poultry litter compost production. *Compost Sci Util* 8(3): 178–189.
34. Bryant FO, Adams MWW (1989) Characterization of hydrogenase from the hyperthermophilic archaeobacterium, *Pyrococcus furiosus*. *J Biol Chem* 264: 5070–5079.

35. Casalot L, Rousset M (2001) Maturation of the [NiFe] hydrogenases. *Trends Microbiol* 9(5): 228–237.
36. Chandan R, Ed. (1997) Properties of milk and its components. *In: Dairy-Based Ingredients*. Ch 1: 1–10.
37. Chandrayan SK, McTernan PM, Hopkins RC, Sun J, Jenney FE, Adams MWW (2012) Engineering hyperthermophilic archaeon *Pyrococcus furiosus* to overproduce its cytoplasmic [NiFe]-hydrogenase. *J Biol Chem* 287(5): 3257–3264.
38. Chou CJ, Shockley KR, Connors SB, Lewis DL, Comfort DA, Adams MWW, Kelly RM (2007) Impact of substrate glycoside linkage and elemental sulfur on bioenergetics and hydrogen production by the hyperthermophilic archaeon *Pyrococcus furiosus*. *Appl Environ Microbiol* 73(21): 6842–6853.
39. Chun J, Rainey FA, (2014) Integrating genomics into the taxonomy and systematics of the Bacteria and Archaea. *Int J Syst Evol Microbiol* 64: 316–324.
40. Cloern JE (2001) Our evolving conceptual model of the coastal eutrophication problem. *Mar Ecol Prog Ser* 210: 223–253.
41. Cohen GN, Barbe V, Flament D, Galperin M, Heilig R, Lecompte O, Poch O, Prieur D, Quérellou J, Ripp R, Thierry J-C, Van der Oost J, Weissenbach J, Zivanovic Y, Forterre P (2003) *Mol Microbiol* 47: 1495-1512.
42. Dabrock B, Bahl H, Gottschalk G (1992) Parameters affecting solvent production by *Clostridium pasteurium*. *Appl Environ Microbiol* 58(4): 1233–1239.
43. Delcher AL, Bratke KA, Powers EC, Salzberg SL (2007) Identifying bacterial genes and endosymbiont DNA with Glimmer. *Bioinformatics* 23: 673–679.
44. Diaz LF, de Bertoldi M, Bidlingmaier W, Ed. (2007) *Compost science and technology*. Amsterdam, The Netherlands: Elsevier.
45. Diggelman C, Ham RK (2003) Household food waste to wastewater or to solid waste? That is the question. *Waste Manag Res* 21(6): 501–504.
46. Dodds WK, Bouska WW, Eitzmann JL, Pilger TJ, Pitts KL, Riley AJ, Schloesser JT, Thornbrugh DJ (2009) Eutrophication of US freshwaters: Analysis of potential economic damages. *Enviro Sci Tech* 43(1): 12–19.
47. Drake HL (1994) Acetogenesis, acetogenic bacteria, and the acetyl-Coa “Wood/Ljungdahl” pathway: Past and current perspectives. *In: Drake HL, Ed. Acetogenesis*. New York, NY: Chapman & Hall.

48. Drake HL, Gößner AS, Daniel SL (2008) Old acetogens, new light. *Ann NY Acad Sci* 1125: 100–128.
49. Dürre P, Kuhn A, Gottwald M, Gottschalk G (1987) Enzymatic investigations on butanol dehydrogenase and butyraldehyde dehydrogenase in extracts of *Clostridium acetobutylicum*. *Appl Microbiol Biotechnol* 26: 268–272.
50. Dürre P, Ed. (2005) *Handbook on Clostridia*. Boca Raton, FL, USA: CRC Press.
51. Dürre P (2008) Fermentative butanol production: Bulk chemical and biofuel. *Ann NY Acad Sci* 1125: 353–362.
52. Eberly JO, Ely RL (2008) Thermotolerant hydrogenases: Biological diversity, properties, and biotechnological applications. *Crit Rev Microbiol* 34: 117–130.
53. Elmore JR, Yokooji, Y, Sato T, Olson S, Glover CVC III, Graveley BR, Atomi H, Terns RM, Terns MP (2013) Programmable plasmid interference by the CRISPR-Cas system in *Thermococcus kodakarensis*. *RNA Biol* 10: 828–840.
54. United States Environmental Protection Agency (2011) Report on the Environment: Science Report. 832B12001.
55. European Commission Directorate-General for the Environment (2009) Environment – Biodegradable Waste. <http://ec.europa.eu/environment/waste/compost/index.htm>. Accessed 06.01.2014.
56. Fang HHP, Liu H (2002) Effect of pH on hydrogen production from glucose by mixed culture. *Bioresour Technol* 82(1): 87–93.
57. Fiala G, Stetter KO (1986) *Pyrococcus furiosus* sp. nov. represents a novel genus of marine heterotrophic archaeobacteria growing optimally at 100°C. *Arch Microbiol* 145(1): 56–61.
58. Fillaudeau L, Blanpain-Avet P, Daufin G (2006) Water, wastewater and waste management in brewing industries. *J Clean Prod* 14(5): 463–471.
59. Frey M (1998) Nickel-iron hydrogenases: Structural and functional properties. *Struct Bond* 90: 97–126.
60. Fukui T, Atomi H, Kanai T, Matsumi R, Fujiwara S, Imanaka T (2005) Complete genome sequence of the hyperthermophilic archaeon *Thermococcus kodakarensis* KOD1 and comparison with *Pyrococcus* genomes. *Genome Res* 15: 352–363.

61. Ganesh R, Torrijos M, Sousbie P, Lugardon A, Steyer JP, Delgenes JP (2014) Single-phase and two-phase anaerobic digestion of fruit and vegetable waste: Comparison of start-up, reactor stability and process performance. *Waste Manag* 34(5): 875–885.
62. Gebler A, Burgdorf T, De Lacey AL, Rüdiger O, Martinez-Arias A, Lenz O, Friedrich B (2007) Impact of alterations near the [NiFe] active site on the function of the H₂ sensor from *Ralstonia eutropha*. *FEBS J* 274(1): 74–85.
63. Ghiradi ML, Posewitz MC, Maness PC, Dubini A, Yu J, Seibert M (2007) Hydrogenases and hydrogen photoproduction in oxygenic photosynthetic organisms. *Annu Rev Plant Biol.* 58: 71–91.
64. Girguis PR and Holden JF (2012) On the potential for bioenergy and biofuels from hydrothermal vent microbes. *Oceanography* 25(1): 213-217.
65. Goff HD, Hill AR (1993) Chemistry and physics. *In: Dairy science and technology handbook*. Vol. 1. Hui YH, Ed. VCH Publishers, New York.
66. Goris J, Konstantinidis T, Klappenback JA, Coenye T, Vandamme P, Tiedje JM (2007) DNA-DNA hybridization values and their relationship to whole-genome sequence similarities. *Int J Syst Evol Microbiol* 57: 81–91.
67. Grissa I, Vergnaud G, Pourcel C (2007) CRISPRFinder: a web tool to identify clustered regularly interspaced short palindromic repeats. *Nucleic Acids Res* 35: W52–W57.
68. Hallenbeck PC (2009) Fermentative hydrogen production: Principles, progress and prognosis. *Int J Hydrogen Energy* 34(17): 7379–7389.
69. Hallenbeck PC, Ghosh D (2009) Advances in fermentative biohydrogen production: The way forward? *Trends Biotechnol.* 27: 287–297.
70. Hartmanis MGN, Gatenbeck S (1984) Intermediary metabolism in *Clostridium acetobutylicum*: Levels of enzymes involved in the formation of acetate and butyrate. *Appl Environ Microbiol* 47(6): 1277–1283.
71. Haug RT (1993) *The practical handbook of compost engineering*. Lewis Publishers, Boca Raton, Florida, USA.
72. Hay J, Kuchenrither RD (1990) Fundamentals and application of windrow composting. *J Environ Eng* 116(4): 746–763.
73. Hedderich R, Forzi L (2005) Energy-converting [NiFe] hydrogenases: More than just H₂ activation. *J Mol Microbio Biotechnol* 10: 92–104.

74. Heider J, Ma K, Adams MWW (1995) Purification, characterization, and metabolic function of tungsten-containing aldehyde ferredoxin oxidoreductase from the hyperthermophilic and proteolytic archaeon *Thermococcus* strain ES-1. *J Bacteriol* 177: 4757–4764.
75. Heider J, Mai X, Adams MWW (1996) Characterization of 2-ketoisovalerate ferredoxin oxidoreductase, a new and reversible coenzyme A-dependent enzyme involved in peptide fermentation by hyperthermophilic archaea. *J Bacteriol* 178: 780–787.
76. Heinekey DM (2009) Hydrogenase enzymes: Recent structural studies and active site models. *J Organomet Chem* 649: 2671–2680.
77. Heinonen JE, Lahti RJ (1981) A new and convenient colorimetric determination of inorganic orthophosphate and its application to the assay of inorganic pyrophosphatase. *Anal Biochem* 113:313–317.
78. Hensley SA, Jung JH, Park CS, Holden JF (2014). *Thermococcus paralvinellae* ES1 sp. nov. and *Thermococcus cleftensis* CL1 sp. nov., new species of hyperthermophilic heterotrophs from deep-sea hydrothermal vents. *IJSEM* In review.
79. Hermann BG, Debeer L, de Wilde B, Blok K, Patel MK (2011) To compost or not to compost: Carbon and energy footprints of biodegradable materials' waste treatment. *Polymer Degradation and Stability* 96(6): 1159–1171.
80. Holden JF, Takai K, Summit M, Bolton S, Zyskowski J, Baross JA (2001) Diversity among three novel groups of hyperthermophilic deep-sea *Thermococcus* species from three sites in the northeastern Pacific Ocean. *FEMS Microbiol Ecol* 36: 51–60.
81. Hornish RE, Kotarski SF (2002) Cephalosporins in veterinary medicine – Ceftiofur use in food animals. *Curr Top Med Chem* 2: 717–731.
82. Huber R, Langworthy TA, König H, Thomm M, Woese CR, Sleytr UB, Stetter KO (1986) *Thermotoga maritima* sp. nov. represents a new genus of unique extremely thermophilic eubacteria growing up to 90°C. *Arch Microbio* 144: 324–333.
83. Hutchins AM, Mai X, Adams MWW (2001) Acetyl-CoA synthetases I and II from *Pyrococcus furiosus*. *Methods in Enzymology* 331: 158–167.
84. Ibrahim N, Jahim JM, Lim SS (2013) Initial study of thermophilic hydrogen production from raw palm oil mill effluent (POME) using mixed microflora. *In: Pogaku R, Bono A, Chu C (Eds.) Developments in Sustainable Chemical and Bioprocess Technology*. 1:43-49. doi: 10.1007/978-1-4614-6208-8_6

85. Ivanova G, Rákhely G, Kovács KL (2009) Thermophilic biohydrogen production from energy plants by *Caldicellulosiruptor saccharolyticus* and comparison with related studies. *Int J Hydrogen Energy* 34: 3659-3670.
86. Jenney FE, Adams MWW (2008) Hydrogenases of the model hyperthermophiles. *Incredible anaerobes: from physiology to genomics to fuels*. *Ann New York Acad Sci* 1125: 252–266. doi: 10.1196/annals.1419.013
87. Jeon E-J, Jung JH, Seo D-H, Holden JF, Park CS (2014) Bioinformatic and biochemical analysis of maltose-forming α -amylase from the hyperthermophilic archaeon *Thermococcus* sp. CL1. *Enzyme Microb Technol* doi: 10.1016/j.enzmictec.2014.03.009
88. Jun X, Lupeng L, Minjuan X, Oger P, Fenping W, Jebbar M, Xiang X (2011) Complete genome sequence of the obligate piezophilic hyperthermophilic archaeon *Pyrococcus yayanosii* CH1. *J Bacteriol* 193(16): 4297-4298.
89. Jung JH, Holden JF, Seo D-H, Park KH, Shin H, Ryu S, Lee JH, Park CS (2012a) Complete genome sequence of the hyperthermophilic archaeon *Thermococcus* sp. strain CL1, isolated from a *Paralvinella* sp. polychaete worm collected from a hydrothermal vent. *J Bacteriol* 194(17): 4769–4770.
90. Jung JH, Lee JH, Holden JF, Seo D-H, Shin H, Kim HY, Kim W, Ryu S, Park CS (2012b) Complete genome sequence of the hyperthermophilic archaeon *Pyrococcus* sp. strain St04, isolated from a deep-sea hydrothermal sulfide chimney on the Juan de Fuca Ridge. *J Bacteriol* 194(16): 4434–4435.
91. Jung JH, Kim YT, Jeon E-J, Seo D-H, Hensley SA, Holden JF, Lee J-H, Park CS (2014) Complete genome sequence of the hyperthermophilic archaeon *Thermococcus* sp. ES1. *J Biotech* 174: 14–15 doi: 10.1016/j.biotech.2014.01.022.
92. Kapdan IK, Kargi F (2006) Biohydrogen production from waste materials. *Enzyme Microb Technol* 38(5): 569–582.
93. Kawarabayasi Y, Sawada M, Horikawa H, Haikawa Y, Hino Y, Yamamoto S, Sekine M, Baba S-I, Kosugi H, Hosoyama A, Nagai Y, Sakai M, Ogura K, Otsuka R, Nakazawa H, Takamiya M, Ohfuku Y, Funahashi T, Tanaka T, Kudoh Y, Yamazaki J, Kushida N, Oguchi A, Aoki K-I, Yoshizawa T, Nakamura Y, Robb FT, Horikoshi K, Masuchi Y, Shizuya H, Kikuchi H (1998) Complete sequence and gene organization of the genome of a hyper-thermophilic archaeobacterium, *Pyrococcus horikoshii* OT3. *DNA Res* 5(2): 55-76.
94. Kengen SWM, Stams AJM (1994) Growth and energy conservation in batch cultures of *Pyrococcus furiosus*. *FEMS Microbiol Lett* 117: 305–309.

95. Kengen SWM, Stams AJM, de Vos WM (1996) Sugar metabolism of hyperthermophiles. *FEMS Microbiol Rev* 18: 119–137.
96. Khanal SK, Chen WH, Li L, Sung S (2004) Biological hydrogen production: effects of pH and intermediate products. *Int J Hydrogen Energy* 29: 1123–1131.
97. Kim J, Bajpai R, and Iannotti EL (1988) Redox potential in acetone-butanol fermentations. *Appl Biochem Biotechnol* 18: 175–186.
98. Kim S-H, Han S-K, Shin H-S (2004) Feasibility of biohydrogen production by anaerobic co-digestion of food waste and sewage sludge. *Int J Hydrogen Energy* 29: 1607–1216.
99. Kim YJ, Lee HS, Kim ES, Bae SS, Lim JK, Matsumi R, Lebedinsky AV, Sokolova TG, Kozhevnikova DA, Cha S-S, Kim S-J, Kwon KK, Imanaka T, Atomi H, Bonch-Osmolovskaya EA, Lee J-H, Kang SG (2010) Formate-driven growth coupled with H₂ production. *Nature* 467: 352-355.
100. Kim M-S, Bae SS, Kim YJ, Kim TW, Lim JK, Lee SH, Choi AR, Jeon JH, Lee J-H, Lee HS, Kand SG (2013) CO-Dependent H₂ production by genetically engineered *Thermococcus onnurineus* NA1. *79(6)*: 2048-2053.
101. Koelmans AA, Van Der Heijde A, Knijff LM, Aalderink RH (2001) Integrated Modelling of Eutrophication and Organic Contaminant Fate & Effects in Aquatic Ecosystems: A Review. *Water Research* 35(15): 3517–3536.
102. Koesnandar A, Nishio N, Nagai S (1991a) Effects of trace metal ions on the growth, homoacetogenesis and corrinoid production by *Clostridium thermoaceticum*. *J Ferment Bioeng* 71(3): 181–185.
103. Koesnandar A, Nishio N, Nagai S (1991b) Enzymatic reduction of cystine into cysteine by cell-free extract of *Clostridium thermoaceticum*. *J Ferment Bioeng* 72 (1): 11–14.
104. Kumar N, Das D (2000) Enhancement of hydrogen production by *Enterobacter cloacae* IIT-BT08. *Process Biochem* 35(6): 589–593.
105. Lagesen K, Hallin P, Rødland EA, Staerfeldt HH, Rognes T, Usserv DW (2007) RNAmmer: consistent and rapid annotation of ribosomal RNA genes. *Nucleic Acids Res.* 35(9): 3100–3108.
106. Lai C-M, Ke G-R, Chung M-Y (2009) Potentials of food wastes for power generation and energy conservation in Taiwan. *Ren Energy.* **34**:1913–1915.

107. Larkin MA, Blackshields G, Brown NP, Chenna R, McGettigan PA, McWilliams H, Valentin F, Wallance IM, Wilm A, Lopez R, Thompson JD, Gibson TJ, Higgins DG (2007). ClustalW and ClustalX version 2.0. *Bioinformatics* 23: 2947–2948.
108. Lee S-H, Choi K-I, Osako M, Dong J-I (2007) Evaluation of environmental burdens caused by changes of food waste management systems in Seoul, Korea. *Sci Total Environ* 387: 42–53.
109. Lee HS, Kang SG, Bae SS, Lim JK, Cho Y, Kim YJ, Jeon JH, Cha S-S, Kwon KK, Kim H-T, Park C-J, Lee H-W, Kim SI, Chun J, Colwell RR, Kim S-J, Lee J-H (2008a) The complete genome sequence of *Thermococcus onnurineus* NA1 reveals a mixed heterotrophic and carboxydrotrophic metabolism. *J Bacteriol* 190: 7491-7499.
110. Lee SY, Park JH, Jang SH, Nielsen LK, Kim J, and Jung KS (2008b) Fermentative butanol production by Clostridia. *Biotechnol Bioeng* 101(2): 209–228.
111. Lee M, Hidaka T, Tsuno H (2009) Two-phased hyperthermophilic anaerobic co-digestion of waste activated sludge with kitchen garbage. *J Biosci Bioengineer* 108(5): 408–413.
112. Lee HS, Bae SS, Kim M-S, Kwon KK, Kang SG, Lee J-H (2011) Complete genome sequence of hyperthermophilic *Pyrococcus* sp. strain NA2, isolated from a deep-sea hydrothermal vent area. *J Bacteriol* 193(14): 3666-3667.
113. Lee JE, Kim IH, Jung JH, Seo D-H, Kang SG, Holden JF, Cha J, Park CS (2013). Molecular cloning and enzymatic characterization of cyclomaltodextrinase from hyperthermophilic archaeon *Thermococcus* sp. CL1. *J Microbiol Biotechnol* 23: 1060–1069.
114. Levis JW, Barlaz MA, Themelis NJ, Ulloa P (2010) Assessment of the state of food waste treatment in the United States and Canada. *Waste Manag* 30(8-9): 1486–1494
115. Lim JK, Kang SG, Lebedinsky AV, Lee J-H, Lee HS (2010) Identification of a novel class of membrane-bound [NiFe]-hydrogenases in *Thermococcus onnurineus* NA1 by *in silico* analysis. *Appl Environ Microbiol* 76(18): 6286–6289.
116. Lin CSK, Pfaltzgraff LA, Herrero-Davila L, Mudofu EB, Abderrahim S, Clark JH, Koutinas AA, Kopsahelis N, Stamatelatos K, Dickson F, Thankappan S, Mohamed Z, Brocklesby R, Luque R (2013) Food waste as a valuable resource for the production of chemicals, materials and fuels. Current situation and global perspective. *Energy Environ Sci* 6: 426–464.

117. Lipscomb GL, Stirret K, Schut GJ, Yang F, Jennery Jr FE, Scott RA, Adams MWW, Westpheling J (2011) Natural competence in the hyperthermophilic archaeon *Pyrococcus furiosus* facilitates genetic manipulation: Construction of markerless deletions of genes encoding the two cytoplasmic hydrogenases. *Appl Environ Microbiol* 77(7): 2232–2238.
118. Ljunggren M, Zacchi G (2010) Techno-economic analysis of a two-step biological process producing hydrogen and methane. *Bioresour Technol* 101(20): 7780–7788.
119. Ljunggren M, Wallberg O, Zacchi G (2011a) Techno-economic comparison of a biological hydrogen process and a 2nd generation ethanol process using barley straw as feedstock. *Bioresour Technol* 102(20): 9524–9531.
120. Ljunggren M, Willquist K, Zacchi G, van Niel EWJ (2011b) A kinetic model for quantitative evaluation of the effect of H₂ and osmolarity on hydrogen production by *Caldicellulosiruptor saccharolyticus*. *Biotechnol Biofuels* 4(1): 31. doi:10.1186/1754-6834-4-31.
121. Lowe TM, Eddy SR (1997) tRNAscan-SE: a program for improved detection of transfer RNA genes in genomic sequence. *Nucleic Acids Res* 25(5): 955–964.
122. Ma K, Adams MWW (1994) Sulfide dehydrogenase from the hyperthermophilic archaeon *Pyrococcus furiosus*: a new multifunctional enzyme involved in the reduction of elemental sulfur. *J Bacteriol* 176: 6509–6517.
123. Ma KS, Hao Z, Adams MWW (1994) Hydrogen production from pyruvate by enzymes purified from the hyperthermophilic archaeon *Pyrococcus furiosus*: A key role for NADPH. *FEMS Microbiol Lett* 122(3): 245–450.
124. Ma K, Loessner H, Heider J, Johnson MK, Adams MWW (1995) Effects of elemental sulfur on the metabolism of the deep-sea hyperthermophilic archaeon *Thermococcus* strain ES-1: Characterization of a sulfur-regulated, non-heme iron alcohol dehydrogenase. *J Bacteriol* 177(16): 4748–4756.
125. Ma K, Adams MWW (1999) An unusual oxygen-sensitive, iron- and zinc-containing alcohol dehydrogenase from the hyperthermophilic archaeon *Pyrococcus furiosus*. *J Bacteriol* 181(4):1163–1170.
126. Ma K, Weiss R, Adams MWW (2000) Characterization of hydrogenase II from the hyperthermophilic archaeon *Pyrococcus furiosus* and assessment of its role in sulfur reduction. *J Bacteriol* 182: 1864–1871.
127. Ma K, Adams MWW (2001a) Hydrogenases I and II from *Pyrococcus furiosus*. *Methods in Enzymol* 331: 208–216.

128. Ma K, Adams MWW (2001b) Ferredoxin:NADP oxidoreductase from *Pyrococcus furiosus*. *Methods in Enzymol* 334: 40–45.
129. Mai X, Adams MWW (1996) Purification and characterization of two reversible and ADP-dependent acetyl coenzyme A synthetases from the hyperthermophilic archaeon *Pyrococcus furiosus*. *J Bacteriol* 178: 5897–5903.
130. Mardanov AV, Ravin NV, Svetlitchnyi VA, Beletsky AV, Miroshnichenko ML, Bonch-Osmolvskaya EA, Skryabin KG (2009) Metabolic versatility and indigenous origin of the archaeon *Thermococcus sibiricus*, isolated from a Siberian oil reservoir, as revealed by genome analysis. *Appl Environ Microbiol* 75: 4580-4588.
131. Matthew AG, Cissell R, Liamthong S (2007) Antibiotic resistance in bacteria associated with food animals: A United States perspective of livestock production. *Food Path Disease* 4(2): 115–133.
132. McGinnis S, Madden TL (2004) BLAST: At the core of a powerful and diverse set of sequence analysis tools. *Nucleic Acids Res* 32: W20-W25.
133. Mende DR, Sunagawa S, Zeller G, Bork P (2013) Accurate and universal delineation of prokaryotic species. *Nature Methods* 10: 881–884.
134. Meyer J (2007) [FeFe] hydrogenases and their evolution: a genomic perspective. *Cell Mol Life Sci* 64(9): 1063–1084.
135. Mnatsakanyan N, Bagramyan K, Trchounian (2004) Hydrogenase 3 but not hydrogenase 4 is major in hydrogen gas production by *Escherichia coli* formate hydrogenlyase at acidic pH and in the presence of external formate. *Cell Biochem Biophys* 41(3): 357–366.
136. Mohee R, Mudhoo A (2005) Analysis of the physical properties of an in-vessel composting matrix. *Powder Technol* 155(1): 92–99.
137. Monier V, Mudgal S, Escalon V, O'Connor C, Gibon T, Anderson G, Montoux H (2010) Preparatory study on food waste across E.U.-27 for the European Commission. European Communities DOI: 10.2779/85947
138. Moon Y-J, Kwon J, Yun S-H, Lim HL, Kim M-S, Kang SG, Lee J-H, Choi J-S, Kim SI, Chung Y-H (2012) Proteome analyses of hydrogen-producing hyperthermophilic archaeon *Thermococcus onnurineus* NA1 in different one-carbon substrate culture conditions. *Mol Cell Proteom* 11(6). doi: 10.1074/mcp.M111.015420-1.
139. Moore DA, Taylor J, Hartman ML, Sisco WM (2009) Quality assessments of waste milk at a calf ranch. *J Dairy Sci* 92(7): 3503–3509.

140. Morimoto M, Atsuko M, Atif AAY, Ngan MA, Fakhru'l-Razi A, Iyuke SE, Bakir AM (2004) Biological production of hydrogen from glucose by natural anaerobic microflora. *Int J Hydrogen Energy* 29: 709–713.
141. Müller V, Blaut M, Heise R, Winner C, Gottschalk G (1990) Sodium bioenergetics in methanogens and acetogens. *FEMS Microbiol Let* 87: 373–376.
142. Müller V, Imkamp F, Biegel E, Schmidt S, Dilling S (2008) Discovery of a ferredoxin NAD⁺-oxidoreductase (Rnf) in *Acetobacterium woodii*: A potential coupling site in acetogens. *Ann N Y Acad Sci* 1125: 137–146.
143. Mukund S, Adams MWW (1991) The novel tungsten-iron-sulfur protein of the hyperthermophilic archaebacterium, *Pyrococcus furiosus*, is an aldehyde ferredoxin oxidoreductase. *J Biol Chem* 266: 14208–14216.
144. Nath K, Das D (2004) Improvement of fermentative hydrogen production: Various approaches. *Appl Microbiol Biotechnol* 65(5): 520–529.
145. Nicolet Y, Cavazza C, Fontecilla-Camps JC (2002) Fe-only hydrogenases: structure, function and evolution. *J Inorg Biochem* 91(1): 1–8.
146. Novotny V (1999) Diffuse pollution from agriculture – A worldwide outlook. *Water Sci Technol* 39(3): 1–13.
147. Ntaikou I, Antonopoulou G, Lyberatos G (2010) Biohydrogen production from biomass and wastes via dark fermentation: A review. *Waste Biomass Valor* 1(1): 21–39.
148. Olivares C, Goldstein N, Rhodes Y (2008) Food composting infrastructure. *BioCycle* 49 (12): 30-31.
149. Osowski DM, Jung JH, Seo D-H, Park CS, Holden JF (2011) Production of hydrogen from α -1,4- and β -1,4-Linked saccharides by marine hyperthermophilic archaea. *Appl Environ Microbiol* 77(10): 3169–3173.
150. Panda H (2011) *The Complete Book on Managing Food Processing Industry Waste*. Asia Pacific Business Press Inc.
151. Partanen P, Hultman J, Paulin L, Auvinen P, Romantschuk M (2010) Bacterial diversity at different stages of the composting process. *BMC Microbiol* 10: 94.
152. Parfitt J, Barthel M, Macnaughton S (2010) Food waste within food supply chains: quantification and potential for change to 2050. *Philos Trans R Soc B* 365(1554): 3065–3081.

153. Pawar SS and van Niel EWJ (2013) Thermophilic biohydrogen production: how far are we? *Appl Microbiol Biotechnol* 97: 7999-8009.
154. Pell AN (1997) Manure and microbes: Public and animal health problem? *J Dairy Sci* 80(10): 2673-2681.
155. Perevalova AA, Svetlichny VA, Kublanov IV, Chernyh NA, Kostrikina NA, Tourova TP, Kuznetsov BB, Bonch-Osmolovskaya EA (2005) *Desulfurococcus fermentans* sp. nov., a novel hyperthermophilic archaeon from a Kamchatka hot spring, and emended description of the genus *Desulfurococcus*. *Int J Sys Evol Microbiol* 55: 995-999.
156. Petersen TN, Brunak S, von Heijne G, Nielsen H (2011) SignalP 4.0: discriminating signal peptides from transmembrane regions. *Nat Methods* 8: 785-786.
157. Pledger RJ, Baross JA (1989) Characterization of an extremely thermophilic archaebacterium isolated from a black smoker polychaete (*Paralvinella* sp.) at the Juan de Fuca Ridge. *Syst Appl Microbiol* 12(3): 249-256.
158. Pledger RJ, Crump BC, Baross JA (1994) A barophilic response by two hyperthermophilic, hydrothermal vent archaea: An upward shift in the optimal temperature and acceleration of growth rate at supra-optimal temperatures by elevated pressure. *FEMS Microbiol Ecol* 14: 233-241.
159. Pisa KY, Huber H, Thomm M, Müller V (2007) A sodium ion-dependent A_1A_0 ATP synthase from the hyperthermophilic archaeon *Pyrococcus furiosus*. *FEBS J* 274(15): 3928-3938.
160. Prince RC, Kheshgi HS (2005) The photobiological production of hydrogen: potential efficiency and effectiveness as a renewable fuel. *Crit Rev Microbiol* 31(1): 19-31.
161. Pütz S, Dolezai P, Gelius-Dietrich G, Bohacova L, Tachezy J, Henze K (2006) Fe-hydrogenase maturases in the hydrogenosomes of *Trichomonas vaginalis*. *Eukaryot Cell* 5(3): 579-586.
162. R Core Team (2013) R: A language and environment for statistical computing. R Foundation for Statistical Computing, Vienna, Austria. ISBN 3-900051-07-0, URL <http://www.R-project.org/>
163. Remmereit J, Thomm M (2008) Energy production with hyperthermophilic organisms. US Patent No: US 2008/0131958 A1.

164. Robb FT, Park JB, Adams MWW (1992) Characterization of an extremely thermostable glutamate dehydrogenase: a key enzyme in the primary metabolism of the hyperthermophilic archaeobacterium, *Pyrococcus furiosus*. *Biochim Biophys Acta* 1120: 276–272.
165. Robb FT, Maeder DL, Brown JR, DiRuggiero J, Stump MD, Yeh RK, Weiss RB, Dunn DM (2001) Genomic sequence of hyperthermophile, *Pyrococcus furiosus*: implications for physiology and enzymology. *Methods Enzymol* 330: 134–157.
166. Robin O, Turgeon S, Paquin P (1993) Functional properties of milk proteins. *In: Dairy Science and Technology Handbook*. Vol. 1 Y.H. Hui, Ed. VCH Publishers, New York.
167. Richter M, Rosselló-Móra R (2009) Shifting the genomic gold standard for the prokaryotic species definition. *Proc Natl Acad Sci USA* 106(45): 19126–19131.
168. Rilling N (2005) Anaerobic fermentation of wet or semi-dry garbage waste fractions. *In: Jördening H-J, Winter J (Eds.) Environmental Biotechnology: Concepts and Applications*. doi: 10.1002/3527604286.
169. Rogers P, Chen J-S, Zidwick MJ (2013) Organic acid and solvent production part I: Acetic, lactic, gluconic, succinic and polyhydroxyalkanoic acids. *In: Rosenberg E, DeLong EF, Lory S, Stackebrandt E, Thompson F (Eds.) Prokaryotes* 18: 3-75.
170. Roy R, Mukund S, Schut GJ, Dunn DM, Weiss R, Adams MWW (1999) Purification and molecular characterization of the tungsten-containing formaldehyde ferredoxin oxidoreductase from the hyperthermophilic archaeon *Pyrococcus furiosus*: the third of a putative five-member tungstoenzyme family. *J Bacteriol* 181: 1171–1180.
171. Roy R, Menon AL, Adams MWW (2001) Aldehyde oxidoreductases from *Pyrococcus furiosus*. *Methods Enzymol* 331: 132–144.
172. Saady NMC (2013) Homoacetogenesis during hydrogen production by mixed cultures dark fermentation: Unresolved challenge. *Int J Hydrogen Energy* 38:13172-13191.
173. Sakai S-I, Yoshida H, Hirai Y, Asari M, Takigami H, Takahashi S, Tomoda K, Peeler MV, Wejchert J, Schmid-Unterseh T, Douvan AR, Hathaway R, Hylander LD, Fischer C, Oh GJ, Jinhui L, Chi NK (2011) International comparative study of 3R and waste management policy developments. *J Mater Cycles Waste Manag* 13: 86–102.

174. Sakurai H, Masukawa H (2007) Promoting R&D in photobiological hydrogen production utilizing mariculture-raised cyanobacteria. *Mar Biotechnol* 9(2): 128–145.
175. Samanidou V, Nisyriou S (2008) Multi-residue methods for confirmatory determination of antibiotics in milk. *J Sep Sci* 31(11): 2068–2090.
176. Sapro R, Verhagen MF, Adams MWW (2000) Purification and characterization of a membrane-bound hydrogenase from the hyperthermophilic archaeon *Pyrococcus furiosus*. *J Bacteriol* 182: 3423–3428.
177. Sapro R, Bagramyan K, Adams MWW (2003) A simple energy-conserving system: Proton reduction coupled to proton translocation. *PNAS* 100(13): 7545–7550.
178. Sato T, Atomi H (2011) Novel Metabolic Pathways in *Archaea*. *Curr Op Microbiol* 14(3):307-314.
179. Schink B, Stams AJM (2006) Syntrophism among prokaryotes. *In: Rosenberg E, DeLong EF, Lory S, Stackebrandt E, Thompson F (Eds.) The Prokaryotes*. Springer Verlag, New York. 471-493.
180. Schmidt CE, Card TR, Kiehl B (2009) Composting trials evaluate VOC emissions control. *Biocycle* 50(4): 33–36.
181. Schut GJ, Brehm SD, Datta S, Adams MWW (2003) Whole-Genome DNA microarray analysis of a hyperthermophile and an archaeon: *Pyrococcus furiosus* grown on carbohydrates or peptides. *J Bacteriol* 185: 3935–3947.
182. Schut GJ, MWW Adams (2009) The iron-hydrogenase of *Thermotoga maritima* utilizes ferredoxin and NADH synergistically: A new perspective on anaerobic hydrogen production. *J Bacteriol* 191: 4451–4457.
183. Schwartz S, Kent WJ, Smit A, Zhang Z, Baertsch R, Hardison RC, Haussler D, Miller W (2003) Human-mouse alignments with BLASTZ. *Genome Res* 13(1): 103-107.
184. Shima S, Thauer RK (2007) A third type of hydrogenase catalyzing H₂ activation. *Chem Rec* 7(1): 37–46.
185. Shin H-S, Youn J-H, Kim S-H (2004) Hydrogen production from food waste in anaerobic mesophilic and thermophilic acidogenesis. *Int J Hydrogen Energy* 29(13): 1355–1363.
186. Silva PJ, Van de Ban EC, Wassink H, Haaker H, de Castró B, Robb FT, Hagen WR (2000) Enzymes of Hydrogen Metabolism in *Pyrococcus furiosus*. *Eur J Biochem* 267(22): 6541–6551.

187. Simmons P, Goldstein N, Kaufman SM, Themelis NJ, Thompson J (2006) The state of garbage in America. *Biocycle* 47: 26-43.
188. Skulachev VP (1989) Bacterial Na⁺ energetics. *FEBS letters* 250: 106–114.
189. Smith-Howard, K (2010) Antibiotics and agricultural change: Purifying milk and protecting health in the postwar era. *Agricultural history* 84(3): 327–351.
190. Smith VH, Tilman GD, Nekola JC (1999) Eutrophication: Impacts of excess nutrients inputs on freshwater, marine, and terrestrial ecosystems. *Environmental Pollution* 100: 179–196.
191. Soboh B, Linder D, Hedderich R (2004) A multisubunit membrane-bound [NiFe] hydrogenase and an NADH-dependent Fe-only hydrogenase in the fermenting bacterium *Thermoanaerobacter tengcongensis*. *Microbiology* 150: 2451–2463.
192. Soderlund C, Bomhoff M, Nelson WM (2011) SyMAP v.3.4: A turnkey synteny system with application to plant genomes. *Nucleic Acids Res* 39(10): e68.
193. Sokolova TG, Jeanthon C, Kostrikina NA, Chernyh NA, Lebedinsky AV, Stackebrandt E, Bonch-Osmolovskaya EA (2004) The first evidence of anaerobic CO oxidation coupled with H₂ production by a hyperthermophilic archaeon isolated from a deep-sea hydrothermal vent. *Extremophiles* 8: 317–323.
194. Staley BF, Barlaz MA (2009) Composition of municipal solid waste in the US and implications for carbon sequestration and methane yield. *J Environ Engineering* 135:901-909.
195. Stams AJ (1994) Metabolic interactions between anaerobic bacteria in methanogenic environments. *Antonie Van Leeuwenhoek* 66: 271–294.
196. Stetter KO (1996) Hyperthermophilic prokaryotes. *FEMS Microbiology Reviews* 18: 149–158.
197. Stetter KO (2003) Hyperthermophilic microorganisms. *EOLSS* 169–184.
198. Sunkara G, Navarre CB, Kompella UB (1999) Influence of pH and temperature on kinetics of ceftiofur degradation in aqueous solutions. *J Pharm Pharmacol* 51(3): 249-255.
199. Takai K, Sugai A, Itoh T, Horikoshi K (2000) *Palaeococcus ferrophilus* gen. nov., sp. nov., a barophilic, hyperthermophilic archaeon from a deep-sea hydrothermal vent chimney. *Int J Syst Evol Microbiol* 50: 489-500.

200. Tamagnini P, Leitão E, Oliveira P, Ferreria D, Pinto F, Harris DJ, Linblad P (2007) Cyanobacterial hydrogenases: diversity, regulation, and applications. *FEMS Microbiol Rev* 31(6): 692–720.
201. Tamura K, Peterson D, Peterson N, Stecher G, Nei M, Kumar S (2011) MEGA5: molecular evolutionary genetics analysis using maximum likelihood, evolutionary distance, and maximum parsimony methods. *Mol Biol Evol* 28(10): 2731–2739.
202. Thauer RK, Jungermann K, Decker K (1977) Energy conservation in chemotrophic anaerobic bacteria. *Bacteriol Rev* 41(1): 100–180.
203. Thiel A, Michoud G, Moalic Y, Flament D, Jebbar M (2014) Genetic manipulations of the hyperthermophilic piezophilic archaeon *Thermococcus barophilus*. *Appl Environ Microbiol* 80: 2299–2306.
204. Tjihuis L, Van Loosdrecht MCM, Heijnen JI (1993) A thermodynamically based correlation for maintenance Gibbs energy requirements in aerobic and anaerobic chemotrophic growth. *Biotechnol Bioeng* 42(4): 509–519.
205. Tilman D, Cassman KG, Matson PA, Naylor R, Polasky S (2002) Agricultural sustainability and intensive production practices. *Nature* 418: 671–677.
206. Ueno Y, Haruta S, Ishii M, Igarashi Y (2001) Characterization of a microorganism isolated from the effluent of hydrogen fermentation by microflora. *J Biosci Bioeng* 92(4): 397–400.
207. Ullmann S, Dürre P (1998) Changes in DNA topology are involved in triggering the onset of solventogenesis in *Clostridium acetobutylicum*. *Recent Res Dev Microbiol* 2: 281-294.
208. Van de Werken HJ, Verhaart MR, Van Fossen AL, Willquist K, Lewis DL, Nichols JD, Goorissen HP, Mongodin EF, Nelson KE, Van Niel EWJ, Stams AJM, Ward DE, de Vos WM, van de Oost J, Kelly RM, Kengen SWM (2008) Hydrogenomics of the extremely thermophilic bacterium *Caldicellulosiruptor saccharolyticus*. *Appl Environ Microbiol* 74(21): 6720–6729.
209. Vanfossen AL, Lewis DL, Nichols JD, Kelly RM (2008) Polysaccharide degradation and synthesis by extremely thermophilic anaerobes. *Ann NY Acad Sci* 1125: 322–337.
210. Van Haaren R, Themelis N, Goldstein N (2010) The state of garbage in America. *Biocycle* 51(10): 16.

211. Vannier P, Marteinson VT, Fridjonsson OH, Oger P, Jebbar M (2011) Complete genome sequence of the hyperthermophilic, pizeophilic, heterotrophic, and carboxydrotrophic archaeon *Thermococcus barophilus* MP. *J Bacteriol* 193: 1481-1482.
212. Verhaart MR, Bielen AA, Van der Oost J, Stams AJM, Kengen SWM (2010) Hydrogen production by hyperthermophilic and extremely thermophilic bacteria and archaea: mechanisms for reductant disposal. *Environ Technol* 31(8-9): 993-1003.
213. Verhees CH, Kengen SWM, Tuininga JE, Schut GJ, Adams MWW, De Vos WM, Van der Oost J (2003) The unique features of glycolytic pathways in Archaea. *Biochem J* 375: 231-246.
214. Vignais PM, Biloud B, Meyer J (2001) Classification and phylogeny of hydrogenases. *FEMS Microbio Rev* 25(4): 455-501.
215. Vignais PM, Colbeau A (2004) Molecular biology of microbial hydrogenases. *Curr Issues Mol Biol* 6(2): 159-188.
216. Waldron TT (2013) IDEXX SNAP beta-lactam ST validation for penicillin G detection. *J AOAC Int* 96(6): 1343-1349.
217. Wang J, Wan W (2009) Experimental design methods for fermentative hydrogen production: A review. *Int J Hydrogen Energy* 34: 235-244.
218. Wang Q, Garrity GM, Tiedje JM, Cole JR (2007) Naïve Bayesian classifier for a rapid assignment of rRNA sequences into the new bacterial taxonomy. *Appl Environ Microbiol* 73: 5261-5267.
219. Wang X, Gao Z, Xu X, Ruan L (2011) Complete genome sequence of *Thermococcus* sp. strain 4557, a hyperthermophilic archaeon isolated from a deep-sea hydrothermal vent area. *J Bacteriol* 193: 5544-5545.
220. Ward DE, Kengen SWM, van der Oost J, de Vos WM (2000) Purification and characterization of the alanine aminotransferase from the hyperthermophilic archaeon *Pyrococcus furiosus* and its role in alanine production. *J Bacteriol* 182: 2559-2566.
221. White D, Drummond JT, Fuqua C (Eds.) (2011) The physiology and biochemistry of prokaryotes. Oxford University Press, New York. 198-201.
222. Wiegel J, Ljungdahl LG, Demain AL (1985) The importance of thermophilic bacteria in biotechnology. *Crit Rev Biotechnol* 3: 39-108.
223. Wong J, Bennett GN (1996) The effect of novobiocin on solvent production by *Clostridium acetobutylicum*. *J Ind Microbiol* 16: 354-359.

224. Wong NP, Jenness R, Keeney M, Marth EH, Eds (1988) Fundamentals of Dairy Chemistry, 3rd ed. Van Nostrand Reinhold, New York.
225. Woods DR (1993) Biochemistry and Regulation of Acid and Solvent Production in Clostridia. *In: The Clostridia and Biotechnology*. Stoneham, MA p. 25-50.
226. Yoki H, Maki R, Hirose J, Hayashi S (2002) Microbial production of hydrogen from starch manufacturing wastes. *Biomass Bioenergy*. 22(5): 89–395.
227. Ying X, Grunden AM, Nie L, Adams MWW, Ma K (2009) Molecular characterization of the recombinant iron-containing alcohol dehydrogenase from the hyperthermophilic archaeon, *Thermococcus* strain ES1. *Extremophiles* 13(2): 299–311.
228. Zdobnov EM, Apweiler R (2001) InterProScan: an integration platform for the signature-recognition methods in InterPro. *Bioinformatics*. 17(9): 847–848.
229. Zeidan AA, Van Niel EWJ (2009) Developing a thermophilic hydrogen-producing co-culture for efficient utilization of mixed sugars. *Int J Hydrogen Energy* 34(10): 4524–4528.
230. Zeng X, Zhang X, Jiang L, Alain K, Jebbar M, Shao Z (2013) *Palaeococcus pacificus* sp. nov., an archaeon from deep-sea hydrothermal sediment. *Int J Sys Evol Microbiol* 63: 2155-2159.
231. Zivanovic Y, Armengaud J, Lagorce A, Leplat C, Guérin P, Dutertre M, Anthouard V, Forterre P, Winker P, Confalonieri F (2009) Genome analysis and genome-wide proteomics of *Thermococcus gammatolerans*, the most radioresistant organism known amongst the Archaea. *Genome Biol* 10: 1-23. doi: 10.1186/gb-2009-10-6-r70.